

Report No. CCEER 00-8

**Seismic Analysis and Design of the  
AISI LRFD Design Examples  
of Steel Highway Bridges**

Ahmad M. Itani  
Hassan Sedarat

Final Report on a Research Project Funded by the American Iron and Steel Institute

---

Center for Civil Engineering Earthquake Research  
Department of Civil Engineering  
University of Nevada, Reno

November 2000

**Seismic Analysis and Design of the  
AISI LRFD Design Examples  
of Steel Highway Bridges**

by

Ahmad M. Itani, Ph.D., P.E.  
Associate Professor  
Department of Civil Engineering  
University of Nevada, Reno

and

Hassan Sedarat, Ph.D., P.E.  
Senior Engineer  
SC Solutions, Inc.  
Santa Clara, CA

Report to American Iron and Steel Institute

Center for Civil Engineering Earthquake Research  
Department of Civil Engineering  
University of Nevada, Reno

November 8, 2000

## **ACKNOWLEDGEMENTS**

This document was prepared for the American Iron and Steel Institute (AISI) by Professor Ahmad M. Itani, P.E. of the University of Nevada, Reno and Dr. Hassan Sedarat, P.E. of SC Solutions, Inc.

The authors would like to gratefully acknowledge the contributions and advice of the AISI Take Force on Seismic Design of Steel Bridges: Mr. John Barsom, Past Chair of the task force, Mr. Edward Wasserman, P.E. of Tennessee Department of Transportation, current chair of the task force, Prof. Hassan Astanteh, P.E. of University of California, Berkeley, Mr. Steve Altman, P.E. and Mark Reno, P.E. of California Department of Transportation, Professor Charles Roeder, P.E. of the University of Washington, Professor Stewart Chen, P.E. of the State University at Buffalo, Professor Karl Frank, P.E. of the University of Texas, Austin, Mr. Alex Krimotat of SC Solutions, Inc and Mr. Mike Grubb of BSDI, Inc.

The authors would like also like to thank Camille G. Rubeiz, of AISI and Alex Wilson of Bethlehem Lukens Plate for their assistance throughout the project.

## **NOTICE**

The materials set fourth herein are for general information only. They are not a substitute for competent professional assistance. Anyone making use of them does so at his or her own risk and assumes any resulting liability

# Table of Contents

**Acknowledgments** .....ii

List of Tables      **iv**

List of Figures      **vii**

## Part I: AASHTO LRFD Seismic Design of Highway Bridges

Introduction .....3  
AASHTO LRFD Seismic Analysis & Design.....3  
AASHTO Seismic Loads .....4  
AASHTO Seismic Design Forces .....7  
AASHTO Analysis for Earthquake Loads .....8  
Seismic Lateral Load Distribution.....8

## Part II: AISI LRFD Design Examples of Highway Bridges

Introduction .....10  
Description of AISI LRFD Example 1 .....10  
Description of AISI LRFD Example 2 .....11  
Description of AISI LRFD Example 2-M.....11  
Description of AISI LRFD Example 3 .....11  
Description of AISI LRFD Example 3-M.....12  
Description of AISI LRFD Example 4 .....12

## Part II: AISI LRFD Design Examples of Highway Bridges

Introduction .....13  
Finite Element Modeling of Steel Highway Bridges .....13  
Space Frame Element Modeling .....14  
Three Dimensional Frame Modeling of the AISI Design Examples .....15  
Mathematical Models of the AISI Design Examples.....16  
Description of AISI LRFD Example 3-M.....12  
Description of AISI LRFD Example 4 .....12

## Part IV: Dynamic Characteristics of the AISI Design Examples

Introduction .....18  
Dynamic Behavior of Design Examples .....18

## Part V: Seismic Analysis of the AISI Design Examples

Introduction .....	22
Seismic Loads .....	22
Analysis for Earthquake Loads .....	24
Seismic Analysis of Design Examples 2 and 2-M .....	25
Seismic Analysis of Design Examples 3 and 3-M .....	25
Seismic Analysis of Design Example 4.....	26

## Part VI: Seismic Design of AISI Design Examples

Introduction .....	27
Seismic Design of Single Span Bridges .....	27
Seismic Design of Multi-Span Bridges .....	28
Seismic Design of Example 1 .....	29
Seismic Design of Example 2.....	35

References   **43**

Tables       **45**

Figures      **79**

## List of Tables

1.1	Response Modification Factors for Bridge Substructure .....	46
1.2	Response Modification Factors for Bridge Connections .....	46
2.1	Cross Sections of Girder in Design Example 1 .....	47
2.2	Cross Sections of Girder in Design Example 2 .....	47
2.3	Cross Sections of Girder in Design Example 3 .....	48
2.2	Cross Sections of Girder in Design Example 4 .....	48
4.1	Dynamic Characteristics of 3-D Finite Element Model of Example 2 .....	49
4.2	Dynamic Characteristics of Space Frame Model of Example 2 .....	50
4.3	Dynamic Characteristics of 3-D Finite Element Model of Example 2-M .....	51
4.4	Dynamic Characteristics of 3-D Finite Element Model of Example 3 .....	52
4.5	Dynamic Characteristics of 3-D Finite Element Model of Example 3 .....	53
4.6	Dynamic Characteristics of 3-D Finite Element Model of Example 3-M .....	54
4.7	Dynamic Characteristics of 3-D Finite Element Model of Example 3-M .....	55
4.8	Dynamic Characteristics of 3-D Finite Element Model of Example 4 .....	56
4.9	Dynamic Characteristics of Space Frame Model of Example 4 using one-stick Model for the Superstructure .....	57
4.10	Dynamic Characteristics of Space Frame Model of Example 4 using one-stick Model for the Superstructure .....	58
5.1	Unreduced Column Forces in Design Example 2 .....	59
5.2	Unreduced Bearing Forces in Design Example 2 .....	60
5.3	Unreduced Cross Frame Forces in Design Example 2 .....	61
5.4	Unreduced Column Forces in Design Example 2-M .....	62
5.5	Unreduced Bearing Forces in Design Example 2-M .....	63
5.6	Unreduced Cross Frame Forces in Design Example 2-M .....	64
5.7	Displacements of Design Example 2 .....	65
5.8	Displacements of Design Example 2-M .....	66
5.9	Unreduced Column Forces in Design Example 3 .....	68
5.10	Unreduced Bearing Forces in Design Example 3 .....	69
5.11	Unreduced Cross Frame Forces in Design Example 3 .....	70
5.12	Displacements of Design Example 3 .....	71
5.13	Unreduced Column Forces in Design Example 3-M .....	72
5.14	Unreduced Bearing Forces in Design Example 3-M .....	73
5.15	Unreduced Cross Frame Forces in Design Example 3-M .....	74
5.16	Displacements of Design Example 3-M .....	75
5.17	Unreduced Column Forces in Design Example 4 .....	76
5.18	Unreduced Bearing Forces in Design Example 4 .....	77
5.19	Unreduced Cross Frame Forces in Design Example 4 .....	78
5.20	Displacements of Design Example 4 .....	79

## List of Figures

2.1	Example 1 Elevation.....	80
2.2	Bridge Cross Section of Example 1 .....	81
2.3	Example 1 Girder Layout .....	82
2.4	Elevation of Example 2 .....	83
2.5	Example 2 Girder Layout .....	84
2.6	Example 2 Cross Section at Bent .....	85
2.7	Details of Cross Frames.....	86
2.8	Girder Layout of Example 2-M.....	87
2.9	Elevation of Example 3 .....	88
2.10	Example 3 Cross Section at Bent Location.....	89
2.11	Girder Layout of Example 3.....	90
2.12	Example 3-M Cross Section at Bent Location.....	91
2.13	Elevation of Example 4 .....	92
2.14	Example 4 Framing System.....	93
2.15	Example 4 Cross Section at Mid-Span.....	94
2.16	Example 4 Cross Section at Bent Location.....	95
3.1	Detailed Finite Element Model of the Design Example 2.....	96
3.2	Simplified Finite Element Model of the Design Example 2 .....	97
3.3	Detailed Finite Element Model of the Design Example 2M .....	98
3.4	Detailed Finite Element Model of the Design Example 3.....	99
3.5	Simplified Finite Element Model of the Design Example 4 .....	100
4.1	Comparison of Mode Shapes of the Model 2 .....	101
4.2	Comparison of Mode Shapes of the Model 2M .....	102
4.3	Comparison of Mode Shapes of the Model 3 With Fixed Base.....	103
4.4	Comparison of Mode Shapes of the Model 3 With Pinned Base.....	104
4.5	Comparison of Mode Shapes of the Model 4 .....	105
6.1	Elevation View of End Cross Frame of Example 1 .....	106
6.2	Elevation View of Intermediate Cross Frame of Example 2.....	107
6.3	Connection Details between Diagonal Members and Top Strut .....	108
6.4	Connection Details between Diagonal Members ant Bottom Strut .....	109
6.5	Connection Details between Top Strut Members at Bent Cross Frame .....	110

# Part I

## AASHTO LRFD SEISMIC DESIGN OF HIGHWAY BRIDGES

---

by  
Ahmad M. Itani, Ph.D., P.E.  
University of Nevada, Reno

---

### Introduction

The seismic specifications for highway bridges went through changes as a result of damaging earthquakes. In 1956, bridge specifications included a static load approach for the design of bridges in seismic zones. This approach was mainly based on the Structural Engineering Association of California (SEAOC) Blue Book, which specifies a percentage of the dead load and use it as lateral loads to account for seismic forces [1]. Recognizing the shortcomings of static forces in accounting for dynamic seismic forces, the California Department of Transportation (Caltrans), in 1968, included the effect of dynamic characteristics of bridges in the seismic design process [2]. Elastic dynamic analyses were performed during the seismic design of California bridges. However, after the significant highway damage during the 1971 San Fernando earthquake, Caltrans adopted in 1973, new seismic design criteria that included:

- Seismicity
- Soil Effect
- Dynamic Characteristics
- Ductility/Risk Reduction Factor

In addition, rigorous reinforcement detail provisions for reinforced concrete bridge columns were incorporated in Caltrans Bridge Design Specifications. In 1975, AASHTO adopted Caltrans criteria for the seismic design of highway bridges. However, recognizing the need that the criteria should be national and should include the effect of



earthquakes that are different from California earthquakes, the Federal Highway Administration (FHWA) commissioned the Applied Technology Council (ATC) in 1978 to develop seismic design guidelines for highway bridges [3]. The guidelines were comprehensive in nature and they embodied several new concepts that were significant departure from existing procedures at that time. Although the guidelines specified ultimate earthquake loads, they utilized an elastic modal analysis procedure in conjunction with a force reduction factor to account for the non-linearity of the response during strong earthquakes. AASHTO adopted the ATC-6 document as “Guide Specifications” for the seismic design of highway bridges.

Another milestone in the seismic design of highway bridges came after the 1989 Loma Prieta earthquake. The Collapse of Cypress Viaduct and the damage to the San Francisco-Oakland Bay Bridge proved the continued vulnerability of highway bridges and the need to modify the seismic specifications. This earthquake also exposed the impact of highway bridges on the national economy and the necessity of having such important structures serviceable after such events. Following the Loma Prieta earthquake, Caltrans increased the seismic bridge research more than twenty folds [4]. Large-scale bridge components were tested under static and dynamic loads to study and improve their seismic performance. In addition, Caltrans commissioned the ATC to study its Bridge Design Specifications and revise it to include latest information in ground motion and seismic design. A new document was prepared, “Improved Seismic Design Criteria for California Bridges: Provisional Recommendation” [5]. This document contains the state-of-art information about seismic design of concrete bridges. In addition, this document can be regarded as a benchmark in bridge seismic design since it placed an emphasis on the deformation capacity of bridge components during cyclic loading.

After the Loma Prieta earthquake, AASHTO adopted the 1983 Guide Specifications of seismic design as a part of the Standard Specification [6] and made it mandatory to include seismic effect during the design process. In 1994 AASHTO published the 1<sup>st</sup> Edition of the “AASHTO LRFD Bridge Design Specifications,” [7] which the seismic effect is an integral part of the bridge design process. The 2<sup>nd</sup> Edition of the AASHTO LRFD [8] is essentially the same as the 1<sup>st</sup> Edition in terms of seismic effects with minor modification.

## **AASHTO LRFD Seismic Analysis and Design**

The AASHTO LRFD Specifications similar to the previous AASHTO Seismic Specifications establish analysis, design, and construction provisions for bridges to minimize their susceptibility to damage from earthquakes. The design earthquake motions and forces specified in the LRFD AASHTO are based on low probability of their being exceeded during the normal life of the bridge. Bridges and their components that are designed according to the LRFD Specifications may suffer damage, but should have low probability of collapse due to seismically induced ground shaking.

The basic concept of the AASHTO seismic design is life safety. However, the specifications also recognized the importance of the functionality of essential bridges after major events. The principles of the AASHTO LRFD that were used to develop the seismic provisions are still based on the three items that appeared in the ATC-6 document. These principles are:

1. Small to moderate earthquakes should be resisted within the elastic range of the structural components without significant damage.
2. Realistic ground motion intensities and forces are used in the design procedures.
3. Exposure to shaking from large earthquakes should not cause collapse of all or part of the bridge. Where possible damage that does occur should be readily detectable and accessible for inspection and repair.

The design equation of AASHTO LRFD is:

$$\sum \eta_i \gamma_i Q_i \leq \phi R_n$$

- $\eta_i$  = load modifier
- $\gamma_i$  = load factor
- $Q_i$  = force effect
- $\phi_i$  = resistance factor

- $R_n$  = nominal resistance

In seismic design the right-hand side of the above equation represents the seismic demand while the left-hand side represents the ultimate section capacity. The seismic loads, and seismic design forces are presented in Section 3 while the seismic analysis methods are presented in Section 4 of the AASHTO LRFD Specifications.

### **AASHTO Seismic Loads**

The determination of appropriate seismic design loads, although complex in reality has been significantly simplified for code application. The dynamic seismic force is equal to:

$$F = \text{mass} \times \text{acceleration}$$

If the acceleration is expressed as a fraction of the acceleration due to gravity, therefore, the seismic force is equal to:

$$F = C W$$

where  $C$  is an acceleration coefficient and  $W$  is the equivalent weight which is a function of the actual weight and bridge configuration. In AASHTO, this coefficient is identified as the elastic seismic response coefficient:

$$C_{sm} = \frac{1.2 A S}{T_m^{2/3}} \leq 2.5 A$$

where:

$T_m$  = period of vibration of the  $m^{\text{th}}$  mode

$A$  = Acceleration coefficient and  $S$  = site coefficient

The acceleration coefficient “A” are based on a uniform risk model of seismic hazard. The probability that the coefficient will not be exceeded at a given location during a 50-year period is estimated to be about 90 percent. The U.S. Geological Survey prepared the contour maps for different areas of the United States. The numbers given on contour maps are expressed in percent. The design earthquake that is used to develop these maps is defined as an earthquake with a return period of 475 years. Figures 1.1, 1.2 and 1.3 show the acceleration coefficient for the United States.

The coefficient “S” is a site coefficient, which accounts for the effect of the soil on the ground motion. Four types of soil profiles are included in the specifications to represent the different subsurface conditions that may exist at the site of the bridge. The subsurface conditions were selected on the basis of a statistical study of spectral shapes developed on such soils close to seismic source zones in previous earthquakes. Figure 1.4 shows the seismic response coefficient for various soil profiles, normalized with respect to Acceleration Coefficient “A”.

Therefore, the earthquake loads, which are horizontal forces applied at the superstructure level, are equal to:

$$EQ = \frac{C_{sm} W^*}{R}$$

where

W\* is the equivalent weight of the bridge that is automatically included in the seismic analysis based on either single-mode or multi-mode methods and R is the Response Modification Factor.

The LRFD Specifications recognize that it is uneconomical to design a bridge to resist large earthquakes elastically. Columns were chosen as the weak link in the structural load path. Thus, bridge columns are designed to deform inelastically during design level earthquakes. This was established by dividing the elastic seismic force effects by the appropriate R-factor. Connections and foundations are designed to accommodate the design ground forces with little if any damage.

The rationale used in development of the R factors for columns, piers and pile bents was based on considerations of redundancy and ductility provided by the various supports. New additional factor was added in the specifications based on a new “Importance Category” criterion. Three types of bridge are defined in the specifications:

- Critical
- Essential
- Other

The R-factors for the “Other” bridges represent the factors that used to be in the Standard Specifications. The “Importance Category” for bridge is primarily based on the Social/Survival and Security/Defense requirements. Essential bridges are generally those that should, as a minimum, be open to emergency vehicles and for security/defense purposes immediately after the design earthquake. Critical bridges must remain open to all traffic after the design earthquake and be useable by emergency vehicles after a large earthquake which has a 2500 year return period.

The wall type pier was judged to have minimal ductility capacity and redundancy in its strong direction and was assigned an R-factor of 2. A multiple column bent with well-detailed column was judged to have good ductility capacity and redundancy and was assigned the highest value of 5. R-factors of 1 and 0.8 were assigned to connections to maintain the overall integrity of the bridge structures at these important locations. Tables 1.1 and 1.2 show the AASHTO R factors for bridge substructure. It is interesting to note here that the steel columns were lumped with composite columns in same row and were given the same value of reinforced concrete columns.

## **AASHTO Seismic Design Forces**

The seismic design of bridge system and components can be divided into two main categories:

- Restrained movement
- Free movement

If restrained movement between the bridge superstructure and substructure is required, then that bridge component should be designed for the code specified seismic forces. On the other hand, if movement was allowed to occur, then ample seat width should be provided to allow the movement without any loss of support.

The seismic design forces are specified according to the different seismic zones except for single-span bridges where the minimum design connection force in the restrained direction is equal to the product of the site coefficient, the acceleration coefficient and the tributary permanent load.

For bridges on sites in Zone 1 where the acceleration coefficient is less than 0.025 and the soil profile is either Type I or Type II, the horizontal design connection force in the restrained direction is equal to 0.1 times the vertical reaction due to the permanent dead load. For all other sites in Zone 1, the seismic force is equal to 0.2 times the vertical reaction due to the tributary dead load.

For bridge in Seismic Zone 2, the seismic forces are determined based on dynamic analysis. Therefore, the seismic force is determined by dividing the elastic seismic forces by the response modification factor.

For bridges in Seismic Zone 3 and 4, the specifications start to lean toward capacity design based on the ultimate column strength. The plastic flexural capacity of the column, in most cases, is less than the seismic design forces. Therefore, the superstructure and substructure components and their connections are designed to resist a lateral shear force from the column determined from the inelastic flexural resistance of the column. The ultimate capacity of concrete and steel sections is 1.3 and 1.25 time the nominal resistance, respectively.

## **AASHTO Analysis for Earthquake Loads**

The specifications specify four analysis methods that can be used to determine the seismic forces for regular bridges. Regularity of the bridge is a function number of the spans and the distribution of weight and stiffness. Regular bridges have less than seven spans, no abrupt or unusual changes in weight, stiffness, or geometry; and no large change in these parameters from span to span. The selection of the analysis method depends on the Seismic Zone, Importance category and bridge regularity. The four analysis methods are:

1. Uniform Load Elastic Method: UL
2. Single-Mode Elastic Method: SM
3. Multi-Mode Elastic Method: MM
4. Time History Method: TH

With the advances with computer technology, the most common method is the Multi-Mode spectral analysis using Space Frame Element models (stick) or Finite Element models. The minimum number of modes that are included in the analysis is equal to three times the number of the span. The member forces and displacements are determined by combining the response quantities from the individual modes by the complete Quadratic Combination (CQC) method.

This study investigated the use of the two modeling techniques for modern steel bridges and identified the details of these methods using the Four AISI LRFD design examples.

## **Seismic Lateral Load Distribution**

The 2<sup>nd</sup> Edition of the LRFD Specifications included for the first time a new section about the seismic lateral load distribution that discusses the seismic load path. The focus for these criteria is steel bridges since they normally do not have monolithic connections as the structural concrete box girder bridges. The specifications specify that a clear and a straightforward load path from the superstructure to the substructure should exist. All elements that lie in the load path are primary seismic member and should be designed to stay elastic during severe ground motion. Diaphragms and cross-frames, lateral bracing and bearings should be part of the seismic load path. Even though the specifications

admit that if these members were designed to respond in a ductile manner or allow some movements, the damage will be limited. However, the specifications require that the cross frames at end diaphragms to stay elastic during earthquakes. Section 3 of the specification presents two flow charts that identify the seismic analysis and design step-by-step. Figures 1.5 and 1.6 shows these flow charts.



## Part II

# AISI LRFD Design Examples of Steel Highway Bridges

---

by  
Ahmad M. Itani, Ph.D., P.E.  
University of Nevada, Reno

---

### Introduction

In 1996 AISI published Vol. II, Chap. 1B of the Highway Structures, Design Handbook, “Four LRFD Design Examples of Steel Highway Bridges” [9]. These design examples covered the gravity design of the superstructure according to the AASHTO LRFD Bridge Specifications. The four examples consisted of:

1. Simple-Span Composite I Girder
2. Two-Span Continuous Composite I Girder
3. Three-Span Continuous Composite I Girder
4. Three-Span Continuous Composite Box Girder

The main purpose of this report is to perform seismic design of the above design examples. Substructures that include single column bent, multi column bents were added to the design example. The following sections will summarize the structural systems of the design examples.

### Description of AISI LRFD Example 1

This design example represents a simple-span composite I girder with a span of 161'-0". The bridge cross section consists of four girders spaced at 13'-0" centers with 4'-3" deck overhang and 44'-0" roadway width. The concrete deck is 10" thick including a 1/2" integral wearing surface. Figure 2.1 shows the elevation of the bridge while Figure 2.2 shows a typical cross section. Each abutment is skewed a positive 35°. Figure 2.3 shows the plan of the bridge that consists six interior cross frames and two exterior cross frames

over the abutments. Table 2.1 presents the dimensions of the of the plate girder along the length of the bridge.

### **Description of AISI LRFD Design Example 2**

Example 2 represents a tangent two-span composite I girder with spans 90'-0"-90'-0". The bridge cross section consists of four girders spaced at 10'-0" centers with 3'-6" overhangs and 34'-0" roadway width. The concrete deck is 8½" thick with ½" integral wearing surface. A single column with a dropped bent cap was added to the bridge. The cap has a 4'-0" depth and 5'-0" width. The column height is 25'-0". Figure 2.4 shows the elevation of the bridge, while figures 2.5 and 2.6 shows the plan of the bridge and the cross section at the bent location. The bridge has two interior cross frame along each span as shown in Figure 2.5. The details of the abutment and bent cross frames are shown in Figure 2.7. Table 2.2 presents the dimensions of the plate girder along the length of the bridge.

### **Description of AISI LRFD Design Example 2-M**

Example 2-M is identical with Example with the abutments and the bent skewed at 35°. The purpose of this example is to study the skew effect on the dynamic behavior of the bridge. All dimensions of the bridge stayed the same as Example 2. The interior cross frames were kept normal to the girders while abutment and bent cross frame were skewed. Figure 2.8 shows the plan of the bridge.

### **Description of AISI LRFD Design Example 3**

Example 3 represents a tangent three-span continuous composite I girder with spans of 140'-0", 175'-0", and 140'-0". Figure 2.9 shows the elevation of the bridge. The bridge cross section consists of four girders spaced at 12'-0" centers with 3'-6" overhangs and 40'-0" roadway width. A two-column bent was added to the bridge with a dropped cap. The columns were fixed at the base. The diameter of the column is 4'-0" while the bent cap has 4'-0" depth and 5'-0" width. Figures 2.10 and 2.11 show the cross section of the bridge at a bent location and the plan of the bridge, respectively. Seven interior cross frames were used in each span as shown in Figure 2.11. Table 2.3 presents the dimensions of the plate girder along the length of the bridge.

### **Description of AISI LRFD Design Example 3-M**

Example 3-M is identical of Example 3 with an integral bent cap. With the use of an integral cap the columns could be pinned at the base. The purpose of this example is to study the dynamic difference between the two examples. Figure 2.12 shows the cross section of the bridge at a bent location.

### **Description of AISI LRFD Design Example 4**

Example 4 presents a three-span continuous composite box girder with spans of 190'-0", 236'-0", and 190'-0". The bridge consists of two trapezoidal box sections spaced at 11'-0" on centers. The substructure consisted of two-column bent with a dropped cap. Figure 2.13 shows the elevation of the bridge. Figure 2.14 shows the plan and the framing system of the bridge, while Figures 2.15 and 2.16 show the cross section of the superstructure at mid-span and the cross section of the bridge at the bent location.

## Part III

# Mathematical Modeling of Steel Highway Bridge for Seismic Analysis

---

by

Hassan Sedarat, Ph.D., P.E.  
SC Solutions, Inc.

Ahmad M. Itani, Ph.D., P.E.  
University of Nevada, Reno

---

### Introduction

Mathematical modeling of bridges is an important part of any seismic evaluation and earthquake resistant design. The basic mathematical model that captures the dynamic behavior of the bridge should include the effect of mass, stiffness, strength, and damping. Generally, two types of mathematical models are used to determine the dynamic response of a bridge:

1. Space Frame Element Models

It is a simplified model of a bridge using stick modeling with finite element beam-columns.

2. Space Finite Element Models

It is a detailed model of a bridge using finite element solids and shells in combination with beam-column elements.

### Finite Element Modeling of Steel Highway Bridges

Key steps in any structural analysis starts with studying the real structure. The engineer should make judgments on modeling idealizations and the purpose of the required results. Nodes and elements define the mathematical model. The elements can be beam, shell, solid elements or other types of elements that suite the idealization of the real structure. In this stage the geometry of the model is built and the structure is ready for analysis, which depends on the computational strategy and available computer programs. The analysis can be linear elastic nonlinear, static or dynamic. Once the analysis is complete,

the results will be extracted for the mathematical model. The last step is to interpret these results for the real structure using engineering judgement. At the analysis part, once the unknown displacement degrees of freedom are selected, the compatibility equations will be used to obtain deformations at element level. Then action-deformation relationship will provide internal forces or member forces from element deformations. The equilibrium will be satisfied based on the applied load in the last step. Each of these three steps can be either linear or nonlinear. Nonlinearity in compatibility equations and equilibrium equations is often referred to as geometric nonlinearity, whereas nonlinear action-deformation relationship is often referred to as material nonlinearity.

### **Space Frame Element Modeling**

A bridge structure may be modeled in a simplified or in a very detailed way. In a detailed finite element modeling of the bridge, the superstructure deck is modeled explicitly with solid elements, the plate girders may be modeled with shell elements that are supporting the deck. On the other hand the simplified modeling of the bridge is based on idealized structural elements that are connected to represent the general geometry of the bridge. Each element in the frame has the equivalent moment of inertia. These elements are connected by nodal points to realistically represent the geometry, stiffness, and strength of the bridge. The nodes have six degrees of freedom, three translational and three rotational. The structural mass is usually lumped with a minimum of three translational inertia terms. The mass includes the deck, and the supporting girders, which are usually the largest mass in the bridge. All structural components such as bent caps, columns, and superstructure deck are included in the model. The mass distribution in the stick model is determined by the refinement in the finite element mesh of individual components. The ATC-6 document recommends that the superstructure should be modeled as a series of beam elements with nodes at the span quarter points in addition to the joints of each span. The ATC-32 document recommends that five elements per span are sufficient for a good representation of the first three vibration modes of a span. If the periods of the higher modes of a span are within the acceleration-control region of the earthquake response spectrum, it is necessary to include more elements to capture higher

modes. In general, if the contribution of the  $i^{\text{th}}$  mode need to be included in the analysis, the span should be modeled by  $2i-1$  elements over the span length.

The columns are also modeled as space frame elements. The masses of columns have a relatively small contribution to the total mass of the bridge, where most of it is resulted from the superstructure mass. The ATC-6 [3] recommends that for short stiff columns having length less than one-third of either adjacent span intermediate nodes along the length of the columns are not necessary. Long, flexible columns are modeled with intermediate nodes at the third points in addition to the joints at the column ends. Bent caps are normally very rigid in comparison with the rest of the bridge; therefore fewer elements are usually sufficient to capture the behavior of this rigid element. However, more elements are needed to represent the stiffness of the bent cap.

Damping for dynamic analysis using the response spectrum method must be specified by modal damping ratio. Viscous damping equal to 5% combined with the effective stiffness is normally used for the analysis of highway bridges.

Figure 3.1 shows a schematic view of a space frame bridge model. The mass was lumped on the nodes and joints in the superstructure and the substructure. The number of the modes that should be included in the analysis depends on the value of effective modal mass that contributes in these modes. The analysis should capture at least 90% of the effective modal mass.

### **Three-Dimensional Frame Modeling of the AISI Examples**

The design examples 2, 2M, 3, 3M, and 4 were modeled with the general-purpose computer program ADINA [10]. The mode shapes and frequencies were extracted followed by a set of response spectrum analysis for each bridge.

The design examples were modeled in two ways. The first approach was to model each bridge with a detailed finite element modeling. In this model the plate girders were modeled with shell elements, whereas the concrete slab were modeled with solid

elements. Columns and braces were modeled with beam elements. The second approach was to represent each bridge with simplified stick models. The superstructure was modeled with beam element. The transformed sectional properties of the composite concrete-girder section were calculated and used in the simplified models.

### **Mathematical Models of AISI Design Examples**

The longitudinal structural system used in the design examples consisted of a constrained movement at the bent cap location and free movement over the two abutments. However, for the design example 3-M, where the superstructure is integral with the bent cap, the model utilized a rigid joint between the superstructure and the substructure. The transverse structural system consisted of constrained movement at the bent cap location and also at the two abutments.

In the detailed 3-D finite element models of the design examples, the plate girders were modeled with linear elastic four-node shell elements. The concrete slab was modeled with linear elastic 20-node solid elements. The bent cap, braces, and columns were all modeled with linear elastic beam elements. For the nonlinear pushover analyses and nonlinear dynamic analyses, the columns and braces were modeled with plastic multi-linear moment-curvature elements.

In the simplified models of the design examples, the superstructure and the substructure were modeled as beam element. The superstructure was connected to four locations at the bent cap representing the bearing of the superstructure.

Figure 3.1 shows the view of the 3-D model and a cross section at the abutment location of Example 2. Figure 3.2 shows the view of the simplified model for that example. This is a two two-span continuous composite I girder with spans of 90 ft. The concrete slab is 8.5 inch thick including a ½inch integral wearing surface.

The modeling of Example 2-M was identical to Example 2 with the exception of the skewed abutment and cross frames above the bent cap and the abutments. Figure 3.3 shows a view of the detailed finite element model of this bridge. While a separate detailed finite element model of the design example 2 was developed when the abutment was skewed, only one simplified model was used because the simplified model cannot capture the effect of skewed abutment.

Modeling of Example 3 was identical to Example 2. Figures 3.4 and 3.5 show the view of the detailed 3-D finite element model and the simplified model respectively. This is a three-span continuous composite I girder with spans of 141 ft, 174 ft, and 141 ft. The concrete slab is 9.8 inch thick including a 0.6 inch integral wearing surface.

The detailed 3-D finite element model of Example 4 is shown in Figure 3.6. The simplified model utilized two beam elements to model each steel box individually and combined together as shown in Figure 3.8. This is a three-span continuous composite box girder with spans of 190 ft, 236 ft, and 190 ft. The concrete slab is 9.6-inch in thickness including a ½inch integral wearing surface. The bridge cross section consists of two trapezoidal box sections with top lateral bracing.



## Part IV

# Dynamic Characteristics of the AISI Design Examples

---

Hassan Sedarat, Ph.D., P.E.  
SC Solutions, Inc.

by  
Ahmad M. Itani, Ph.D., P.E.  
University of Nevada, Reno

---

### Introduction

The objective of this chapter is to determine and compare the dynamic characteristics of the AISI Design Examples modeled with the detailed finite element method and the simplified procedure as discussed in Part III of this report.

### Dynamic Characteristic of the AISI Examples

Table 4.1 presents the results of the dynamic characteristics of the 3-D detailed finite element model of the design Example 2. As it can be seen from this table, thirty modes were included in the analysis to capture almost 90%, 80%, and 70% of the mass in the longitudinal, transverse and vertical directions, respectively. The first mode was a longitudinal mode with a fundamental period of 1.36 seconds, the 6<sup>th</sup> mode was a transverse mode with a fundamental period of 0.23 seconds, and the 5<sup>th</sup> mode was a vertical mode with a fundamental period of 0.29 seconds.

Table 4.2 presents the results of the dynamic characteristics of the simplified model of the design Example 2. As can be seen from this table, twenty modes were extracted to capture almost 99%, 89%, and 89% of the mass in the longitudinal, horizontal, and vertical direction, respectively. The first mode was a longitudinal mode with a fundamental period of 1.39 seconds, the third mode was a vertical mode with a fundamental period of 0.25 seconds, and the 4<sup>th</sup> mode was a transverse mode with a fundamental period of 0.2 seconds.

Comparing Tables 4.1 and 4.2 shows that the simplified model of the design example was capable of capturing the basic dynamic characteristics of the detailed 3-D finite element model. Figure 4.1 shows comparison between the transverse modes of the two models.

To understand the effect of the skewed abutment on the dynamic properties of Example 2, a 30° skew angle was added at the abutment and the bent. The results of the dynamic characteristics for Example 2M are presented in Table 4.3. As can be seen from this table, thirty mode shapes were extracted to capture 91%, 88%, and 78% of the mass in the longitudinal, transverse, and vertical directions. Similar to Example 2, the first mode was a longitudinal mode with a fundamental period of 1.35 seconds, the 5<sup>th</sup> mode was a vertical mode with a fundamental period of 0.29 seconds, and the 6<sup>th</sup> mode is a transverse mode with a fundamental period of 0.24 seconds.

From the comparison of the results of the Examples 2 and 2M, it is clear that the 30° skew did not alter the general dynamic characteristics. The mode shapes, mass participation factor and the fundamental periods were close in these two examples.

Table 4.4 summarizes the results of the dynamic characteristics of the detailed 3-D finite element model for the design Example 3. Thirty modes were extracted in the analysis to capture almost 99%, 96%, and 68% of the mass in the longitudinal, horizontal, and vertical direction, respectively. The first mode was a longitudinal mode with a fundamental period of 1.28 seconds, the third mode was a transverse mode with a fundamental period of 0.55 seconds, and the 7<sup>th</sup> mode was a vertical mode with a fundamental period of 0.33 seconds.

Table 4.5 presents the results of the dynamic characteristics of the simplified model of the design Example 3. As can be seen from this table, twenty modes were extracted to capture almost 99%, 91%, and 85% of the mass in the longitudinal, horizontal, and vertical direction, respectively. The first mode was a longitudinal mode with a fundamental period of 1.23 seconds, the third mode was a transverse mode with a

fundamental period of 0.43 seconds, and the 5<sup>th</sup> mode was a vertical mode with a fundamental period of 0.28 seconds.

From the comparison of Tables 4.4 and 4.5, it is obvious that the simplified model was capable of capturing the basic dynamic characteristics that were obtained from the detailed 3-D finite element model. Figure 4.2 shows comparison between the transverse modes of the two models.

To understand the effect of integral bent cap and framing the superstructure and the substructure by rigid joint, Example 3 model was modified accordingly to represent the structural detailing properly. The base of the columns was changes to pinned conditions since fixity is not needed in integral bridges. Table 4.6 presents the results of the dynamic characteristics of the detailed 3-D finite element model for Example 3M. As can be seen from this table, thirty modes were included in the analysis to capture almost 99%, 96%, and 67% of the mass in the longitudinal, horizontal, and vertical direction, respectively. The first mode was a longitudinal mode with a fundamental period of 1.29 seconds, the 2<sup>nd</sup> mode was a transverse mode with a fundamental period of 0.8 seconds, and the 6<sup>th</sup> mode was a vertical mode with a fundamental period of 0.33 seconds.

Table 4.7 presents the results of the dynamic characteristics of the simplified model of the design Example 3M. As can be seen from this table, twenty modes were included in the analysis to capture almost 99%, 92%, and 93% of the mass in the longitudinal, horizontal, and vertical direction, respectively. The first mode was a longitudinal mode with a fundamental period of 1.21 seconds, the 2<sup>nd</sup> mode was a vertical mode with a fundamental period of 0.7 seconds, and the 5<sup>th</sup> mode was a transverse mode with a fundamental period of 0.27 seconds.

From the comparison of Tables 4.6 and 4.7, it becomes clear that the simplified model was capable of capturing the basic dynamic characteristics that were obtained from the detailed 3-D finite element model. Figure 4.3 shows comparison between the transverse modes of the two models.

The results of examples 3 and 3M show that the longitudinal mode is almost the same, however, the transverse mode in Example 3M has a higher period than Example 3. This indicates the integral bridge is more flexible than the dropped cap bridge in the transverse direction, which will put more demands on the columns during seismic events.

Table 4.8 presents the results of the dynamic characteristics of the detailed 3-D finite element model of the design Example 4. As can be seen from this table, twenty modes were included in the analysis to capture almost 98%, 96%, and 71% of the mass in the longitudinal, horizontal, and vertical direction, respectively. The first mode was a longitudinal mode with a fundamental period of 1.5 seconds, the 3<sup>rd</sup> mode was a transverse mode with a fundamental period of 1.1 seconds, and the 5<sup>th</sup> mode was a vertical mode with a fundamental period of 0.58 seconds.

Tables 4.9 and 4.10 present the results of the dynamic characteristics of the two simplified Models (one-stick and two-stick) for Example 4. As can be seen from the two tables, twenty modes were included in the analysis to capture most of the mass. The two tables show that the superstructure could be modeled with one beam element without any significant loss of the dynamic properties. However, it must be emphasized that in a curved bridge where the effects of torsion can become important, the two-stick model is a better representation of the bridge. Figure 4.2 shows a comparison between the transverse modes of the three models.

It can be concluded that the dynamic characteristics of straight steel box girder bridges can be captured by the simplified modeling procedure.

## Part V

# Seismic Analysis of the AISI Design Examples

---

Hassan Sedarat, Ph.D., P.E.  
SC Solutions, Inc.

by

Ahmad M. Itani, Ph.D., P.E.  
University of Nevada, Reno

---

## Introduction

The four bridge examples were assumed to be located in regions of high and low seismicity to determine the effect of seismic forces on the overall bridge design process.

Series of linear elastic response spectrum analyses were performed for the detailed and simplified models of each bridge, the results of which are summarized in this Chapter. The design spectra for AASHTO soil type S2 and S3 were defined as discussed for each example. Once the mode shapes and frequencies were extracted they need to be combined, using a modal combination method, to obtain the dynamic response of the structure. The Complete Quadratic Combination (CQC) procedure was used in these analyses since the modes were closely spaced.

The spatial combination of the responses is also another important task in a response spectrum analysis. In some cases a SRSS spatial combination of the results is acceptable by the design criteria. In this study, however, the spatial combination was based on the 100% and 30% rule as prescribed in AASHTO.

## Seismic Loads

The AASHTO earthquake loads, which are horizontal forces applied at the superstructure level, are equal to:

$$EQ = \frac{C_{sm} W^*}{R}$$

where:

$C_{sm}$  is AASHTO seismic coefficient

$W^*$  is the equivalent weight of the bridge that is automatically included in the seismic analysis based on the multi-mode method

R is the Response Modification Factor

The seismic coefficient factor is given by:

$$C_{sm} = \frac{1.2 A S}{T_m^{2/3}} \leq 2.5 A$$

where:

A = Acceleration coefficient

S = Site coefficient

$T_m$  = Period of vibration of the  $m^{\text{th}}$  mode

The Acceleration Coefficient A for the design examples were selected as:

- Example 1 is located between the 0.1 and 0.2 contours and has  $A=0.15$
- Example 2 is located within the 0.4 contour and has  $A=0.4$
- Example 3 is located within the 0.2 contour and has  $A=0.2$
- Example 4 is located within the 0.1 contour and has  $A=0.1$

Therefore based on the assumed acceleration coefficients the design examples were located in the following Seismic Zones:

- Example 1 is located in Seismic Zone 2
- Example 2 is located in Seismic Zone 4
- Example 3 is located in Seismic Zone 3
- Example 4 is located in Seismic Zone 1

The Site Coefficient  $S$  for the design examples were selected as:

- Example 1 is on a Soil Profile III and has  $S=1.5$
- Example 2 is on Soil Profile III and has  $S=1.5$
- Example 3 is on Soil Profile II and has  $S=1.2$
- Example 4 is on Soil Profile II and has  $S=1.2$

All the design examples were classified as Essential Bridges, which they should as a minimum be open to the emergency vehicles and for security/defense purposes immediately after the design earthquake. Therefore, based on this the Response Modification Factors for the substructure and their connections of the design examples were:

- Example 1:  $R_{\text{substructure}} = \text{N/A}$ ,  $R_{\text{Super-to-Abut}} = 0.8$ , and  $R_{\text{Super-to-Bent}} = \text{N/A}$  (Single Span)
- Example 2:  $R_{\text{substructure}} = 2$ ,  $R_{\text{Super-to-Abut}} = 0.8$ , and  $R_{\text{Super-to-Bent}} = 1$  (Single-Column Bent)
- Example 3:  $R_{\text{substructure}} = 3.5$ ,  $R_{\text{Super-to-Abut}} = 0.8$ , and  $R_{\text{Super-to-Bent}} = 1$  (Two-Column Bent)
- Example 4:  $R_{\text{substructure}} = 3.5$ ,  $R_{\text{Super-to-Abut}} = 0.8$ , and  $R_{\text{Super-to-Bent}} = 1$  (Two-Column Bent)

### **Analysis for Earthquake Loads**

Based on the AASHTO Specifications of minimum design requirements for seismic effect:

- Example 1: No Seismic Analysis Required
- Example 2: Multimode Elastic Method Required
- Example 3: Multimode Elastic Method Required
- Example 4: No Seismic Analysis Required

The results of the seismic analysis are presented in terms of unreduced seismic forces on columns, bearings, cross frames, longitudinal and transverse displacements at bents/abutments.

### **Seismic Analysis of Design Example 2 and 2M**

Two detailed finite element models of this bridge were analyzed using response spectra method. In one case, the abutments were considered to be straight (Example 2), whereas in the other skew abutments were taken into consideration (Example 2M). The third model of this bridge was a simplified stick model. The maximum forces of columns, and bearings for Example 2 and Example 2M were compared with those of the stick model in Tables 5.1 and 5.2. Table 5.3 presented the forces in the cross frames.

The maximum forces of columns, bearings for Example 2M were compared with those of the stick model in Tables 5.4 and 5.5. Table 5.6 presented the maximum forces in the cross frames. The seismic displacements for examples 2 and 2M are presented in tables 5.7 and 5.8, respectively.

### **Seismic Analysis of Design Examples 3 and 3M**

Two detailed finite element models of Example 3 and Example 3M were analyzed using response spectra method. The maximum forces of columns, and bearings for Example 3 were compared with those of the stick model in tables 5.9 and 5.10. Table 5.11 presented the forces in the cross frames. Table 5.12 presented the seismic displacements.

The maximum forces of columns, bearings for Example 3M were compared with those of the stick model in tables 5.13 and 5.14. Tables 5.15 and 5.16 presented the maximum cross frame forces and the seismic displacements.



## **Seismic Analysis of Design Example 4**

According to AASHTO Specification, this design example does not require seismic analysis since it is in Seismic Zone 1. However, it was decided to perform multimode elastic analyses on this example to compare between the three mathematical models and to determine the cross frame forces in the steel box girder. A detailed finite element model of this bridge was analyzed using response spectra method. Two stick models were developed for this design example as discussed in Part IV. In one case the entire superstructure was modeled with one stick, whereas in the other each deck was modeled with one stick and they were connected with transverse beams. The maximum forces of columns, and bearings were compared with those of the one- and two-stick models in Tables 5.17 and 5.18. Tables 5.19 and 5.20 presented forces in the cross braces and the seismic displacements.

## Part VI

# Seismic Design of the AISI Design Examples

---

by  
Ahmad M. Itani, Ph.D., P.E.  
University of Nevada, Reno

---

### Introduction

This chapter discusses the seismic design of two AISI Design Examples. As mentioned earlier, the current AASHTO LRFD Specifications do not allow inelasticity to occur in the superstructure, therefore the components of the superstructure were designed to stay elastic. Thus, the inelasticity is limited to the reinforced concrete bent columns. Therefore, two examples were selected to show the design of end cross frames at abutment location and intermediate cross frame at bent location. It is expected that current research that is conducted by Professors Itani and Buckle at the University of Nevada, Reno will shed some light about the seismic design of several type of bearings and the behavior of non-composite deck to plate girders. In addition, to the use of unbonded brace and other smart material as cross frame members. The outcome of these research projects will improve and refine the seismic design of modern steel bridges.

The AASHTO Specifications specify that the resistance factor,  $\phi$ , for the extreme event limit state is taken as 1 except for bolts. Bolted joints not protected by capacity design or fuses can be assumed to behave as bearing type connections at the extreme event limit state.

### Seismic Design of Single Span Bridges

For single span bridges regardless of the seismic zone, the minimum design connection force effect in the restrained direction between the superstructure and the substructure is not less than:

$$F_{EQ} = S A W^*$$

Where S is the site coefficient, A is the acceleration coefficient and W\* is the tributary permanent load.

If the bridge was allowed to move, ample seat width is required to prevent unseating of the superstructure. The seat width is specified to accommodate the empirical seat width, N specified:

$$N = (8 + 0.02L + 0.08H)(1 + 0.000125S^2)$$

Where N is the minimum support length measured normal to the centerline of bearing, L is the length of the bridge deck to the adjacent expansion joint or to the end of the bridge deck, H column height, and S is the skew of the support measured from the line normal to the span. Depending of the seismic zone, a percentage of the seat width can be used according to table 4.7.4.4-1 in the specifications.

### **Seismic Design of Multi-Span Bridges**

The seismic design forces of multi-span bridges depend on the seismic zone. These forces ranges from simply reduced seismic forces to forces based on inelastic hinging of the substructure using limit state analysis.

For bridges on sites in seismic Zone 1, the horizontal seismic force in the restrained direction is equal to 0.1 or 0.2 times the vertical reaction due to the tributary gravity load depending on the acceleration level and the soil type. For bridges is seismic Zone 2 the seismic design forces is determined by dividing the elastic seismic forces by the appropriate response modification factor, R. The seismic design forces for the foundation are based on the elastic seismic forces divided by half of the response modification factor. For seismic Zones 3 and 4, the seismic forces are calculated as outlined in seismic Zone 2 or by plastic hinging forces.

According to the AASHTO Specifications, the inelastic hinges shall be ascertained to form before any other failure due to overstress and instability in the structure and/or in the foundation. Inelastic hinging is only permitted at locations in columns where they can readily inspected and/or repaired. The superstructure and substructure components and their connections to columns are designed to resist a lateral shear force from the column determined from the inelastic flexural resistance of the column section. These shear forces, calculated on the basis of inelastic hinging, may be taken as the extreme seismic forces that the bridge is capable of developing.

### **Seismic Design of Example 1**

This design example illustrate the seismic design of a tangent simple-span composite span of 161'-0". This example illustrates the seismic analysis of a simple span bridge and the design of end cross frames. The bridge cross section consists of four girders spaced at 13'-0" centers with 4'-3" deck overhang and 44'-0" roadway width. The concrete deck is 10 in. in thickness including a ½in. integral wearing surface. Each abutment is skewed a positive 35. The bridge is located on site in Seismic Zone 2 and with soil profile type III.

Specifications:	1998 AASHTO LRFD Bridge Design Specifications, Customary US Units, 2 <sup>nd</sup> Edition
Structural Steel:	AASHTO M270, Grade 50W (ASTM A709, Grade 50 W) uncoated weathering steel with $F_y=50$ ksi
Concrete:	$f_c=4.5$ ksi; modular ratio $n=8$
Slab Reinforcing Steel:	AASHTO M31, Grade 60 (ASTM A615, Grade 60) $F_y=60$ ksi

### **Lateral Load at End Cross Frame Bridge**

The end cross frames of the bridge should transmit the lateral forces that is caused by either wind or seismic forces. The seismic forces that are generated in the superstructure should be transmitted from the deck level to the bearings. For single span bridges

regardless of the seismic zone, the minimum design connection force effect in the restrained direction between the superstructure and the substructure is not less than:

$$F_{EQ} = S A W^*$$

Where S is the site coefficient, A is the acceleration coefficient and W\* is the tributary permanent load.

As specified in the AISI Design examples the dead load of one interior girder is equal to 2.118 k/ft for slab, concrete haunch, steel girders, cross frames and stay-in-place forms. The weight of the two barriers is equal to 1.01 k/ft while the future wearing surface is equal to 0.275 k/ft per girder. Therefore, the total dead load of the bridge (two interior girders and two exterior girders) equal to:

$$W_{DL} = 2.188 \times 3 + 1.01 + 0.275 \times 3 = 8.4 \text{ k/ft}$$

The total weight of the bridge is

$$W = 8.4 \text{ k/ft} \times 161 \text{ ft} = 1352 \text{ kips}$$

Therefore, W\* for one end of the bridge is equal to  $1352 / 2 = 676$  kips

The seismic load horizontal load at the end of the bridge is equal to:

$$F_{EQ} = A \times S \times W^* = 0.15 \times 1.5 \times 676 = 152 \text{ kips}$$

Since the abutment has a skew of 35°, therefore the applied seismic force on the cross frame is equal to  $152 / \cos 35^\circ = 186$  kips.

## Top Strut Design

The top strut of the end cross frame should be designed to resist the axial compression of the seismic forces in addition to the dead load according to the load combination Extreme Event I.

The dead loads acting on the top strut are computed as follows:

Slab (including integral wearing surface) =  $10 \times (14 + 12 + 7.5) / 144 \times 0.15 = 0.35$  k/ft

Concrete haunch =  $7.5 \times (14 + 12 + 7.5/2) / 144 \times 0.15 = 0.23$  k/ft

Steel girder = 0.03 k/ft

Therefore, the top strut should resist  $M_{DL} = 4.52$  k-ft and an axial load equal to 186 kips. In addition, this section should resist the combination of dead, live and wind loads as shown in the AISI design example 3 page 3-93.

Trying a section W10x30, which satisfy the minimum material thickness requirements and is adequate for connection details. The section should be checked for combined axial force and flexure. Since the section is compositely attached to the deck, therefore buckling is not expected to occur. Applying the beam column equations for this section it can shown that section would satisfy the requirements.

## Diagonal Member Design

The compressive force in the diagonal members is the result of the seismic load and the dead load reaction that is transmitted by the top strut. The unbraced length of the diagonal member is 96". The axial compressive load on the diagonal member from the seismic forces and the dead load is equal to 45 kips, assuming that each bay carries an equal portion of the total seismic force.

The member will be selected based on the limiting slenderness ratio for bracing members in the compression and minimum material thickness requirements. The unbraced length  $L$  will be conservatively computed as the distance between the working point.

Try a single angle 5 x 5x 1/2 with 1/2 in. thick gusset plate connection. The single angle will be subjected to combined flexure and axial force due to the eccentricity at the connection.

### Axial Compression

The axial compression capacity of the diagonal member is equal to  $P_r = \phi P_n$  where  $\phi$  is taken as 1.

$$P_n = A_g F_{cr}$$

$$\lambda_c = \frac{KL}{r\pi} \sqrt{\frac{F_y}{E}} = \frac{(0.5)(96)}{(0.983)\pi} \sqrt{\frac{50}{29000}} = 0.65 < 1.5$$

$$\frac{b}{t} = \frac{5}{0.5} = 10 < 0.446 \sqrt{\frac{E}{F_y}} = 10.74, \quad Q = 1$$

$$F_{cr} = (0.658^{\lambda_c^2}) F_y = 42 \text{ ksi}, \quad P_n = 200 \text{ kips}$$

### Flexure Capacity about Minor and Major Axes

The minor axis bending capacity about the Z-Z axis is calculated according to the AISC Specifications [11]:

$$M_{nz} = 1.25 M_y = 1.25 F_y \left( \frac{I_z}{C_z} \right) = 1.25 F_y \left( \frac{Ar_z^2}{C_z} \right) = (1.25)(50) \left( \frac{4.59}{2.02} \right) = 142 \text{ k-in.}$$

The major axis bending capacity about the W-W axis is calculated according to the AISC specifications:

$$M_{nw} = F_y \frac{I_w}{C_w} \left[ 1.25 - 1.49 \left( \frac{b/t}{0.382 \sqrt{\frac{E}{F_y}}} - 1 \right) \right] = 285 \text{ k-in}$$

Lateral torsional buckling capacity  $M_{ob}$  is computed as:

$$M_{ob} = C_b \frac{0.46Eb^2 t^2}{L} = 869 \text{ k-in}$$

$$M_y = F_y S_w = F_y \frac{I_w}{C_w} = 254 \text{ k-in}$$

Since  $M_{ob} > M_y$  the nominal flexural resistance for the limit state of lateral torsional buckling about the major axis is computed as:

$$M_{nw} = (1.58 - 0.83 \sqrt{\frac{M_y}{M_{ob}}}) M_y \leq 1.25 M_y$$

$$M_{nw} = (1.58 - 0.83(0.54)) M_y = 1.13 M_y = 287 \text{ k-in}$$

### Combined Flexure and Axial Compression

$$\frac{P_u}{P_r} = \frac{48}{199} = 0.24 > 0.2$$

$$\left[ \frac{P_u}{P_r} + \frac{8}{9} \left( \frac{M_{uw}}{\phi_b M_{nw}} + \frac{M_{uz}}{\phi_b M_{nz}} \right) \right] \leq 1.0$$

$M_{uz}$  and  $M_{uw}$  are the applied moments at the end connection. They are computed as:

$$M_{uz} = B_{1z} M_z = B_{1z} P_u e_z$$

$$M_{uw} = B_{1w} M_w = B_{1w} P_u e_w$$

Where:



$$B_1 = \frac{C_m}{1 - \frac{P_u}{P_{e1}}} \geq 1$$

$$C_m = 1, \quad P_{e1} = \frac{A_g F_y}{\lambda_c^2}$$

$$\lambda_{cz} = 0.65, \quad P_{e1z} = 562k, \quad B_{1z} = 1.09$$

$$\lambda_{cw} = 0.33, \quad P_{e1z} = 2244k, \quad B_{1w} = 1.02$$

$$M_{uz} = B_{1z} M_z = B_{1z} P_u e_z = (1.09)(45)(0.61) = 30 \text{ k-in}$$

$$M_{uw} = B_{1w} M_w = B_{1w} P_u e_w = (1.02)(45)(2.12) = 97.3 \text{ k-in}$$

Therefore, the interaction equation:

$$\left[ 0.24 + \frac{8}{9} \left( \frac{97.3}{285} + \frac{30}{142} \right) \right] = 0.73 \leq 1.0$$

## Bottom Strut Design

It is assumed that each end of the bridge of the bridge is fixed against transverse movement so that the force from the diagonals is transmitted directly to the bearings. Therefore, no force is induced in the bottom strut. Based on this a 5 x 5 x 1/2 single angle may be used for the bottom strut. Figure 6.1 shows the elevation view of end cross frame in one bay.

## Minimum Displacement Requirements

The bridge minimum seat width at the abutment can be computed by:

$$N = (8 + 0.02L + 0.08H) (1 + 0.000125S^2)$$

Where N is the minimum support length measured normal to the centerline of bearing, L is the bridge length, H is equal to 0.0 for single span bridges, S is the skew angle. The minimum seat width is equal to:

$$N = (8 + 0.02(163)(1 + 0.000125(35)^2)) = 13 \text{ in.}$$

## Seismic Design of Example 2

This design example illustrates the seismic design of a tangent two-span continuous I girder with spans of 90'-0"-90'-0". This seismic analysis for this example was conducted in Chapter V using the multimode elastic method. This example discusses the design process of cross frames over bent cap. The bridge cross section consists of four girders spaced at 10'-0" centers with 3'-6" deck overhang and 34'-0" roadway width. The concrete deck is 8½in. in thickness including a ½in. integral wearing surface. The bridge has a single column bent with a dropped cap. The column diameter is 5'-0" and its height is 25'-0". The bridge is located on site in Seismic Zone 4 and with soil profile type III.

Specifications:	1998 AASHTO LRFD Bridge Design Specifications, Customary US Units, 2 <sup>nd</sup> Edition
Structural Steel:	AASHTO M270, Grade 50W (ASTM A709, Grade 50 W) uncoated weathering steel with $F_y=50$ ksi
Concrete:	$f_c=4.5$ ksi; modular ratio $n=8$
Slab Reinforcing Steel:	AASHTO M31, Grade 60 (ASTM A615, Grade 60) $F_y=60$ ksi

## Lateral Load at Bent Cross Frame

The bent cross frame should be designed to transmit the lateral forces to the column. Since the bridge is located in Seismic zone 4, inelastic hinges shall be ascertained to form before any other failure due to overstress or instability in the structure. Therefore, according to the AASHTO Specifications, the superstructure and substructure and their connections to the columns shall be also designed to resist a lateral shear force from the

column determined from inelastic flexural resistance of the column. This shear force, calculated on the basis of elastic, may be taken as the extreme seismic forces that the bridge is capable of developing.

### Column Seismic Design

The unreduced seismic forces on the base of the single column bent determined by the seismic analysis were:

Case I	ML = 17,190 k-ft	MT=298 k-ft
Case II	ML = 5,157 k-ft	MT=993 k-ft

The R-factor for single column bent in Essential Bridges is equal to 2. The axial dead load on the column is equal to 365 kips. Using the corresponding R factor the column design forces are:

$$M_u = 8,600 \text{ k-ft and } P_u=365 \text{ k}$$

A curvature analysis was conducted for reinforced concrete 5'-0"-diameter column with 36#11 longitudinal bars and #8 @4" using Colduct computer program [12]. The results of the analysis based on idealized M- $\phi$  response are:

$M_p=8,614 \text{ k-ft}$	$V_p=M_p/L=345 \text{ k}$
$\Phi_y= 0.000\text{rad/in}$	$\Phi_u=0.02 \text{ rad/in}$
$\Delta_y=3.06''$	$\Delta_u=22.8 \text{ in}$

where  $\Phi$  is the curvature and the  $\Delta$  is the lateral displacement

### Plate Girder Connection to R/C Deck

The top flange of the plate girder has to be adequately connected to the R/C deck to enable to the transfer of the seismic force to the top strut. The ultimate capacity of shear connectors is given by:

$$Q_r = \phi_{sc} Q_n$$

where  $Q_r$  is the factored resistance of shear connector,  $Q_n$  is nominal resistance of shear connector and  $\phi_{sc}$  is equal to 1. The nominal resistance is given by:

$$Q_n = 0.5A_{sc} \sqrt{f_c E} \leq A_{sc} F_u$$

using 7/8-in diameter AASHTO M160 studs. Therefore,  $Q_n = 36.1$  kips. The number of required shear studs on the girders is equal to:

$$n = \frac{V_{EQ}}{Q_r} = \frac{364}{36.1} = 10$$

Therefore, each plate girder should have 3 shear connectors on its top flange along the location of the bent cross frame.

### **Top Strut Design**

The top strut is designed for the lateral seismic force  $345 / 3 = 115$  kips. Try 2L 2½x 2½ x ½ back-to-back connected to 1/2-in. thick gusset plate.

### **Axial Compression Capacity**

The AISC specifications will be used to compute the axial compression capacity of the built-up section. The slenderness ratios of the built-up section:

Slenderness ratio in the y-y axis

$$I_{yy} = 2(I_y + Ad^2) = 2(1.23 + 2.25(0.81 + 0.25)^2) = 7.48 \text{ in}^4$$

$$r_{yy} = \sqrt{\frac{7.48}{2 \times 2.25}} = 1.66$$

$$\left(\frac{KL}{r}\right)_{yy} = \frac{0.75 \times 10 \times 12}{1.66} = 54$$

Slenderness ratio in the x-x axis:

$$\left(\frac{KL}{r}\right)_{xx} = \frac{0.5 \times 5 \times 12}{0.74} = 40.6$$

Therefore, would occur about the y-y axis and it involves a shear transfer between the main components of the built-up section. This shear transfer would require to modify the governing slenderness ratio.

To delay the individual component buckling after member buckling it requires:

$$\left(\frac{a}{r_z}\right) \leq \frac{3}{4} \left(\frac{KL}{r}\right)_{yy}$$

where a is the spacing between the stitches between the built-up section. Based on this equation, the spacing between the stitches should not exceed 20" along the length of the member.

The modified slenderness ratio, shear transfer occur between the main components of the built-up section is given by:

$$\left(\frac{KL}{r}\right)_m = \sqrt{\left(\frac{KL}{r}\right)_{yy}^2 + 0.82 \frac{\alpha^2}{1 + \alpha^2} \left(\frac{a}{r_{ib}}\right)^2}$$

where

$\alpha$  is the separation ratio  $=h/2r_{ib}$ ,  $h$  is the distance between centroids of individual components perpendicular to the member axis of buckling

$a/r_{ib}$  is the member slenderness ratio of individual components relative to its centroidal axis parallel to axis of buckling.

$$\left(\frac{KL}{r}\right)_m = \sqrt{54^2 + 0.82 \frac{1.31^2}{1 + 1.31^2} (24.8)^2} = 56.9$$

Therefore the buckling stress is equal to  $F_{cr}=39.4$  ksi and  $P_r= 177$  kips.

The connection of top strut to the stiffener is based on limit state analysis to achieve the following three criteria:

- Prevent excessive local yielding in the connections and stitches
- Design the connections and stitches to have sufficient ductility
- The capacity of the connection is larger than the member

The end force at the end of the connection is equal to:

$$P_u = F_{cre} A_g = R_y F_{cr} A_g = (1.1)(39.4)(4.5) = 195 \text{ kips}$$

where  $R_y$  is a factor to account for steel overstrength based on the AISC Specifications.

The fillet weld capacity is equal to:

$$R_r = 0.6\phi_{e2} F_{EXX} = (0.6)(0.8)(70) = 33.6 \text{ ksi}$$

The maximum size of the fillet weld is equal to the thickness of the angle – 1/16.

Therefore, the size of the fillet weld is equal to 7/16 in. The capacity of the fillet weld is equal to

$$R_w = 0.707sR_r = (0.707)(7/16)(33.6) = 10.4 \text{ k/in}$$

Therefore, the total length of the weld at the end of the top strut is equal to 20 in. The connection is designed by using balanced fillet weld. The force acting on the weld of each angle:

$$P_1 = P_u/2 = 195/2 = 97.5 \text{ kips}$$

The total weld length for this angle is 12 in. with the length of the weld at the toe and the heel of the angle is 4 in. and 8 in. respectively.

The 97.5 kips should be transmitted to the gusset plate. The effective area of the gusset plate along the section a-a as shown in Figure XX, using the Whitmore's critical section,

$$A_{\text{eff}} = W_{\text{eff}} t_g = [(L_1 + L_2) \tan 30 + b](t_g) = [(4 + 8) \tan 30 + 2.5](0.5) = 4.71 \text{ in}^2$$

The compressive capacity of the gusset plate =  $4.71 \times 50 \times 0.9 = 213$  kips, assuming the buckling will not occur on this gusset plate because of its small slenderness ratio.

### **Diagonal Member Design**

The compressive force in the diagonal members is the result of the seismic load that is transmitted by the top strut. The axial compressive load on the diagonal member from the seismic force is equal to 45 kips, assuming that each bay carries an equal portion of the total seismic force.

The member will be selected based on the limiting slenderness ratio for bracing members in the compression and minimum material thickness requirements. The unbraced length  $L$  will be conservatively computed as the distance between the working point which is equal to 94.3 in.

The top strut is designed for the lateral seismic force  $345 / 6 \cos 51 = 91.4$  kips. Try 2L 2 1/2 x 2 1/2 x 1/2 back-to-back connected to 1/2-in. thick gusset plate.

## Axial Compression Capacity

The AISC specifications will be used to compute the axial compression capacity of the built-up section. The slenderness ratios of the built-up section:

Slenderness ratio in the y-y axis

$$I_{yy} = 2(I_y + Ad^2) = 2(1.23 + 2.25(0.81 + 0.25)^2) = 7.48 \text{ in}^4$$

$$r_{yy} = \sqrt{\frac{7.48}{2 \times 2.25}} = 1.66$$

$$\left(\frac{KL}{r}\right)_{yy} = \frac{0.75 \times 94.3}{1.66} = 54$$

Slenderness ratio in the x-x axis:

$$\left(\frac{KL}{r}\right)_{xx} = \frac{0.5 \times 94.3}{0.74} = 63.7$$

Therefore, would occur about the x-x axis and does not involve a shear transfer between the main components of the built-up section.

To delay the individual component buckling after member buckling it requires:

$$\left(\frac{a}{r_z}\right) \leq \frac{3}{4} \left(\frac{KL}{r}\right)_{xx}$$

where a is the spacing between the stitches between the built-up section. Based on this equation, the spacing between the stitches should not exceed 23" along the length of the member.

Therefore the buckling stress is equal to  $F_{cr}=37.1$  ksi and  $P_r= 167$  kips.



Connection design between the two braces and the top strut is based on the compression force of the diagonal member, 167 kips. The force horizontal component of the two diagonal members is equal to:  $167 \times 2 \times \cos 51 = 210$  kips. The total weld length around the gusset plate at this connection is equal to 22 in. as shown in Figure XX.

### **Bottom Strut Design**

It is assumed that each end of the bridge of the bridge is fixed against transverse movement so that the force from the diagonals is transmitted directly to the bearings. Therefore, no force is induced in the bottom strut. Based on this a  $2\frac{1}{2} \times 2\frac{1}{2} \times \frac{1}{2}$  single angle may be used for the bottom strut. Figure 6.2 shows the elevation of the cross frame in one bay, while Figures 6.3, 6.4 and 6.5 show the connection details between cross frame members and the plate girder.

### **Superstructure Lateral Capacity**

The lateral capacity of the superstructure is equal to the horizontal components of the diagonal members,  $167 \times 6 \times \cos 51 = 630$  k < 364 k, the plastic shear capacity of the column. Therefore, the expected inelastic activity in the system is the formation of the plastic hinge at the base of the reinforced concrete column.

## **References**

1. Seismic Design of Highway Bridges, FHWA-H1-91-019, U.S. Department of Transportation, Training Course Prepared by Imbsen and Associates, March 92
2. Bridge Design Specification Manual, California Department of Transportation, Sacramento, CA, 1983
3. Seismic Design Guidelines for Highway Bridges, Report No. FHWA/RD-81/081, October 91
4. Robert, J., "Research Based Seismic Design and Retrofit of California Bridges," 2<sup>nd</sup> Caltrans Seismic Research Workshop, Sacramento, CA, March, 93
5. Improved Seismic Design Criteria for California Bridges, Provisional Recommendations, Applied Technology Council, Redwood City, CA, 1996
6. Standard Specifications for Highway Bridges, American Association for State Highway and Transportation Officials, 15<sup>th</sup> Edition, 1989.
7. AASHTO LRFD Bridge Design Specifications, American Association for State Highway and Transportation Officials, 1<sup>st</sup> Edition, 1994
8. AASHTO LRFD Bridge Design Specifications, American Association for State Highway and Transportation Officials, 2<sup>nd</sup> Edition, 1998
9. Four LRFD Design Examples of Steel Highway Bridges, American Iron and Steel Institute, 1997
10. Automatic Dynamic Nonlinear Analysis, Adina R & D Inc., Water town, MA, 1996
11. Bridge Column Ductility Program, ColDuct, California Department of Transportation, Sacramento, CA 1994
12. Load and Resistance Factor Design Specifications for Structural Buildings, American Institute of Steel Construction, 2<sup>nd</sup> Edition, 1993

## Tables

Substructure	Importance Category		
	Critical	Essential	Other
<b>Wall-Type-Larger Dimension</b>	1.5	1.5	2.0
<b>Reinforced Concrete Pile Bent</b>			
• Vertical Piles Only	1.5	2.0	3.0
• With Batter Piles	1.5	1.5	2.0
<b>Single Columns</b>	1.5	2.0	3.0
<b>Steel or Composite Steel and Concrete Pile Bents</b>			
• Vertical Pile Only	1.5	3.5	5.0
• With Batter Piles	1.5	2.0	3.0
<b>Multiple Column Bent</b>	1.5	3.5	5.0

Table 1.1: Response Modification Factors for bridge substructure

Connection	All Importance Categories
<b>Superstructure to abutment</b>	0.8
<b>Expansion Joint within a span of the superstructure</b>	0.8
<b>Columns, Piers, or Pile Bents to Cap Beam or superstructure</b>	1.0
<b>Columns or Piers to Foundation</b>	1.0

Table 1.2: Response Modification Factors for bridge connections

	<b>Cross Sections of Girders</b>		
<b>Region</b>	<b>Web</b>	<b>To flange</b>	<b>Bottom flange</b>
0-18,800 mm (0-62 ft)	11mm x 925mm	22mm x 400mm	22mm x 400mm
18,800-35,200 mm (62-116 ft)	14mm x 925mm	22mm x 400mm	35mm x 400mm
35,200-54000 mm (116-177 ft)	11mm x 925mm	20mm x 325mm	22mm x 400mm

Table 2.2: Cross Sections of Girders of the design Example 2

	<b>Cross Sections of Girders</b>		
<b>Region</b>	<b>Web</b>	<b>To flange</b>	<b>Bottom flange</b>
0-12,500 mm (0-41 ft)	14mm x 2100mm	20mm x 375mm	20mm x 375mm
12,500-30,300 mm (41-99 ft)	14mm x 2100mm	20mm x 375mm	38mm x 375 mm
30,300-38,100 mm (99-125 ft)	14mm x 2100mm	20mm x 375mm	25mm x 475 mm
38100-47,900 mm (125-157 ft)	14mm x 2100mm	45mm x 375mm	45mm x 475mm
47900-55,700 mm (157-183 ft)	14mm x 2100mm	20mm x 375 mm	25mm x 475mm
55,700-69,500 mm (183-273 ft)	14mm x 2100mm	20mm x 375mm	25mm x 375mm
Symmetric to the end			

Table 2.3: Cross Sections of Girders of the Design Example 3

<b>Cross Sections of the Box Girders</b>			
<b>Region</b>	<b>Web late</b>	<b>To late</b>	<b>Bottom late</b>
0-33,500 mm (0-110 ft)	14mm x 1850mm	20mm x 475mm	14mm x 2550mm
33,500-37,000 mm (110-121 ft)	14mm x 1850mm	20mm x 475mm	22mm x 2550mm
37,000-47,000 mm (121-154 ft)	14mm x 1850mm	40mm x 675mm	22mm x 2550mm
47,000-52,500 mm (154-172 ft)	14mm x 1850mm	40mm x 675mm	35mm x 2550mm
52,500-58,000 mm (172-190 ft)	14mm x 1850mm	65mm x 675mm	35mm x 2550mm
58,000-63,500 mm (190-208 ft)	14mm x 1850mm	65mm x 675mm	35mm x 2550mm
63,500-69,000 mm (208-226 ft)	14mm x 1850mm	40mm x 675mm	35mm x 2550mm
69,000-79,000 mm (226-259 ft)	14mm x 1850mm	40mm x 675mm	22mm x 2550mm
79,000-83,500 mm (259-274 ft)	14mm x 1850mm	18mm x 350mm	22mm x 2550mm
83,500-94,000 mm (274-308 ft)	14mm x 1850mm	18mm x 350mm	14mm x 2550mm
Symmetric to the end			

Table 2.4: Cross Sections of Box Girders of the Design Example 4

Total Mass =		629337	kg						
Mode Shape No.	Freq. (HZ)	Period (sec)	Mass Participation			Cumulated Mass		Participation	
			Long.(X) (%)	Trans.(Y) (%)	Verti. (Z) (%)	Long.(X) (%)	Trans.(Y) (%)	Verti. (Z) (%)	
1	0.73	1.3630	89.41	0.00	0.00	89.41	0.00	0.00	
2	2.22	0.4512	0.03	0.00	0.00	89.44	0.00	0.00	
3	2.55	0.3919	0.00	0.00	0.00	89.44	0.00	0.00	
4	2.89	0.3460	0.00	2.37	0.00	89.44	2.37	0.00	
5	3.43	0.2916	0.00	0.00	62.86	89.44	2.37	62.86	
6	4.41	0.2270	0.00	73.46	0.00	89.44	75.83	62.86	
7	6.36	0.1573	0.00	2.32	0.00	89.44	78.15	62.86	
8	7.39	0.1354	0.00	0.00	0.00	89.44	78.15	62.86	
9	7.75	0.1290	0.00	0.00	0.16	89.44	78.15	63.02	
10	8.67	0.1153	0.00	0.00	0.00	89.44	78.15	63.02	
11	9.15	0.1093	0.00	0.00	0.00	89.44	78.15	63.02	
12	9.37	0.1067	0.00	0.00	3.92	89.44	78.15	66.94	
13	11.83	0.0845	0.00	0.00	0.00	89.44	78.15	66.94	
14	12.08	0.0828	0.00	0.00	0.45	89.44	78.15	67.39	
15	12.14	0.0824	0.00	0.00	0.00	89.44	78.15	67.39	
16	12.66	0.0790	0.00	0.36	0.00	89.44	78.50	67.39	
17	12.71	0.0787	0.00	0.00	0.00	89.44	78.50	67.39	
18	12.75	0.0784	0.00	0.00	0.00	89.44	78.50	67.39	
19	12.83	0.0779	0.00	0.00	0.03	89.44	78.50	67.42	
20	12.83	0.0779	0.00	0.01	0.00	89.44	78.51	67.42	
21	12.88	0.0776	0.00	0.00	0.00	89.44	78.51	67.42	
22	12.89	0.0776	0.00	0.00	0.00	89.44	78.51	67.42	
23	12.99	0.0770	0.00	0.00	0.17	89.44	78.51	67.59	
24	13.01	0.0769	0.00	0.19	0.00	89.44	78.70	67.59	
25	15.13	0.0661	0.00	0.00	0.00	89.44	78.70	67.59	
26	15.19	0.0658	0.00	0.00	0.00	89.44	78.71	67.59	
27	15.57	0.0642	0.00	0.00	11.50	89.44	78.71	79.08	
28	17.69	0.0565	0.00	0.00	0.00	89.44	78.71	79.08	
29	17.77	0.0563	0.00	0.92	0.00	89.44	79.63	79.08	
30	17.92	0.0558	0.01	0.00	0.00	89.45	79.63	79.08	

Table 4.1: Dynamic characteristics of 3-D finite element model of Example 2



Total Mass =		600000	kg					
Mode Shape No.	Freq. (Hz)	Period (sec)	Mass Participation			Cumulated Mass		Participation
			Long.(X) (%)	Trans.(Y) (%)	Verti. (Z) (%)	Long. (X) %	Trans.(Y) %	Verti. (Z) %
1	0.72	1.3910	97.91	0.00	0.00	97.91	0.00	0.00
2	2.47	0.4045	0.03	0.00	0.00	97.93	0.00	0.00
3	3.97	0.2517	0.00	0.00	62.89	97.93	0.00	62.89
4	4.81	0.2080	0.00	78.09	0.00	97.93	78.09	62.89
5	9.38	0.1066	0.00	0.00	0.00	97.94	78.09	62.89
6	10.66	0.0938	0.00	2.53	0.00	97.94	80.62	62.89
7	11.71	0.0854	0.00	0.00	7.26	97.94	80.62	70.15
8	20.23	0.0494	0.00	0.00	0.00	97.94	80.62	70.15
9	22.27	0.0449	0.01	0.00	0.00	97.95	80.62	70.15
10	22.29	0.0449	0.00	0.00	10.89	97.95	80.62	81.04
11	27.31	0.0366	0.00	0.00	0.00	97.95	80.62	81.04
12	27.72	0.0361	0.95	0.00	0.00	98.90	80.62	81.04
13	30.62	0.0327	0.00	0.00	8.46	98.90	80.62	89.50
14	42.41	0.0236	0.00	7.05	0.00	98.90	87.67	89.50
15	44.60	0.0224	0.07	0.00	0.00	98.96	87.67	89.50
16	49.26	0.0203	0.05	0.00	0.00	99.01	87.67	89.50
17	59.81	0.0167	0.00	0.00	0.34	99.01	87.67	89.84
18	60.24	0.0166	0.00	0.79	0.00	99.01	88.46	89.84
19	66.67	0.0150	0.00	0.00	0.00	99.01	88.46	89.84
20	72.52	0.0138	0.19	0.00	0.00	99.20	88.46	89.84

Table 4.2: Dynamic characteristics of space frame model of Example 2

Total Mass =			629337			kg		
Mode Shape No.	Freq. (Hz)	Period (sec)	Mass Participation			Cumulated Mass		Participation
			Long.(X) (%)	Trans.(Y) (%)	Verti. (Z) (%)	Long(X) 9L)	Trans.(Y)	Verd. (Z)
1	0.74	1.3480	86.54	0.05	0.00	86.54	0.05	0.00
2	2.20	0.4542	0.39	4.12	0.00	86.93	4.16	0.00
3	2.84	0.3523	3.68	0.40	0.00	90.61	4.56	0.00
4	2.88	0.3474	0.00	0.00	3.88	90.61	4.56	3.88
5	3.44	0.2909	0.00	0.00	60.26	90.61	4.56	64.14
6	4.16	0.2402	0.20	76.29	0.00	90.81	80.85	64.14
7	5.83	0.1715	0.44	1.23	0.00	91.25	82.08	64.14
8	7.41	0.1350	0.00	0.00	0.21	91.25	82.08	64.34
9	7.55	0.1324	0.02	0.03	0.00	91.27	82.11	64.34
10	8.48	0.1179	0.00	0.00	5.17	91.27	82.11	69.52
11	8.76	0.1142	0.00	0.01	0.00	91.27	82.12	69.52
12	9.17	0.1090	0.00	0.00	0.00	91.27	82.12	69.52
13	9.23	0.1084	0.00	0.13	0.00	91.27	82.25	69.52
14	9.95	0.1005	0.00	0.00	0.32	91.27	82.25	69.84
15	10.37	0.0964	0.00	0.00	0.34	91.27	82.25	70.18
16	11.32	0.0884	0.00	0.09	0.00	91.27	82.34	70.18
17	11.39	0.0878	0.00	0.00	0.00	91.27	82.34	70.18
18	11.56	0.0865	0.00	0.08	0.00	91.27	82.42	70.18
19	12.13	0.0825	0.00	0.00	0.18	91.27	82.42	70.36
20	13.27	0.0754	0.00	0.27	0.00	91.28	82.70	70.36
21	14.19	0.0705	0.00	0.00	3.70	91.28	82.70	74.06
22	14.27	0.0701	0.00	0.23	0.00	91.28	82.93	74.06
23	14.36	0.0696	0.00	0.00	2.65	91.28	82.93	76.71
24	15.15	0.0660	0.01	0.97	0.00	91.29	83.89	76.71
25	15.38	0.0650	0.00	0.00	0.74	91.29	83.90	77.45
26	15.39	0.0650	0.01	0.83	0.00	91.29	84.73	77.45
27	15.86	0.0630	0.00	0.00	0.12	91.29	84.73	77.58
28	16.02	0.0624	0.00	1.86	0.00	91.29	86.59	77.58
29	16.93	0.0591	0.00	1.74	0.00	91.30	88.34	77.58
30	16.98	0.0589	0.00	0.00	0.01	91.30	88.34	77.59

Table 4.3: Dynamic characteristics of 3-D finite element model of Example 2M

Total Mass =		2006810 kg		Mass Participation			Cumulated Mass		Participation
Mode Shape NO.	Freq. (Hz)	Period (sec)	Long.(X) (%)	Trans.(Y) (%)	Verti. (Z) (%)	Long.(X) (%)	Trans.(Y) (%)	Verti. (Z) (%)	
1	0.78	1.2800	98.39	0.00	0.00	98.39	0.00	0.00	
2	1.67	0.5981	0.00	0.00	0.08	98.39	0.00	0.08	
3	1.82	0.5500	0.00	75.19	0.00	98.39	75.19	0.08	
4	1.92	0.5201	0.00	7.82	0.00	98.39	83.02	0.08	
5	2.51	0.3991	0.03	0.00	0.00	98.42	83.02	0.08	
6	2.69	0.3719	0.00	0.00	0.00	98.42	83.02	0.08	
7	3.05	0.3280	0.00	0.00	67.55	98.42	83.02	67.63	
8	3.22	0.3103	0.00	0.28	0.00	98.42	83.30	67.63	
9	3.52	0.2841	0.00	0.00	0.00	98.42	83.30	67.63	
10	5.92	0.1688	0.01	0.00	0.00	98.43	83.30	67.63	
11	5.93	0.1687	0.00	12.50	0.00	98.43	95.79	67.63	
12	6.15	0.1626	0.00	0.00	0.00	98.43	95.79	67.63	
13	7.91	0.1264	0.00	0.00	0.05	98.43	95.79	67.67	
14	7.96	0.1257	0.00	0.00	0.52	98.43	95.79	68.19	
15	8.14	0.1229	0.00	0.00	0.00	98.43	95.79	68.19	
16	8.16	0.1225	0.00	0.01	0.00	98.43	95.80	68.19	
17	8.19	0.1221	0.00	0.00	0.00	98.43	95.80	68.19	
18	8.31	0.1204	0.00	0.00	0.00	98.43	95.80	68.19	
19	8.31	0.1203	0.00	0.00	0.02	98.43	95.80	68.22	
20	8.80	0.1136	0.00	0.00	0.00	98.43	95.80	68.22	

Table 4.4: Dynamic characteristics of 3-D finite element model of Example 3

Total Mass -		1879500 kg						
Mode Shape No.	Freq. (Hz)	Period (sec)	Mass Participation			Cumulated Mass Participation		
			Long.(X) (%)	Trans.(Y) (%)	Verti. (Z) (%)	Long.(X) (%)	Trans.(Y) (%)	Verti. (Z) (%)
1	0.81	1.2310	97.30	0.00	0.00	97.30	0.00	0.00
2	1.88	0.5307	0.00	0.00	0.04	97.30	0.00	0.04
3	2.34	0.4275	0.00	80.70	0.00	97.30	80.70	0.04
4	2.90	0.3449	0.04	0.00	0.00	97.33	80.70	0.04
5	3.63	0.2752	0.00	0.00	63.27	97.33	80.70	63.31
6	4.40	0.2273	0.00	0.00	0.00	97.33	80.70	63.31
7	7.10	0.1409	0.01	0.00	0.00	97.34	80.70	63.31
8	8.87	0.1127	0.00	8.52	0.00	97.34	89.22	63.31
9	9.70	0.1031	0.00	0.00	0.61	97.34	89.22	63.92
10	10.49	0.0953	0.00	0.00	0.00	97.35	89.22	63.92
11	11.19	0.0894	0.00	0.00	0.01	97.35	89.22	63.93
12	15.23	0.0656	0.00	0.00	6.85	97.35	89.22	70.78
13	15.37	0.0651	0.00	0.00	0.00	97.35	89.22	70.78
14	20.12	0.0497	0.03	0.00	0.00	97.37	89.22	70.78
15	20.37	0.0491	0.00	0.00	13.46	97.37	89.22	84.24
16	22.68	0.0441	0.05	0.00	0.00	97.43	89.22	84.24
17	22.71	0.0440	0.00	1.87	0.00	97.43	91.09	84.24
18	23.71	0.0422	0.02	0.00	0.00	97.45	91.09	84.24
19	27.21	0.0368	0.00	0.00	0.48	97.45	91.09	84.72
20	29.20	0.0343	1.03	0.00	0.00	98.48	91.09	84.72

Table 4.5: Dynamic characteristics of space frame model of Example 3

Total Mass =		2006810 kg		Mass Participation			CuPnulated Mass		Participation
Mode Shape No.	Freq. (HZ)	Period (sec)	Long.(X) (%)	Trans.(Y) %	Verti. (Z) (%)	Long.(X) (%)	Trans.(Y) %	Verti. (Z) %	
1	0.78	1.2860	98.76	0.00	0.00	98.76	0.00	0.00	
2	1.25	0.7986	0.00	83.98	0.00	98.76	83.98	0.00	
3	1.86	0.5389	0.00	0.00	0.09	98.76	83.98	0.09	
4	2.60	0.3841	0.81	0.00	0.00	99.57	83.98	0.09	
5	3.04	0.3293	0.00	0.00	0.00	99.57	83.98	0.09	
6	3.07	0.3259	0.00	0.00	66.71	99.57	83.98	66.80	
7	3.11	0.3215	0.00	0.17	0.00	99.57	84.15	66.80	
8	3.28	0.3048	0.00	0.37	0.00	99.57	84.52	66.80	
9	3.41	0.2936	0.00	0.00	0.00	99.57	84.52	66.80	
10	5.93	0.1687	0.00	12.13	0.00	99.57	96.65	66.80	
11	6.06	0.1649	0.11	0.00	0.00	99.68	96.65	66.80	
12	7.45	0.1342	0.00	0.00	0.00	99.68	96.65	66.80	
13	8.04	0.1244	0.00	0.00	0.35	99.68	96.65	67.15	
14	8.22	0.1216	0.00	0.00	0.09	99.68	96.65	67.24	
15	8.33	0.1201	0.00	0.00	0.00	99.68	96.65	67.24	
16	8.36	0.1196	0.00	0.00	0.00	99.68	96.65	67.24	
17	8.38	0.1193	0.00	0.00	0.01	99.68	96.65	67.25	
18	8.45	0.1184	0.01	0.00	0.00	99.69	96.65	67.25	
19	8.99	0.1112	0.00	0.18	0.00	99.69	96.83	67.25	
20	9.23	0.1084	0.00	0.00	0.00	99.69	96.83	67.25	

Table 4.6: Dynamic characteristics of 3-D finite element model of Example 3M

Total Mass =		1879500 kg						
Mode Shape No.	Freq. (Hz)	Period (sec)	Mass Participation			Cumulated Mass		Participation
			Long.(X) (%)	Trans.(Y) (%)	Verti. (Z) (%)	Long.(X) (%)	Trans.(Y)	Verti. (Z)
1	0.83	1.2080	97.83	0.00	0.00	97.83	0.00	0.00
2	1.44	0.6948	0.00	81.77	0.00	97.83	81.77	0.00
3	2.10	0.4757	0.00	0.00	0.06	97.83	81.77	0.06
4	3.01	0.3318	0.75	0.00	0.00	98.58	81.77	0.06
5	3.64	0.2749	0.00	0.00	63.11	98.58	81.77	63.17
6	3.87	0.2584	0.00	0.00	0.00	98.58	81.77	63.17
7	7.23	0.1384	0.12	0.00	0.00	98.70	81.77	63.17
8	8.83	0.1133	0.00	7.88	0.00	98.70	89.65	63.17
9	9.76	0.1025	0.00	0.00	0.58	98.70	89.65	63.75
10	10.53	0.0950	0.01	0.00	0.00	98.70	89.65	63.75
11	11.11	0.0900	0.00	0.00	0.03	98.70	89.65	63.78
12	15.22	0.0657	0.00	0.00	6.12	98.70	89.65	69.90
13	15.22	0.0657	0.00	0.00	0.00	98.70	89.65	69.90
14	19.86	0.0504	0.04	0.00	0.00	98.75	89.65	69.90
15	20.37	0.0491	0.00	0.00	13.43	98.75	89.65	83.33
16	22.26	0.0449	0.00	1.88	0.00	98.75	91.53	83.33
17	22.62	0.0442	0.01	0.00	0.00	98.76	91.53	83.33
18	23.75	0.0421	0.02	0.00	0.00	98.79	91.53	83.33
19	27.90	0.0358	0.00	0.00	1.43	98.79	91.53	84.76
20	30.53	0.0328	0.00	0.00	8.02	98.79	91.53	92.78

Table 4.7: Dynamic characteristics of space frame model of Example 3M

Total Mass =		2749351	kg					
Mode Shape No.	Freq. (HZ)	Period (sec)	Mass Participation			Cumulated Mass		Participation
			Long.(X) (%)	Trans.(Y) (%)	Verti. (Z) %	Long.(X) (%)	Trans.(Y) %	Verti. (Z) (%)
1	0.67	1.5010	98.28	0.00	0.00	98.28	0.00	0.00
2	0.92	1.0830	0.00	0.00	0.00	98.28	0.00	0.00
3	1.37	0.7278	0.00	81.71	0.00	98.28	81.71	0.00
4	1.38	0.7267	0.07	0.00	0.00	98.35	81.71	0.00
5	1.73	0.5779	0.00	0.00	65.84	98.35	81.71	65.84
6	1.95	0.5127	0.00	0.00	0.00	98.35	81.71	65.84
7	2.45	0.4085	0.00	0.03	0.00	98.35	81.73	65.84
8	2.50	0.4004	0.00	1.36	0.00	98.35	83.09	65.84
9	2.78	0.3600	0.00	0.00	0.00	98.35	83.09	65.84
10	3.31	0.3020	0.00	0.00	0.00	98.35	83.09	65.84
11	3.44	0.2904	0.00	12.55	0.00	98.35	95.64	65.84
12	4.27	0.2344	0.00	0.00	0.00	98.35	95.64	65.84
13	4.43	0.2256	0.00	0.00	0.35	98.35	95.64	66.19
14	4.70	0.2126	0.00	0.00	0.00	98.35	95.64	66.19
15	4.87	0.2053	0.00	0.00	0.00	98.35	95.64	66.19
16	5.29	0.1892	0.00	0.03	0.00	98.35	95.67	66.19
17	5.62	0.1778	0.00	0.00	0.00	98.35	95.67	66.19
18	6.35	0.1576	0.00	0.00	5.09	98.35	95.67	71.28
19	6.50	0.1538	0.00	0.00	0.04	98.35	95.67	71.32
20	6.57	0.1523	0.00	0.49	0.00	98.35	96.16	71.33

Table 4.8: Dynamic characteristics of 3-D finite element model of Example 4

Total Mass =		2751900	kg						
Mode Shape No.	Freq. (HZ)	Period (sec)	Mass Participation			Cumultbed Mass		Participation	
			Long.(X) (%)	Trans.(Y) (%)	Verti. (Z) (%)	Long.(X) (%)	Trans.(Y) (%)	Verti. (Z) (%)	
1	0.67	1.4980	98.12	0.00	0.00	98.12	0.00	0.00	
2	0.99	1.0080	0.00	0.00	0.02	98.12	0.00	0.02	
3	1.53	0.6519	0.04	0.00	0.00	98.16	0.00	0.02	
4	1.84	0.5431	0.00	81.57	0.00	98.16	81.57	0.02	
5	2.01	0.4981	0.00	0.00	62.80	98.16	81.57	62.82	
6	3.05	0.3280	0.00	0.00	0.00	98.16	81.57	62.82	
7	3.92	0.2549	0.00	0.00	0.00	98.16	81.57	62.82	
8	5.32	0.1880	0.00	0.00	0.59	98.16	81.57	63.41	
9	5.47	0.1827	0.00	9.18	0.00	98.16	90.74	63.41	
10	5.83	0.1714	0.00	0.00	0.00	98.16	90.74	63.41	
11	8.42	0.1188	0.00	0.00	5.29	98.16	90.74	68.70	
12	8.54	0.1171	0.00	0.00	0.02	98.16	90.74	68.73	
13	9.75	0.1026	0.00	0.00	0.00	98.16	90.74	68.73	
14	11.40	0.0877	0.00	0.00	0.00	98.16	90.74	68.73	
15	11.79	0.0848	0.00	0.00	11.73	98.16	90.74	80.45	
16	14.18	0.0705	0.00	0.00	0.00	98.16	90.74	80.45	
17	15.03	0.0665	0.00	1.85	0.00	98.16	92.59	80.45	
18	17.69	0.0565	0.01	0.00	0.00	98.17	92.59	80.45	
19	19.42	0.0515	0.00	0.00	1.28	98.17	92.59	81.73	
20	19.46	0.0514	0.00	0.00	0.00	98.17	92.59	81.73	

Table 4.9: Dynamic characteristics of space frame model of Example 4 using one stick model for the superstructure



Total Mass =		2746589 kg		Mass Participation			Cumulated Mass		Participation
Mode Shape No.	Freq. HZ)	Period (sec)	Long.(X) (%)	Trans.(Y) %	Verti. (Z) %	Long.(X) (%)	Trans.(Y)	Verti. (Z)	
1	0.67	1.5000	95.78	0.00	0.00	95.78	0.00	0.00	
2	0.92	1.0880	0.00	0.00	0.01	95.78	0.00	0.01	
3	1.44	0.6950	0.06	0.00	0.00	95.83	0.00	0.01	
4	1.64	0.6111	0.00	76.93	0.07	95.83	76.93	0.07	
5	1.87	0.5352	0.00	0.08	62.44	95.83	77.01	62.52	
6	2.38	0.4201	0.00	0.03	0.00	95.83	77.03	62.52	
7	3.57	0.2802	0.00	0.90	0.02	95.83	77.93	62.53	
8	3.61	0.2770	0.00	0.00	0.00	95.84	77.93	62.53	
9	3.66	0.2729	0.00	9.26	0.00	95.84	87.19	62.54	
10	4.24	0.2360	0.00	0.00	0.00	95.84	87.19	62.54	
11	4.29	0.2330	0.00	0.33	0.01	95.84	87.52	62.55	
12	4.95	0.2019	0.00	0.00	0.49	95.84	87.52	63.04	
13	5.40	0.1853	0.00	0.00	0.00	95.84	87.52	63.04	
14	6.39	0.1566	0.00	0.01	0.00	95.84	87.54	63.04	
15	6.74	0.1484	0.00	0.00	0.00	95.84	87.54	63.04	
16	7.28	0.1374	0.01	0.00	0.01	95.85	87.54	63.06	
17	7.72	0.1296	0.00	0.00	5.15	95.85	87.54	68.21	
18	8.20	0.1220	0.00	0.02	0.04	95.85	87.56	68.25	
19	8.33	0.1200	0.00	0.00	0.00	95.85	87.56	68.25	
20	9.55	0.1047	0.00	1.68	0.00	95.85	89.23	68.25	

Table 4.10: Dynamic characteristics of space frame model of Example 4 using two stick models for the superstructure

**\*Force in Column**

Soil Type= 3, Zone = 4 (0.40g)

Model Type	Combination		Force-R kips	Force-S kips	Force-T kips	Mom.-S k-ft	Mom.-T k-ft
	Long. (%)	Trans. (%)					
3D	100	30	0.00	20.51	732.49	21220.69	248.52
	30	100	0.00	68.35	219.75	6366.20	828.40
Stick	100	30	0.00	5.81	749.66	21852.54	106.33
	30	100	0.00	19.38	224.90	6555.76	354.44
3D	Dead Load		352.44	0.00	0.00	0.00	0.00
Stick	Dead Load		358.94	0.00	0.00	0.00	0.00

**Note:**

Force-R= Axial Force

Force-S= Shear Force in the Transverse Direction

Force-T= Shear Force in the Longitudinal Direction

Mom.-S= Moment about the Transverse Direction

Mom.-T= Moment about the Longitudinal Direction

**Table 5.1: Unreduced column forces in Design Example 2**

**\*force in bearing**

Soil Type= 3, Zone = 4  
(0.40g)

Model Type	Combination		Force-R <i>kips</i>	Force-S <i>kips</i>	Force-T <i>kips</i>	Mom.-S <i>k-ft</i>	Mom.-T <i>k-ft</i>
	Long. (%)	Trans. (%)					
3D	100	30	8.03	17.95	718.91	2845.02	284.72
	30	100	26.78	59.83	215.67	853.50	949.06
Stick	100	30	6.94	2.93	404.29	829.00	6.01
	30	100	23.12	9.77	121.29	248.70	20.04
3D	Dead Load		326.49	31.35	0.00	0.00	64.27
Stick	Dead Load		178.66	118.45	0.00	0.00	242.88

**Note:**

Force-R= Axial Force

Force-S= Shear Force in the Transverse Direction

Force-T= Shear Force in the Longitudinal Direction

Mom.-S= Moment about the Transverse Direction

Mom.-T= Moment about the Longitudinal Direction

**Table 5.2: Unreduced bearings forces in Design Example 2**

**\*force in Cross Frame**

Soil Type= 3, Zone = 4 (0.40g)

Model Type	Combination		Force-R <i>kips</i>	Force-S <i>kips</i>	Force-T <i>kips</i>	Mom.-S <i>k-ft</i>	Mom. -T <i>k-ft</i>
	Long. (%)	Trans. (%)					
3D	100	30	11.19	0.49	0.10	0.32	2.05
	30	100	36.61	1.35	0.05	0.18	6.10
<b>3D Dead Load</b>			26.76	1.43	0.03	0.12	6.79

**Note:**

Force-R= Axial Force

Force-S= Shear Force in the Transverse Direction

Force-T= Shear Force in the Longitudinal Direction

Mom. -S= Moment about the Transverse Direction

Mom. -T= Moment about the Longitudinal Direction

**Table 5.3: Unreduced cross frame forces in Design Example 2**

\*Force in Column

Soil Type= 3, Zone = 4 (0.40g)

Model Type	Combination		Force-R <i>kips</i>	Force-S <i>kips</i>	Force-T <i>kips</i>	Mom.-S <i>k-ft</i>	Mom.-T <i>k-ft</i>
	Long. (%)	Trans. (%)					
<i>Stick</i>	100	30	0.00	5.81	749.66	21852.54	106.33
	30	100	0.00	19.38	224.90	6555.76	354.44
<i>3D Skew</i>	100	30	0.06	403.17	611.85	17656.63	10280.77
	30	100	0.04	176.99	206.43	5815.16	3832.46
<i>Stick</i>	<i>Dead Load</i>		358.94	0.00	0.00	0.00	0.00
<i>3D Skew</i>	<i>Dead Load</i>		351.59	0.00	0.00	0.72	0.36

Note:  
 Force-R= Axial Force  
 Force-S= Shear Force in the Transverse Direction  
 Force-T= Shear Force in the Longitudinal Direction  
 Mom.-S= Moment about the Transverse Direction  
 Mom.-T= Moment about the Longitudinal Direction

Table 5.4: Unreduced column forces in Design Example 2M

**\*force in bearing**

Cell Type = 2 Zone = 4

Model Type	Combination		Force-R <i>kips</i>	Force-S <i>kips</i>	Force-T <i>kip.</i>	Mom.-S <i>k-ft</i>	Mom.-T <i>k-ft</i>
	Long. (%)	Trans. (%)					
<i>Stick</i>	100	30	6.94	2.93	404.29	829.00	6.01
	30	100	23.12	9.77	121.29	248.70	20.04
<i>3D Skew</i>	100	30	49.80	394.94	598.73	2345.70	1450.30
	30	100	30.67	167.05	196.84	770.71	1140.83
<hr/>							
<i>Stick</i>	<i>Dead Load</i>		178.66	118.45	0.00	0.00	242.88
<i>3D Skew</i>	<i>Dead Load</i>		334.63	52.86	22.09	45.29	107.97

Note:  
 Force-R= Axial Force  
 Force-S= Shear Force in the Transverse Direction  
 Force-T= Shear Force in the Longitudinal Direction  
 Mom.-S= Moment about the Transverse Direction  
 Mom.-T= Moment about the Longitudinal Direction

Table 5.5: Unreduced bearing forces in Design Example 2M

**\*Force in Cross Frame**

**Soil Type**= 3, Zone = 4 (0.40q)

Model Type	Combination		Force-R <i>kips</i>	Force-S <i>kips</i>	Force-T <i>kips</i>	Mom.-S <i>k-ft</i>	Mom. -T <i>k-ft</i>
	Long. (%)	Trans. (%)					
3D Skew	100	30	101.18	10.47	1.07	5.05	35.16
	30	100	80.01	5.36	0.37	1.68	20.45
3D Skew	Dead Load-		31.00	1.55	0.11	0.42	8.26

**Note:**

Force-R= Axial Force

Force-S= Shear Force in the Transverse Direction

Force-T= Shear Force in the Longitudinal Direction

Mom.-S= Moment about the Transverse Direction

Mom.-T= Moment about the Longitudinal Direction

**Table 5.6: Unreduced cross frame forces in Design Example 2M**

Soil Type- 3, Zone = 4 (0.40g)								
	Long.	Trans.	Vert.		Long.	Trans.	Vert.	
Exterior Girder -1	(inch)	(inch)	(inch)	Exterior Girder -2	(inch)	(inch)	(inch)	
<b>Dead Load</b>				<b>Dead Load</b>				
at the abutment	-0.0028	-0.0002	-0.0027	at the abutment	-0.0028	0.0002	-0.0027	
at the bent	0.0000	0.0014	-0.0733	at the bent	0.0000	-0.0014	-0.0733	
at the abutment	-0.0028	-0.0002	-0.0027	at the abutment	0.0028	0.0002	-0.0027	
<b>100% Long. + 30% Trans.</b>				<b>100% Long. + 30% Trans.</b>				
at the abutment	10.7805	0.0097	0.0010	at the abutment	10.7805	0.0097	0.0010	
at the bent	10.7622	0.0627	0.0517	at the bent	10.7622	0.0627	0.0517	
at the abutment	10.7805	0.0097	0.0010	at the abutment	10.7805	0.0097	0.0010	
<b>30% Long. + 100% Trans.</b>				<b>30% Long. + 100% Trans.</b>				
at the abutment	3.2742	0.0320	0.0017	at the abutment	3.2742	0.0320	0.0017	
at the bent	3.2286	0.2090	0.1723	at the bent	3.2286	0.2090	0.1723	
at the abutment	3.2742	0.0320	0.0017	at the abutment	3.2742	0.0320	0.0017	
	<b>Long.</b>	<b>Trans.</b>	<b>Vert.</b>		<b>Long.</b>	<b>Trans.</b>	<b>Vert.</b>	
<b>Interior Girder -1</b>	<b>(inch)</b>	<b>(inch)</b>	<b>(inch)</b>	<b>Interior Girder -2</b>	<b>(inch)</b>	<b>(inch)</b>	<b>(inch)</b>	
<b>Dead Load</b>				<b>Dead Load</b>				
at the abutment	-0.0031	-0.0001	-0.0028	at the abutment	-0.0031	0.0001	-0.0028	
at the bent	0.0000	0.0005	-0.0303	at the bent	0.0000	-0.0005	-0.0303	
at the abutment	0.0031	-0.0001	-0.0028	at the abutment	0.0031	0.0001	-0.0028	
<b>100% Long. + 30% Trans.</b>				<b>100% Long. . + 30% Trans.</b>				
at the abutment	10.7720	0.0095	0.0006	at the abutment	10.7720	0.0095	0.0006	
at the bent	10.7570	0.0628	0.0165	at the bent	10.7570	0.0628	0.0165	
at the abutment	10.7720	0.0095	0.0006 4	at the abutment	10.7720	0.0095	0.0006	
<b>30% Long. + 100% Trans.</b>				<b>30% Lon . + 100% Frans.</b>				
at the abutment	3.2445	0.0317	0.0005	at the abutment	3.2445	0.0317	0.0005	
at the bent	3.2271	0.2092	0.0551	at the bent	3.2271	0.2092	0.0551	
at the abutment	3.2445	0.0317	0.0005	at the abutment	3.2445	0.0317	0.0005	

**Table 5.7: Displacements of Design Example 2**



<b>Soil Type= 3, Zone = 4 (0.40g)</b>							
<b>Exterior Girder</b>	<b>Long. (inch)</b>	<b>Trans. (inch)</b>	<b>Vert. (inch)</b>	<b>Exterior Girder</b>	<b>Long. (inch)</b>	<b>Trans. (inch)</b>	<b>Vert. (inch)</b>
Dead Load				Dead Load			
at the abutment	-0.0114	0.0329	-0.0027	at the abutment	0.0051	0.0443	-0.0027
at the bent	-0.0082	-0.0067	-0.1117	at the bent	0.0070	0.0066	-0.1123
at the abutment	-0.0063	-0.0443	-0.0027	at the abutment	0.0102	-0.0329	-0.0027
<b>100% Long. + 30% Trans.</b>				<b>100% Long. + 30% Trans.</b>			
at the abutment	10.1567	0.0513	0.0099	at the abutment	10.1179	0.0909	0.0017
at the bent	10.1329	0.3907	4.3053	at the bent	10.1329	0.3907	4.3089
at the abutment	10.1179	0.0908	0.0017	at the abutment	10.1567	0.0513	0.0099
<b>30°/a Lon . + 100% Trans.</b>				<b>30% Long. + 100% Trans.</b>			
at the abutment	3.2622	0.1044	0.0044	at the abutment	3.2497	0.0715	0.0021
at the bent	3.2506	0.3363	1.4520	at the bent	3.2506	0.3363	1.4531
at the abutment	3.2497	0.0714	0.0021	at the abutment	3.2622	0.1044	0.0044
<b>Interior Girder</b>	<b>Long. (inch)</b>	<b>Trans. (inch)</b>	<b>Vert. (inch)</b>	<b>Interior Girder</b>	<b>Long. (inch)</b>	<b>Trans. (inch)</b>	<b>Vert. (inch)</b>
Dead Load				Dead Load			
at the abutment	-0.0065	0.0363	-0.0028	at the abutment	-0.0011	0.0400	-0.0028
at the bent	-0.0026	-0.0020	-0.0381	at the bent	0.0014	0.0019	-0.0383
at the abutment	-0.0001	-0.0400	-0.0028	at the abutment	0.0053	-0.0363	-0.0028
<b>100% Long. + 30% Trans.</b>				<b>100% Long. + 30% Trans.</b>			
at the abutment	10.1518	0.0587	0.0053	at the abutment	10.1403	0.0711	0.0034
at the bent	10.1331	0.3937	1.4397	at the bent	10.1331	0.3937	1.4429
at the abutment	10.1403	0.0710	0.0034	at the abutment	10.1518	0.0586	0.0053
<b>30% Long. + 100% Trans.</b>				<b>30% Long. + 100% Trans.</b>			
at the abutment	3.2574	0.0896	0.0034	at the abutment	3.2533	0.0782	0.0029
at the bent	3.2507	0.3398	0.4838	at the bent	3.2507	0.3398	0.4848
at the abutment	3.2533	0.0782	0.0029	at the abutment	3.2574	0.0896	0.0034

**Table 5.8: Displacements of Design Examples 2M**

**\*Force in Column**

Soil Type= 2, Zone = 2 (0.19g)

Model Type	Combination		Force-R kips	Force-S kips	Force-T kips	Mom.-S k-ft	Mom.-T k-ft
	Long. (%)	Trans. (%)					
3D Fixed	100	30	159.74	84.03	266.19	7486.42	1208.00
	30	100	506.78	279.70	92.07	2444.77	4023.08
Stick Fixed	100	30	215.04	98.66	247.98	7075.56	1269.72
	30	100	673.33	328.65	84.75	2283.51	4230.62
3D Fixed	Dead Load		166.89	1.82	0.17	5.00	29.45
Stick Fixed	Dead Load		156.37	0.56	0.04	1.56	9.53

**Note:**

- Force-R= Axial Force
- Force-S= Shear Force in the Transverse Direction
- Force-T= Shear Force in the Longitudinal Direction
- Mom.-S= Moment about the Transverse Direction
- Mom.-T= Moment about the Longitudinal Direction

**Table 5.9: Unreduced column forces in Design Example 3**

***\*force in bearing***

**Soil Type=2, Zone=2 (0.19g)**

Model Type	Combination		Force-R kips	Force-S kips	Force-T kips	Mom. -S k-ft	Mom.-T k-ft
	Long %	Trans. %					
3D Fixed	100	30	45.12	58.46	146.57	301.03	120.07
	30	100	136.18	194.76	48.13	98.85	400.00
Stick Fixed	100	30	304.34	93.13	144.38	296.05	190.95
	30	100	990.76	281.59	49.98	102.48	577.39
3D Fixed	Dead Load		158.83	4.69	0.17	0.70	33.17
Stick Fixed	Dead Load		86.11	101.59	0.03	0.07	208.30

Force-R= Axial Force  
 Force-S= Shear Force in the Transverse Direction  
 Force-T= Shear Force in the Longitudinal Direction  
 Mom.-S= Moment about the Transverse Direction  
 Mom.-T= Moment about the Longitudinal Direction

**Table 5.10: Unreduced bearing forces in Design Example 3**

**\*forces in cross frame**

Soil Type= 2, Zone = 2 (0.19g)

Model Type	Combination		Force-R <i>kips</i>	Force-S <i>kips</i>	Force-T <i>kips</i>	Mom.-S <i>k-ft</i>	Mom.-T <i>k-ft</i>
	Long. (%)	Trans. (%)					
<i>3D Fixed</i>	100	30	48.57	1.38	0.04	0.19	7.49
	30	100	161.82	4.54	0.10	0.46	24.77
<i>3D Fixed</i>	<i>Dead Load</i>		4.41	0.47	0.01	0.09	1.65

**Note:**

- Force-R= Axial Force
- Force-S= Shear Force in the Transverse Direction
- Force-T= Shear Force in the Longitudinal Direction
- Mom.-S= Moment about the Transverse Direction
- Mom.-T= Moment about the Longitudinal Direction

**Table 5.11: Unreduced cross frame forces in Design Example 3**

Soil Type= 2, Zone = 2		(0.19g)							
		Long.	Trans.	Vert.			Long.	Traps.	Vert.
		(inch)	(inch)	(inch)			(inch)	(inch)	(inch)
<b>Exterior Girder Dead Load</b>					<b>Exterior Girder Dead Load</b>				
at the abutment	0.0000	0.0000	0.0000	at the abutment	0.0000	0.0000	0.0000	0.0000	
at the bent	0.0026	-0.0002	-0.0031	at the bent	0.0023	0.0001	-0.0033	-0.0033	
at the bent	-0.0011	0.0010	-0.0196	at the bent	-0.0011	-0.0005	-0.0133	-0.0133	
at the abutment	0.0011	0.0010	-0.0196	at the abutment	0.0011	-0.0005	-0.0133	-0.0133	
<b>100% Long. + 30% Traps.</b>					<b>100% Long. + 30% Traps.</b>				
at the abutment	0.0000	0.0000	0.0000	at the abutment	0.0000	0.0000	0.0000	0.0000	
at the bent	3.8021	0.0314	0.0015	at the bent	3.8021	0.0314	0.0015	0.0015	
at the bent	3.7771	0.3676	0.0372	at the bent	3.7771	0.3676	0.0372	0.0372	
at the abutment	3.7771	0.3676	0.0372	at the abutment	3.7771	0.3676	0.0372	0.0372	
<b>30% Long. + 100% Traps.</b>					<b>30% Long. + 100% Traps.</b>				
at the abutment	0.0000	0.0000	0.0000	at the abutment	0.0000	0.0000	0.0000	0.0000	
at the bent	1.2978	0.1045	0.0033	at the bent	1.2978	0.1045	0.0033	0.0033	
at the bent	1.2288	1.2248	0.1205	at the bent	1.2288	1.2248	0.1205	0.1205	
at the abutment	1.2288	1.2248	0.1205	at the abutment	1.2288	1.2248	0.1205	0.1205	
<b>Interior Girder Dead Load</b>					<b>Interior Girder Dead Load</b>				
at the abutment	0.0000	0.0000	0.0000	at the abutment	0.0000	0.0000	0.0000	0.0000	
at the bent	0.0023	-0.0001	-0.0033	at the bent	0.0026	0.0002	-0.0031	-0.0031	
at the bent	-0.0011	0.0005	-0.0133	at the bent	-0.0011	-0.0010	-0.0196	-0.0196	
at the abutment	0.0011	0.0005	-0.0133	at the abutment	0.0011	-0.0010	-0.0196	-0.0196	
<b>100% Long. + 30% Traps.</b>					<b>100% Long. + 30% Traps.</b>				
at the abutment	0.0000	0.0000	0.0000	at the abutment	0.0000	0.0000	0.0000	0.0000	
at the bent	3.7674	0.0314	0.0007	at the bent	3.7674	0.0314	0.0007	0.0007	
at the bent	3.7555	0.3684	0.0018	at the bent	3.7555	0.3684	0.0018	0.0018	
at the abutment	3.7555	0.3684	0.0018	at the abutment	3.7555	0.3684	0.0018	0.0018	
<b>30% Long. + 100% Traps.</b>					<b>30% Long. + 100% Traps.</b>				
at the abutment	0.0000	0.0000	0.0000	at the abutment	0.0000	0.0000	0.0000	0.0000	
at the bent	1.1821	0.1045	0.0008	at the bent	1.1821	0.1045	0.0008	0.0008	
at the bent	1.1582	1.2279	0.0041	at the bent	1.1582	1.2279	0.0041	0.0041	
at the abutment	1.1582	1.2279	0.0041	at the abutment	1.1582	1.2279	0.0041	0.0041	

**Table 5.12: Displacements of Design Example 3**

**\*Force in Column**  
**Soil Type=2, Zone=2 (0.19g)**

Model Type	Combination		Force-R <i>kips</i>	Force-S <i>kips</i>	Force-T <i>kips</i>	Mom.-S <i>k-ft</i>	Mom.-T <i>k-ft</i>
	Long. (%)	Trans. (%)					
3D Pinned	100	30	180.86	46.36	258.50	6419.62	1129.58
	30	100	452.83	154.46	85.56	2122.10	3763.71
Stick Pinned	100	30	209.69	51.30	249.79	6209.78	1248.29
	30	100	544.17	170.81	82.53	2048.31	4156.77
3D Pinned	Dead Load		166.82	0.07	0.47	11.87	1.72
Stick Pinned	Dead Load		156.33	0.17	0.21	5.55	3.98

**Note:**

Force-R= Axial Force

Force-S= Shear Force in the Transverse Direction

Force-T= Shear Force in the Longitudinal Direction

Mom.-S= Moment about the Transverse Direction

Mom.-T= Moment about the Longitudinal Direction

**\*force in bearing**

Soil Tyne= 2\_ Zone = 2 (0.19g)

Model Type	Combination		Force-R kips	Force-S kips	Force-T kips	Mom.-S k-ft	Mom.-T k-ft
	Long. (%)	Trans. %					
3D Pinned	100	30	50.95	74.07	148.34	3955.10	684.16
	30	100	92.17	229.84	48.47	1633.10	2117.94
Stick Pinned	100	30	287.96	23.64	132.75	3999.48	591.51
	30	100	870.08	78.42	44.10	1319.37	1717.62
3D Pinned	Dead Load		158.76	24.36	0.47	12.82	237.19
Stick Pinned	Dead Load		80.14	0.36	0.13	3.60	243.59

Force-R= Axial Force  
 Force-S= Shear Force in the Transverse Direction  
 Force-T= Shear Force in the Longitudinal Direction  
 Mom.-S= Moment about the Transverse Direction  
 Mom.-T= Moment about the Longitudinal Direction

**Table 5.14: Unreduced bearing forces in Design 3M**

**\*forces in cross frame**

**Soil Type= 2, Zone = 2 (0.19g)**

Model Type	Combination		Force-R <i>kips</i>	Force-S <i>kips</i>	Force-T <i>kips</i>	Mom.-S <i>k-ft</i>	Mom.-T <i>k-ft</i>
	Long. (%)	Trans. (%)					
<i>3D Pinned</i>	100	30	26.78	1.32	0.04	0.15	6.52
	30	100	88.19	3.53	0.04	0.29	18.84
<i>3D Pinned</i>	<i>Dead Load</i>		2.49	0.41	0.01	0.07	1.27

**Note:**  
 Force-R= *Axial Force*  
 Force-S= *Shear Force in the Transverse Direction*  
 Force-T= *Shear Force in the Longitudinal Direction*  
 Mom.-S= *Moment about the Transverse Direction*  
 Mom.-T= *Moment about the Longitudinal Direction*

**Table 5.15: Unreduced cross frame forces in Design Example 3M**



**Soil Type= 2, Zone = 2 (0.19g)**

<b>Exterior Girder</b>	<b>Long. (inch)</b>	<b>Traps. (inch)</b>	<b>Vert. (inch)</b>	<b>Exterior Girder</b>	<b>Long. (inch)</b>	<b>Traps. (inch)</b>	<b>Vert. (inch)</b>
<b>Dead Load</b>				<b>Dead Load</b>			
at the abutment	0.0000	0.0000	0.0000	at the abutment	0.0000	0.0000	0.0000
at the bent	0.0028	-0.0002	-0.0031	at the bent	0.0028	0.0002	-0.0031
at the bent	-0.0011	-0.0003	-0.0098	at the bent	-0.0011	0.0003	-0.0098
at the abutment	0.0011	-0.0003	-0.0098	at the abutment	0.0011	0.0003	-0.0098
<b>100% Long. + 30% Traps.</b>				<b>100% Long. + 30% Traps.</b>			
at the abutment	0.0000	0.0000	0.0000	at the abutment	0.0000	0.0000	0.0000
at the bent	3.8140	0.0414	0.0036	at the bent	3.8140	0.0414	0.0036
at the bent	3.7977	0.6256	0.0225	at the bent	3.7977	0.6256	0.0225
at the abutment	3.7977	0.6256	0.0225	at the abutment	3.7977	0.6256	0.0225
<b>30% Long. + 100% Traps.</b>				<b>30% Long. + 100% Traps.</b>			
at the abutment	0.0000	0.0000	0.0000	at the abutment	0.0000	0.0000	0.0000
at the bent	1.4057	0.1374	0.0045	at the bent	1.4057	0.1374	0.0045
at the bent	1.2895	2.0848	0.0661	at the bent	1.2895	2.0848	0.0661
at the abutment	1.2895	2.0848	0.0661	at the abutment	1.2895	2.0848	0.0661
<b>Interior Girder</b>	<b>Long. (inch)</b>	<b>Traps. (inch)</b>	<b>Vert. (inch)</b>	<b>Interior Girder</b>	<b>Long. (inch)</b>	<b>Traps. (inch)</b>	<b>Vert. (inch)</b>
<b>Dead Load</b>				<b>Dead Load</b>			
at the abutment	0.0000	0.0000	0.0000	at the abutment	0.0000	0.0000	0.0000
at the bent	0.0025	-0.0001	-0.0033	at the bent	0.0025	0.0001	-0.0033
at the bent	-0.0011	0.0007	-0.0091	at the bent	-0.0011	-0.0007	-0.0091
at the abutment	0.0011	0.0007	-0.0091	at the abutment	0.0011	0.0001	-0.0091
<b>100% Long. + 30% Traps.</b>				<b>100% Long. + 30% Traps.</b>			
at the abutment	0.0000	0.0000	<u>0.0000</u>	at the abutment	0.0000	0.0000	0.0000
at the bent	3.7564	0.0413	<u>0.0026</u>	at the bent	3.7564	0.0413	0.0026
at the bent	3.7627	0.6240	<u>0.0048</u>	at the bent	3.7627	0.6240	0.0048
at the abutment	3.7627	0.6240	0.0048	at the abutment	3.7627	0.6240	0.0048
<b>30% Long. + 100% Traps.</b>				<b>30% Long. + 100% Traps.</b>			
at the abutment	0.0000	0.0000	0.0000	at the abutment	0.0000	0.0000	0.0000
at the bent	1.2133	0.1375	0.0015	at the bent	1.2133	0.1375	0.0015
at the bent	1.1785	2.0792	0.0076	at the bent	1.1785	2.0792	0.0076
at the abutment	1.1785	2.0792	0.0076	at the abutment	1.1785	2.0792	0.0076

**Table 5.16: Displacements of Design Example 3M**

**\*Force in Column**

**Soil Tyne= 2\_ Zone = 1 (0.09a1**

Model Type	Combination		Force-R kips	Force-S kips	Force-T kips	Mom.-S k-ft	Mom.-T k-ft
	Long. (%)	Trans.(%)					
3D	100	30	97.96	51.14	153.66	4362.15	737.31
	30	100	312.57	170.44	51.67	1400.96	2457.35
One Stick	100	30	119.16	64.20	153.58	4361.03	829.59
	30	100	384.10	213.93	51.45	1392.48	2764.84
Two Stick	100	30	115.62	61.53	154.36	4375.17	825.52
	30	100	371.28	204.72	53.54	1426.65	2746.80
3D	Dead Load		109.09	0.38	0.06	1.69	6.14
One Stick	Dead Load		110.84	0.42	0.00	0.20	6.94
Two Stick	Dead Load		122.15	0.04	0.12	3.50	3.50

**Note:**

- Force-R= *Axial Force*
- Force-S= *Shear Force in the Transverse Direction*
- Force-T= *Shear Force in the Longitudinal Direction*
- Mom. -S= *Moment about the Transverse Direction*
- Mom. -T= *Moment about the Longitudinal Direction*

**Table 5.17: Unreduced column forces in Design Example 4**

**\*Force in bearing**

**Soil Tyne- 2. Zone = 1 10.09a)**

Model Type	Combination		Force-R kips	Force-S kips	Force-T kips	Mom. -S k-ft	Mom. -T k-ft
	Long. (%)	Trans.(%)					
3D	100	30	24.30	79.26	76.56	157.23	162.78
	30	100	73.93	262.58	34.79	71.45	539.28
One Stick	100	30	185.89	52.13	90.79	186.16	106.89
	30	100	611.49	164.75	30.51	62.57	337.82
Two Stick	100	30	16.47	171.32	91.94	188.53	351.29
	30	100	48.67	563.78	34.08	69.88	1156.03
3D	Dead Load		105.28	0.86	0.06	0.22	6.92
One Stick	Dead Load		63.87	73.45	0.00	0.01	150.61
Two Stick	Dead Load		59.46	67.09	0.79	1.62	126.41

**Note:**

- Force-R= Axial Force
- Force-S= Shear Force in the Transverse Direction
- Force-T= Shear Force in the Longitudinal Direction
- Mom.-S= Moment about the Transverse Direction
- Mom.-T= Moment about the Longitudinal Direction

**Table 5.18: Unreduced bearing forces in Design Example 4**

**\*Force in Braces**  
**Soil Type= 2, Zone = 1**

Model	Combination		Maximum Force in To	Maximum Force
Type	Long. (%)	Trans. (%)	Lateral Bracing (kips)	Diaphragm Bracing (kips)
3D	100	30	4.74	19.36
	30	100	15.78	64.40
3D	Dead Load		1.16	0.42

**Table 5.19: Unreduced cross frame forces in Design Example 4**

<b>Soil Type= 2, Zone = 1 (0.09g)</b>								
	<b>Long. (inch)</b>	<b>Trans. (inch)</b>	<b>Vert. (inch)</b>		<b>Long. (inch)</b>	<b>Trans. (inch)</b>	<b>Vert. (inch)</b>	
<b>Box Girder</b>				<b>Box Girder</b>				
<b>Dead Load</b>				<b>Dead Load</b>				
at the abutment	-0.0420	0.0000	-0.0136	at the abutment	-0.0419	0.0000	-0.0136	
at the bent	-0.0008	0.0002	-0.0137	at the bent	-0.0009	-0.0001	-0.0138	
at the bent	0.0008	0.0002	-0.0137	at the bent	0.0009	-0.0001	-0.0138	
at the abutment	0.0420	0.0000	-0.0136	at the abutment	0.0419	0.0000	-0.0136	
<b>100% Long. + 30% Trans.</b>				<b>100% Long. + 30% Trans.</b>				
at the abutment	2.2211	0.0002	0.0075	at the abutment	2.2210	0.0002	0.0012	
at the bent	2.1869	0.1839	0.0059	at the bent	2.1869	0.1839	0.0063	
at the bent	2.1869	0.1839	0.0059	at the bent	2.1869	0.1840	0.0063	
at the abutment	2.2211	0.0002	0.0074	at the abutment	2.2210	0.0002	0.0012	
<b>30% Long. + 100% Trans.</b>				<b>30% Long. + 100% Trans.</b>				
at the abutment	0.7301	0.0007	0.0243	at the abutment	0.7298	0.0007	0.0034	
at the bent	0.6835	0.6131	0.01 B3	at the bent	0.6834	0.6131	0.0197	
at the bent	0.6835	0.6131	0.0183	at the bent	0.6834	0.6131	0.0197	
at the abutment	0.7301	0.0007	0.0241	at the abutment	0.7298	0.0007	0.0034	

**Table 5.20: Displacements of Design Example 4**

## Figures

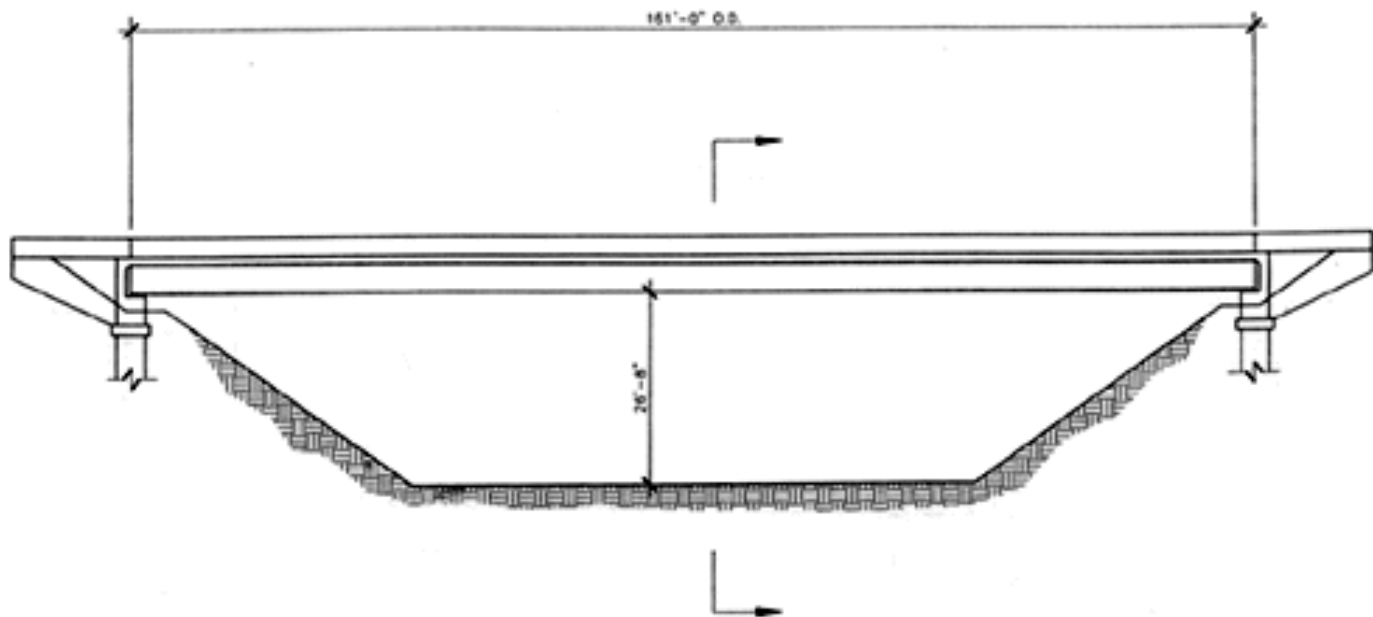


Figure 2.1: Example 1 elevation

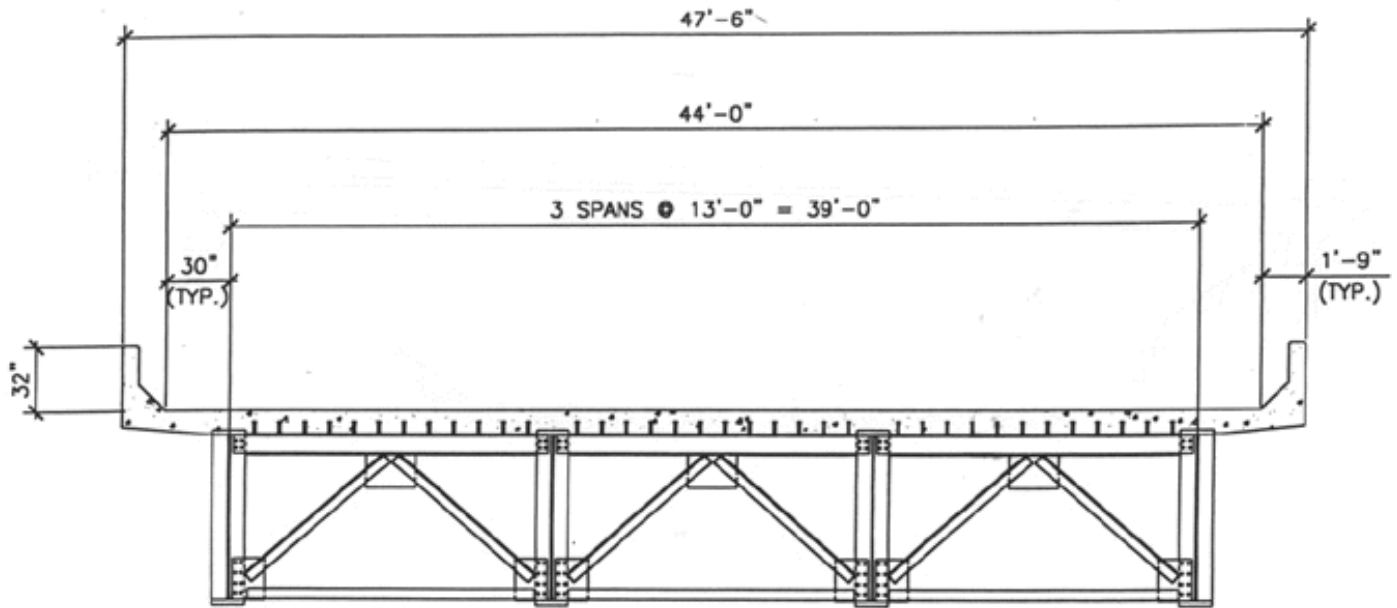


Figure 2.2: Bridge cross section of Example 1



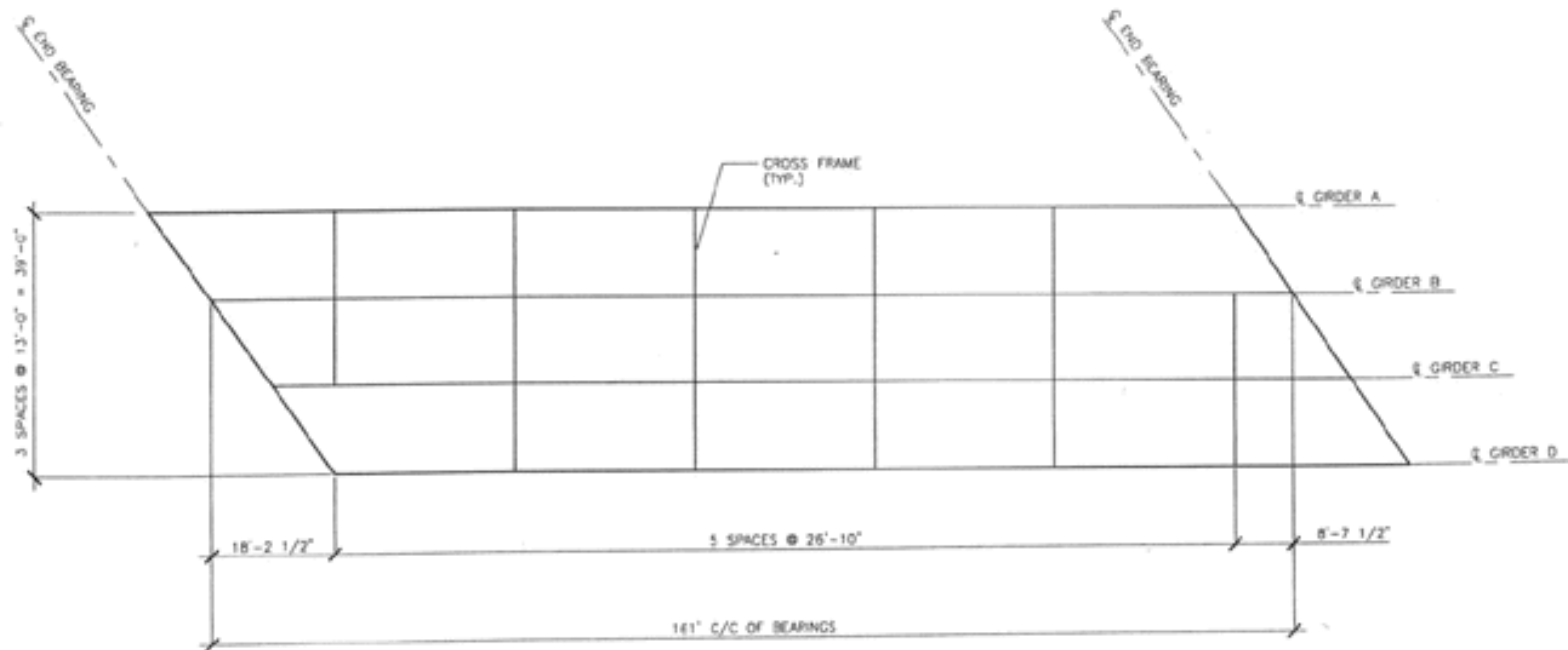


Figure 2.3: Example 1 girder layout

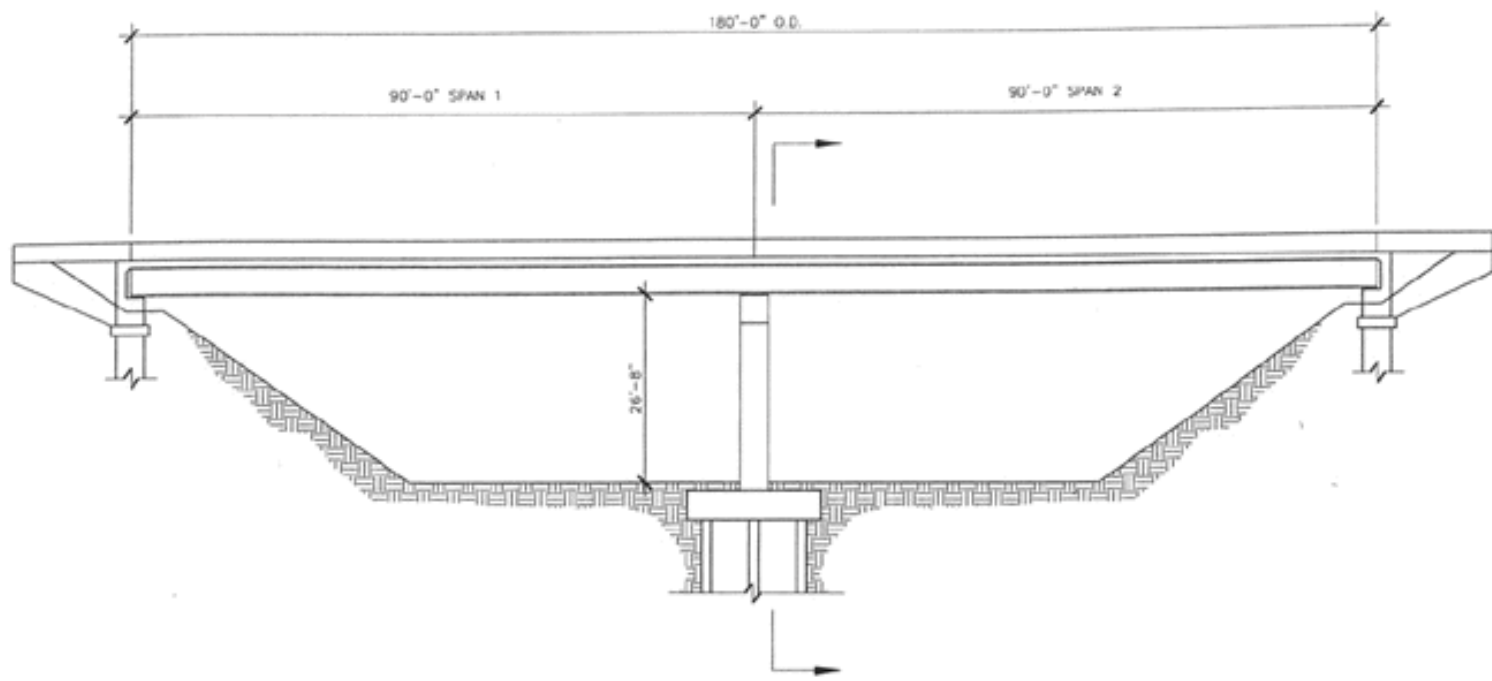


Figure 2.4: Elevation of Example 2

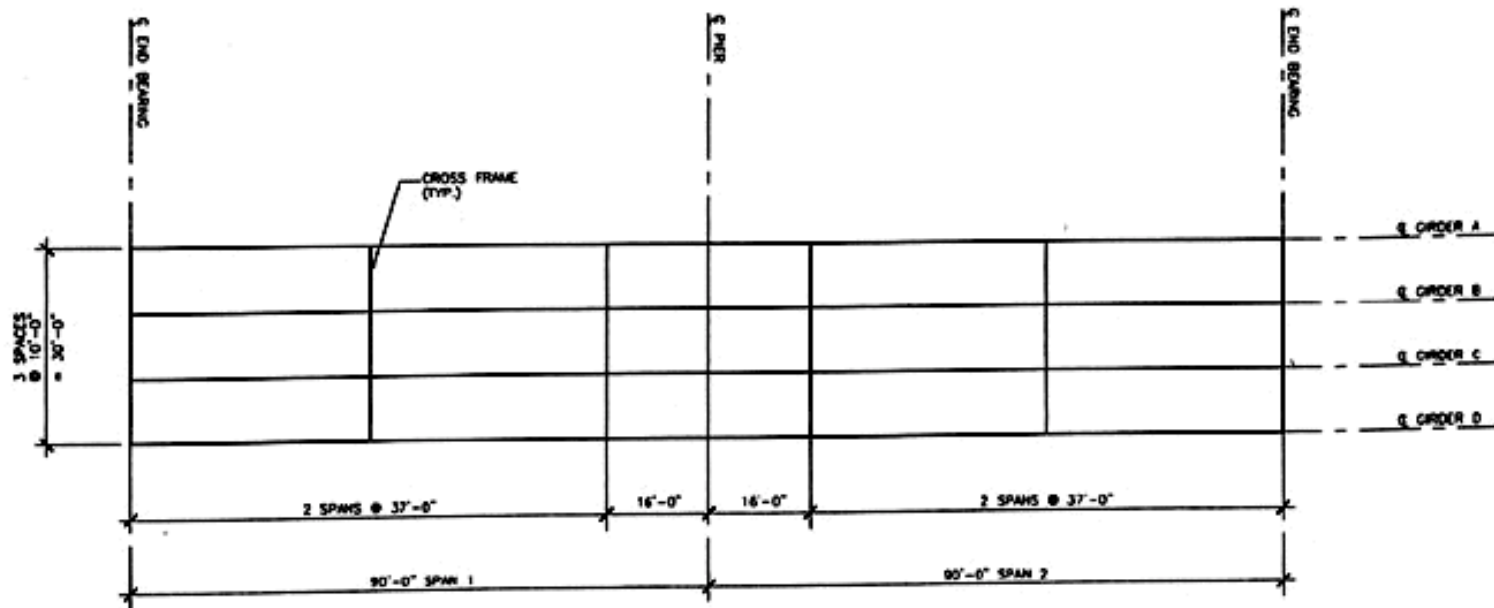


Figure 2.5: Example 2 girder layout

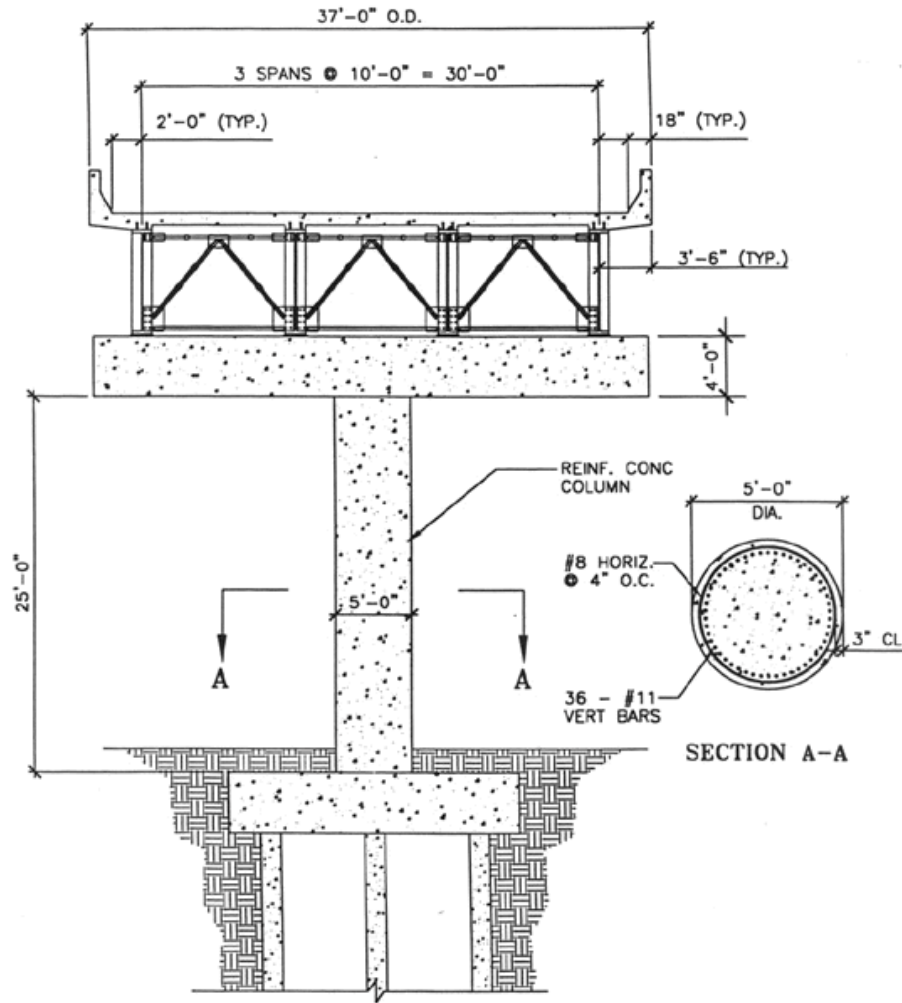


Figure 2.6 Elevation at bent cap location of Example 2

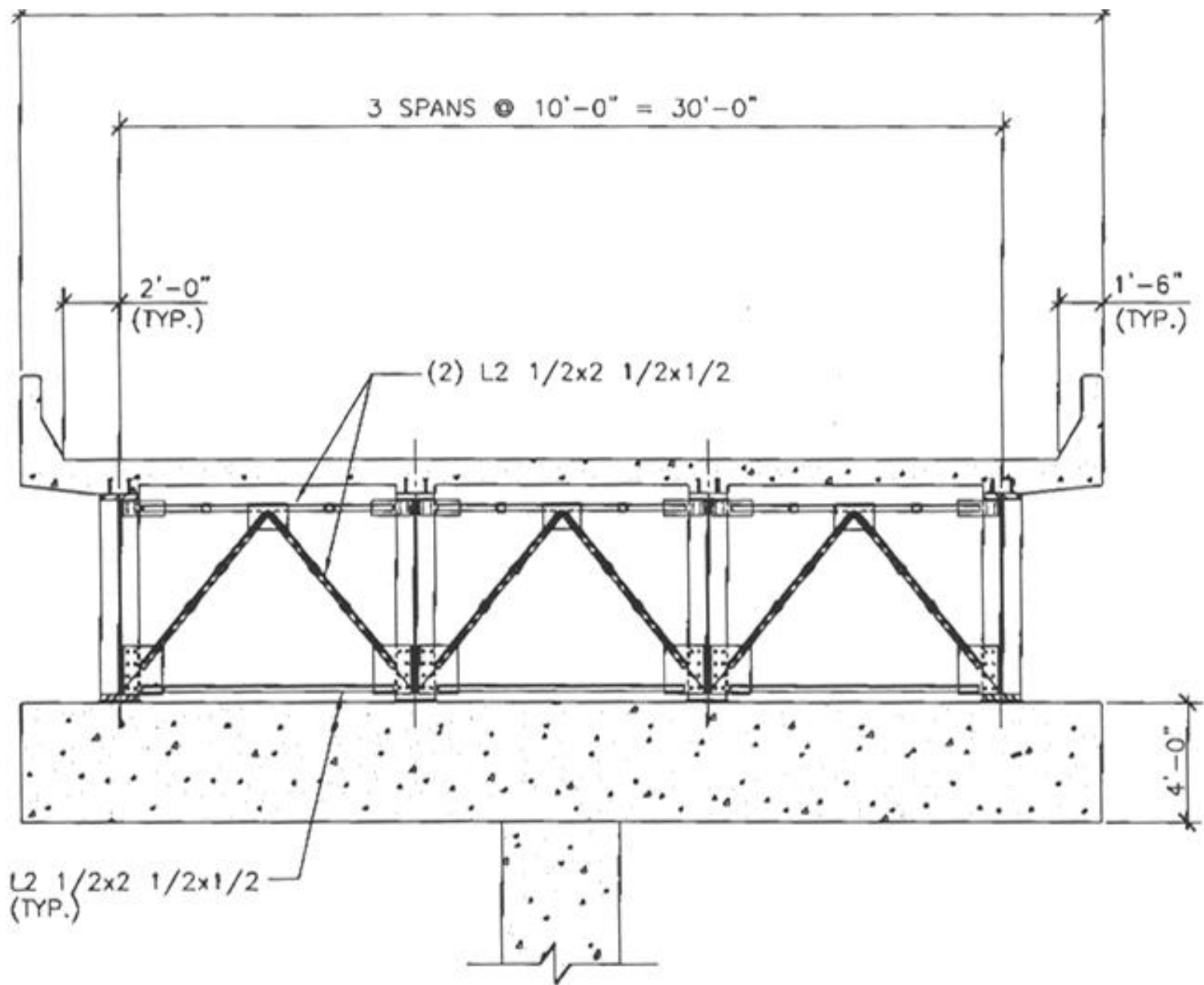


Figure 2.7 Elevation details of Example 2

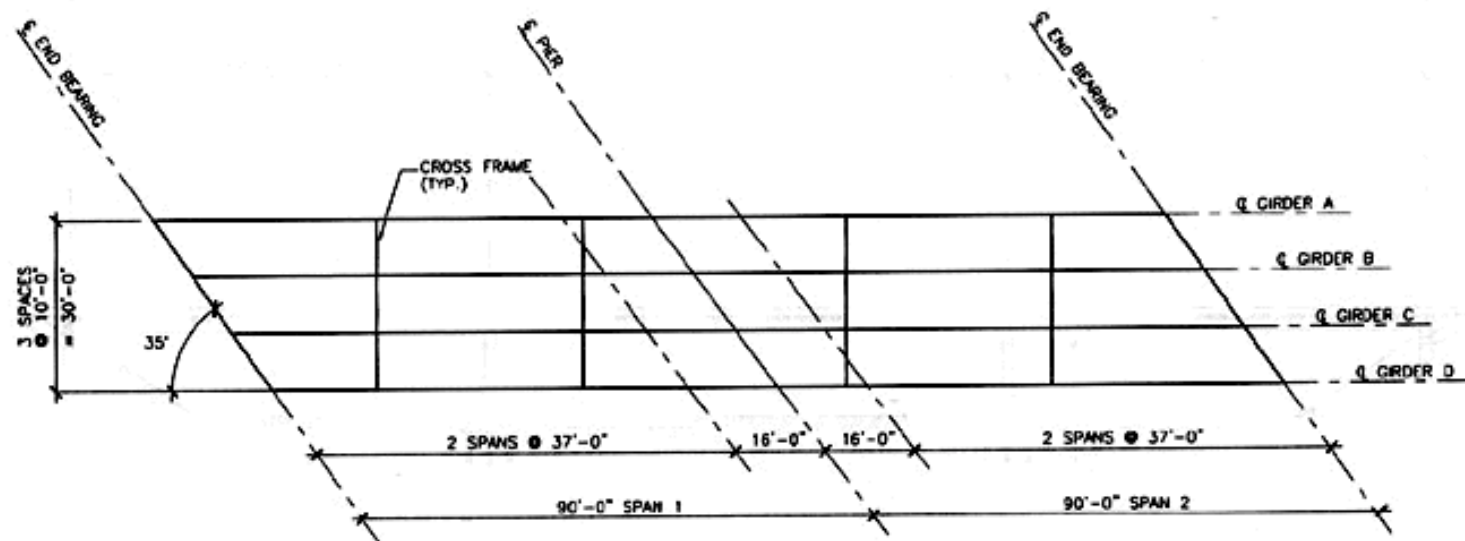


Figure 2.8: Girder layout of Example 2-M

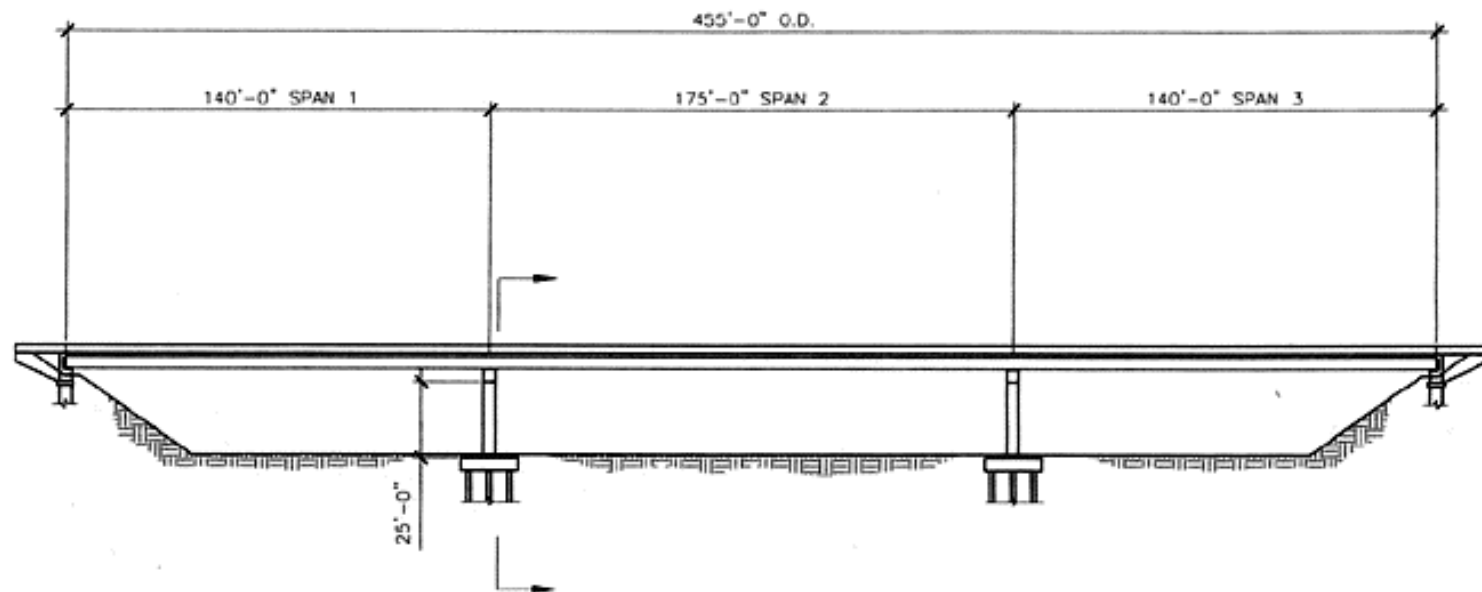


Figure 2.9: Elevation of Example 3

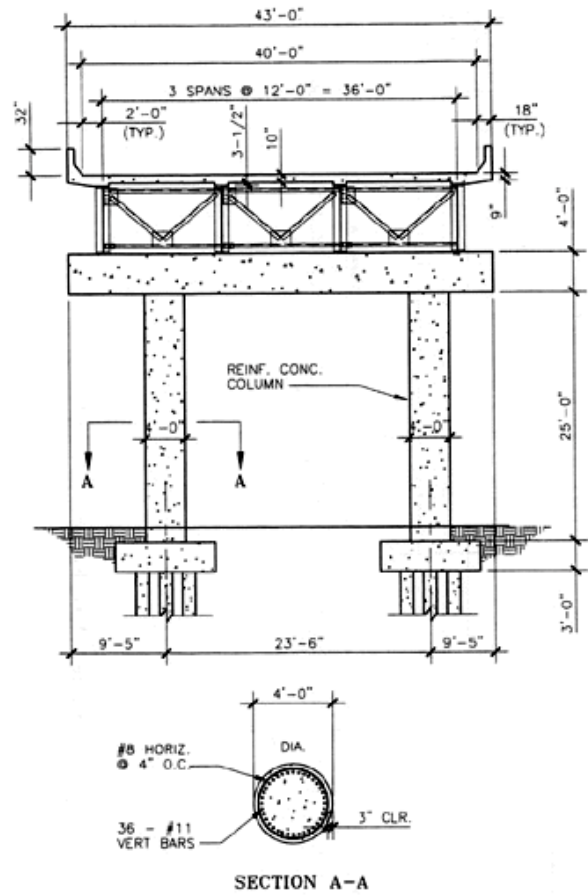


Figure 2.10: Example 3 cross section at bent location



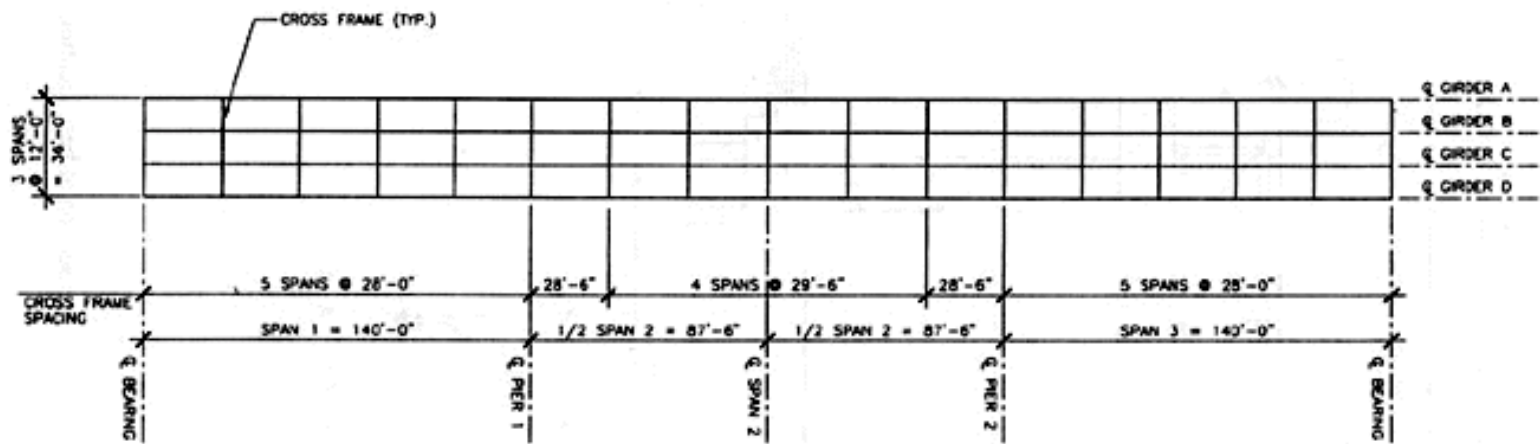


Figure 2.11: Girder layout of Example 3

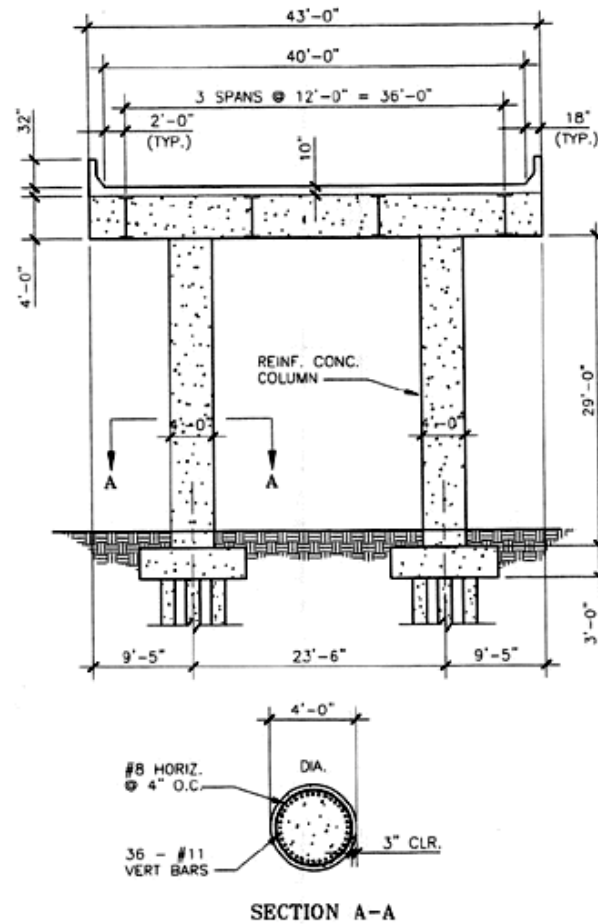


Figure 2.12: Example 3-M cross section at bent location

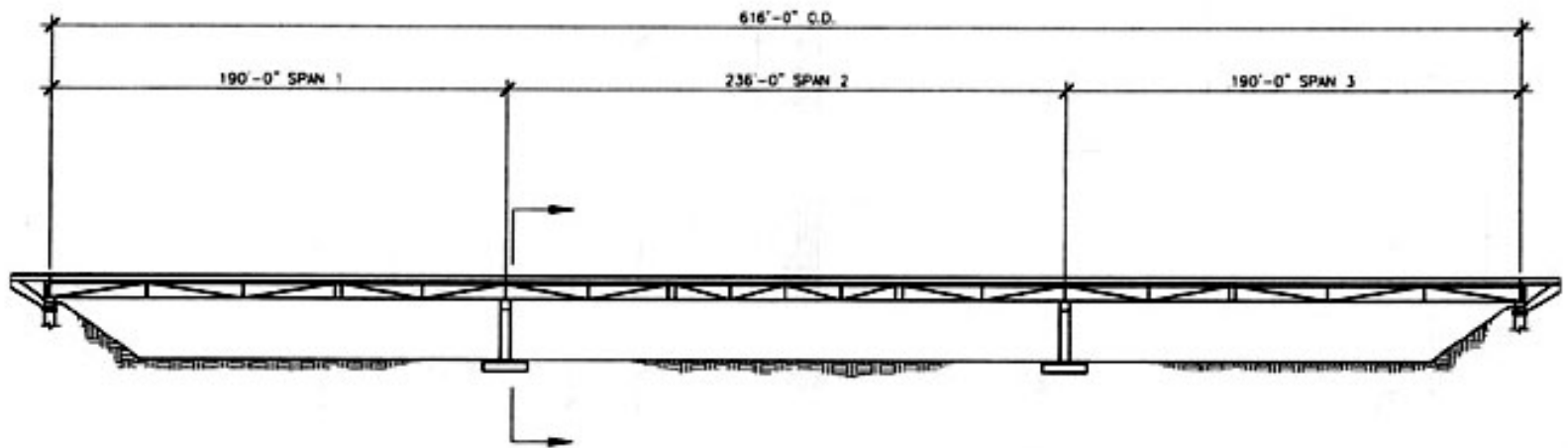


Figure 2.13: Elevation of Example 4

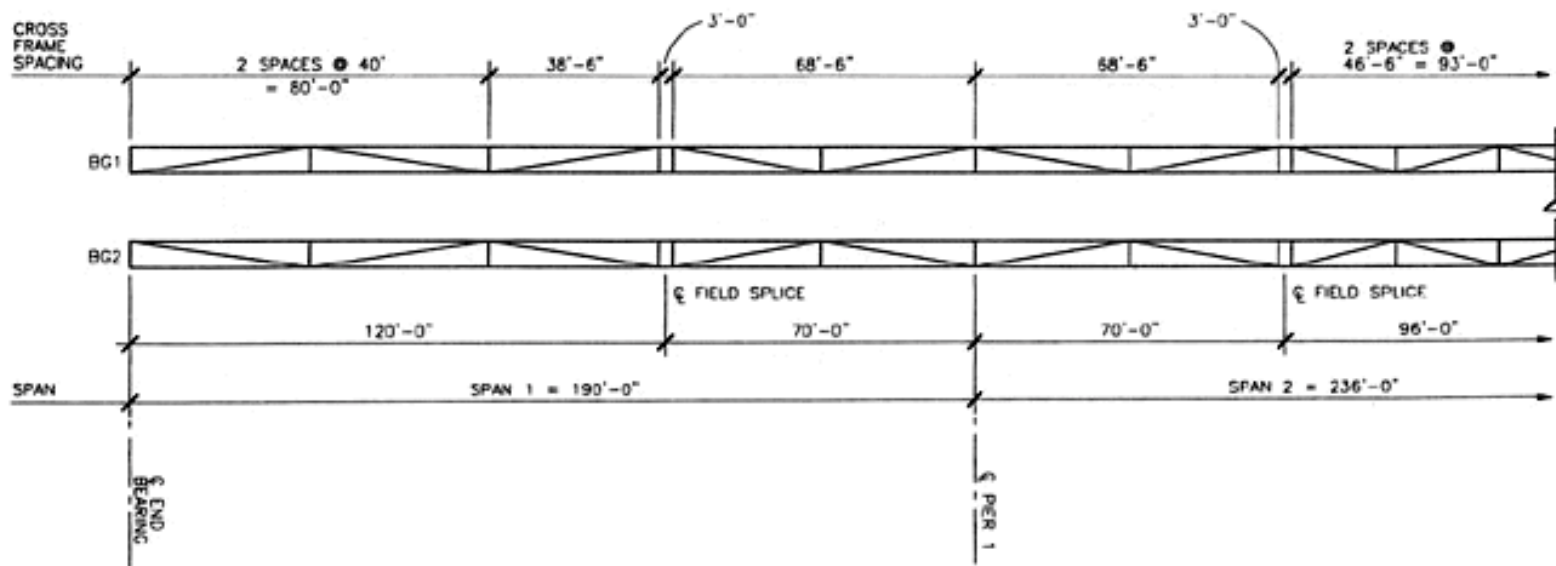


Figure 2.14: Example 4 framing system

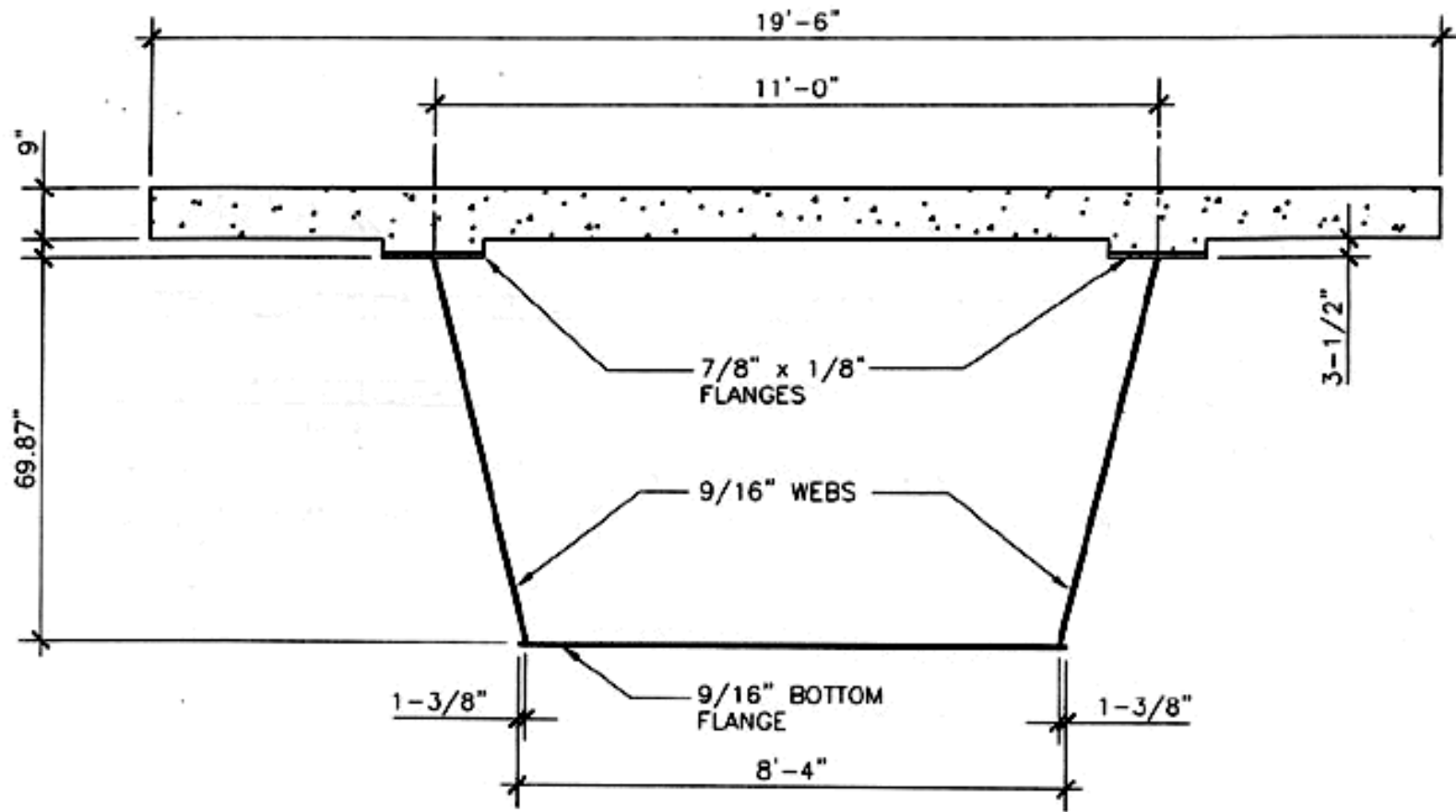


Figure 2.15: Example 4 cross section at mid-span

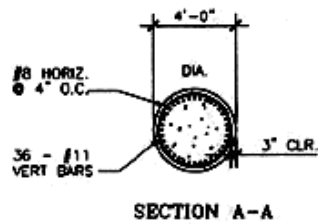
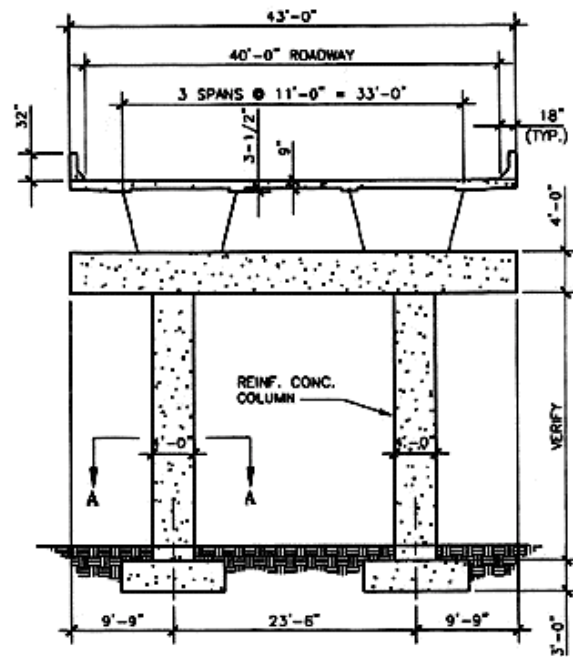


Figure 2.16: Example 4 cross section at bent location

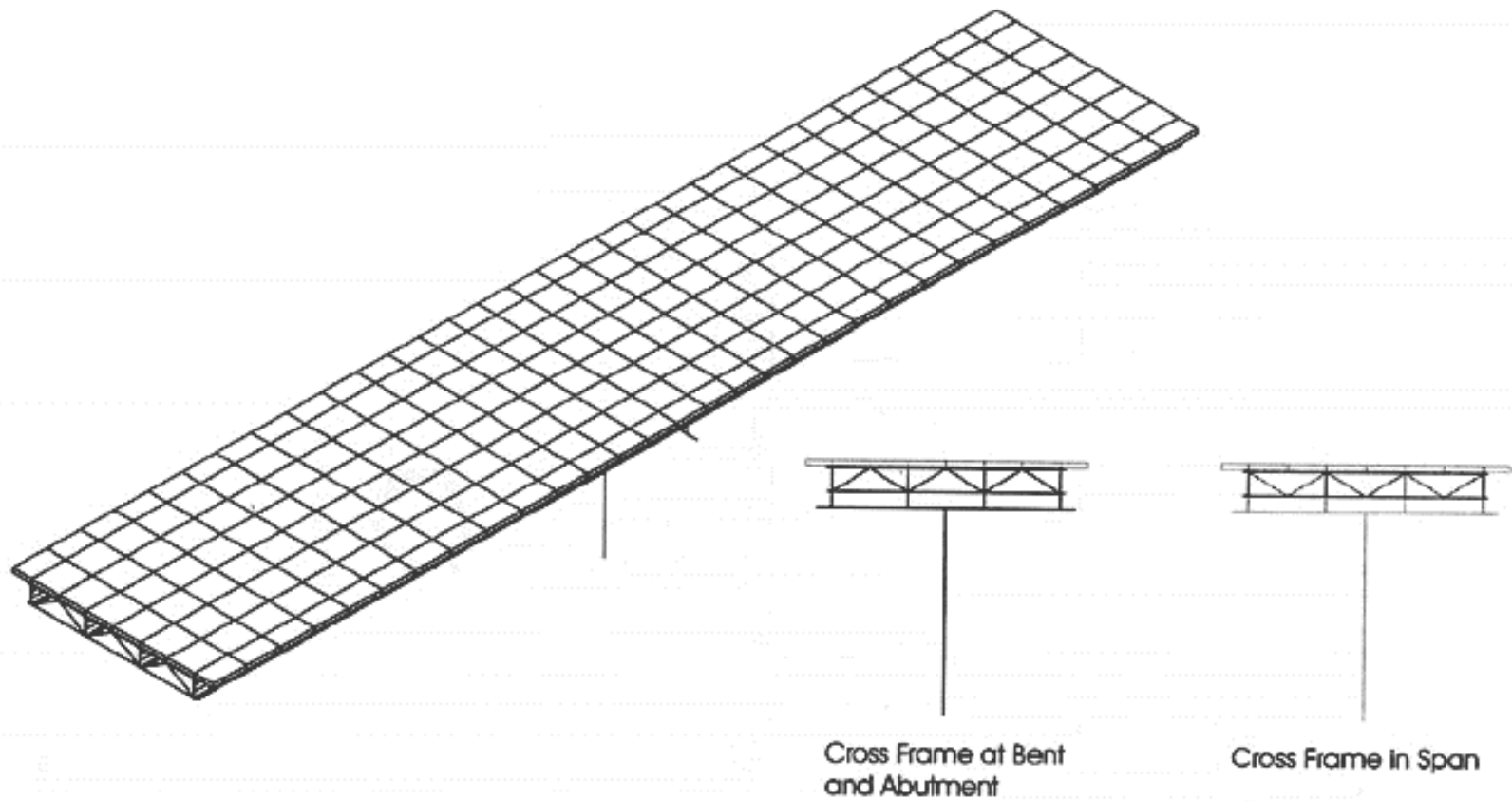
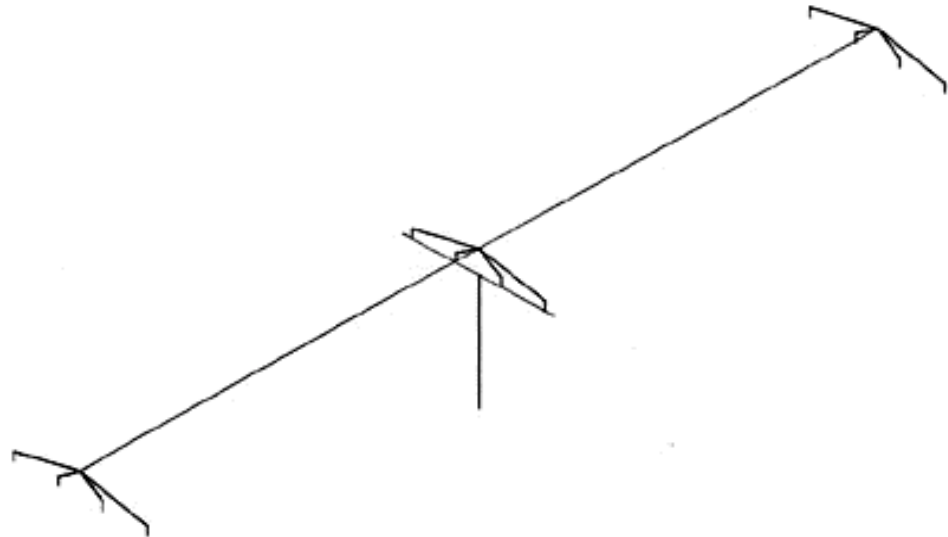


Figure 3.1: Detailed Finite Element Model of the Design Example 2



**Figure 3.2: Simplified Finite Element Model of the Design Example 2**



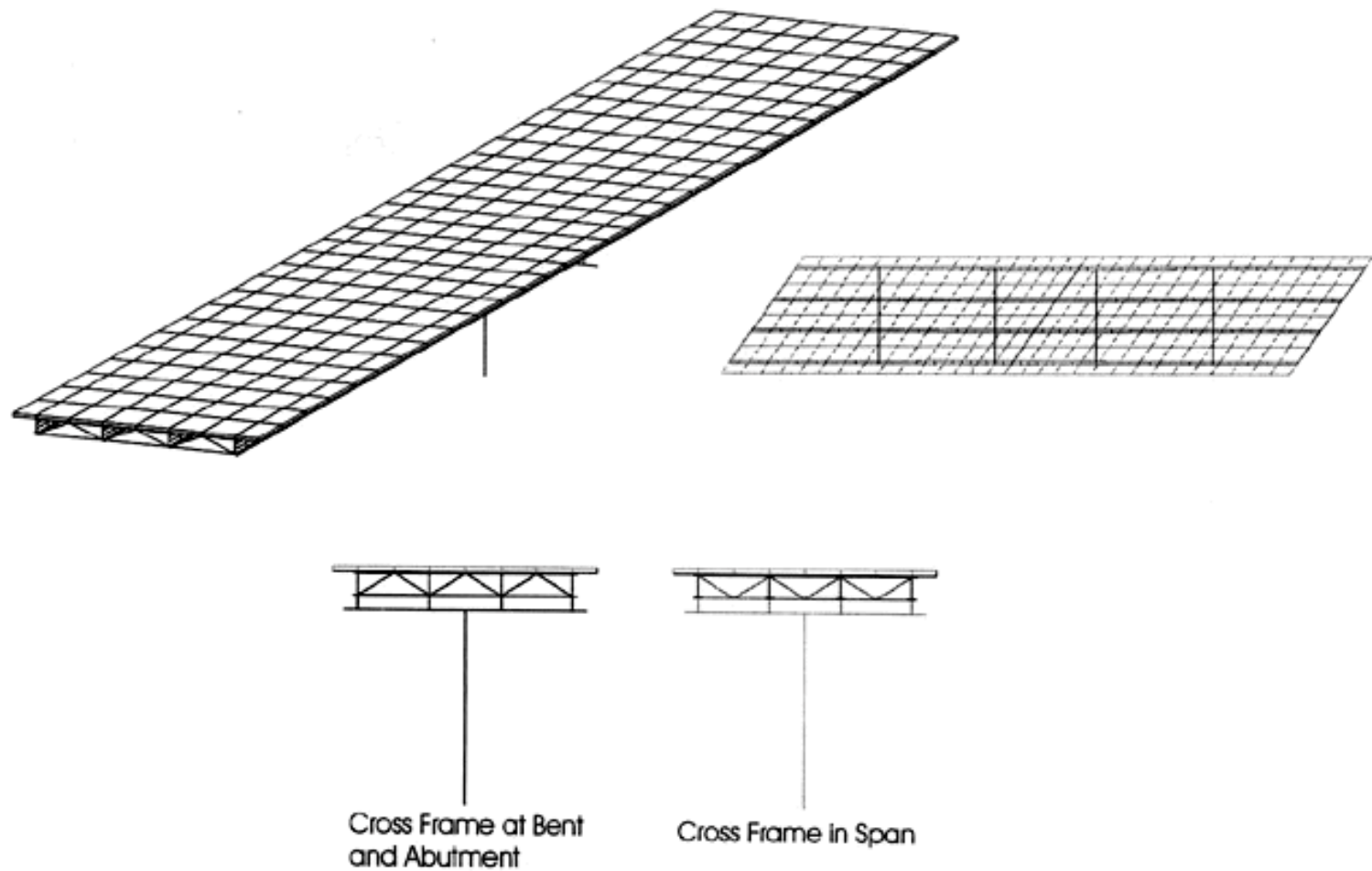


Figure 3.3: Detailed Finite Element Model of the Design Example 2M

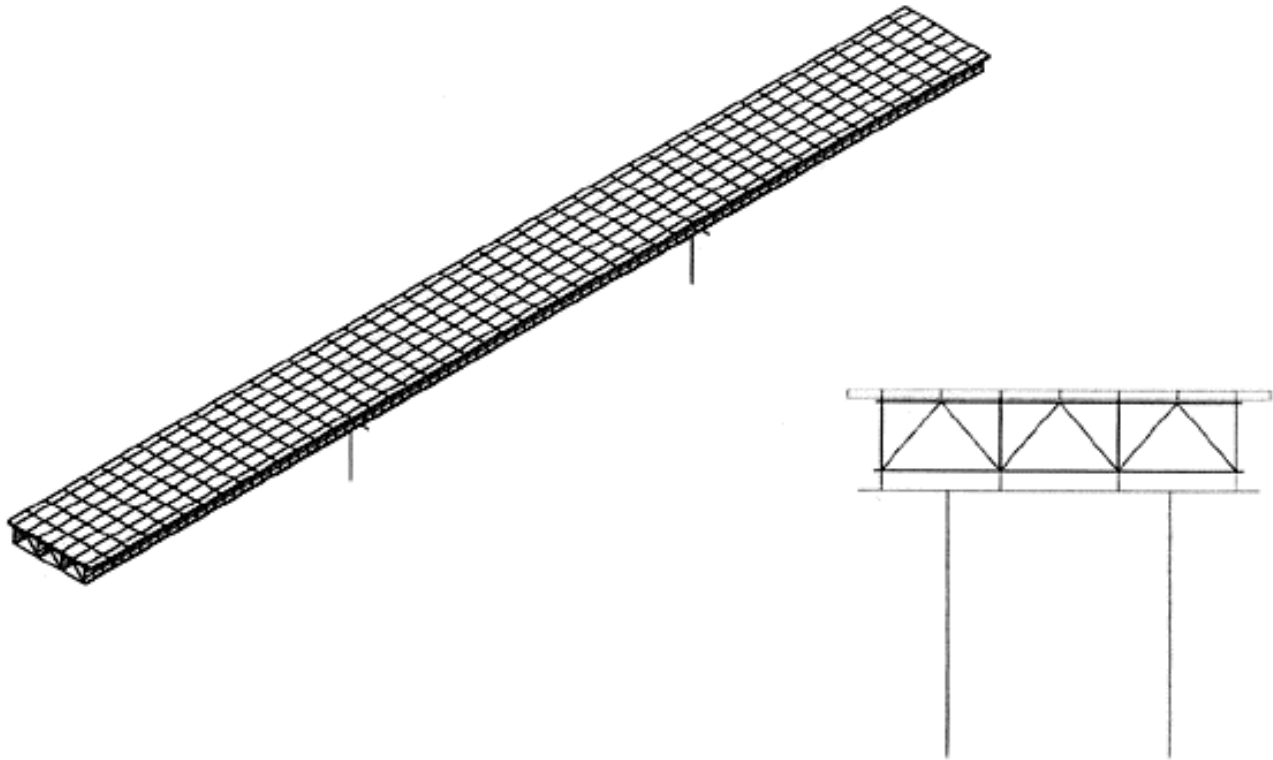


Figure 3.4: Detailed Finite Element Model of the Design Example 3

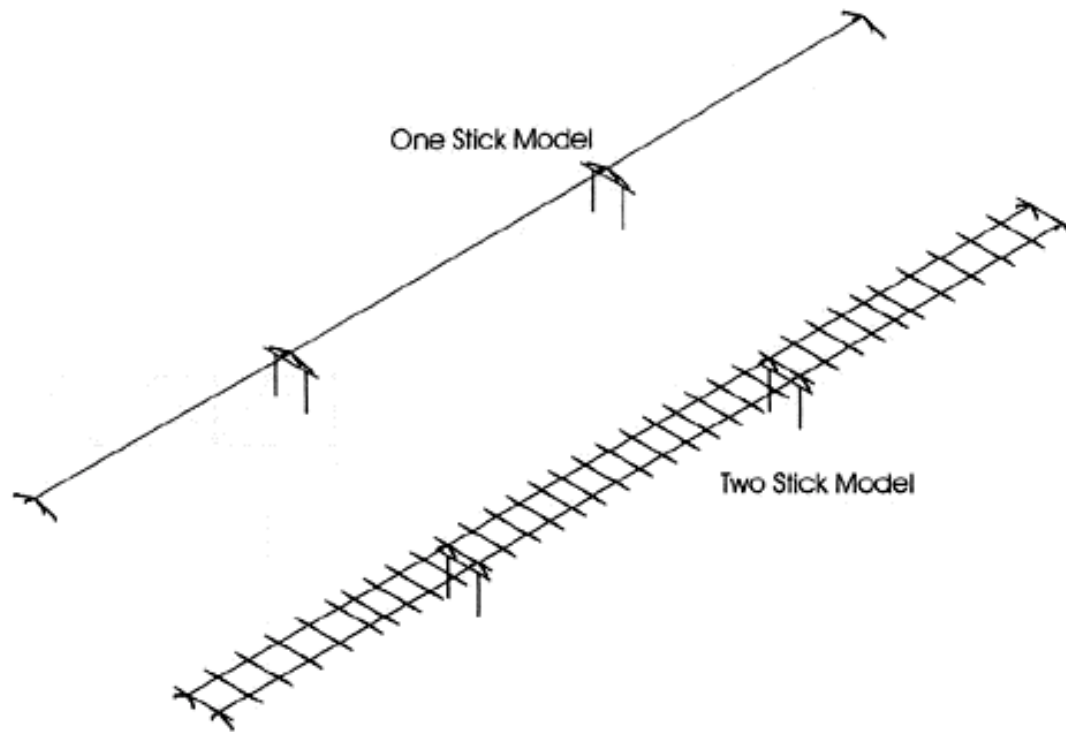
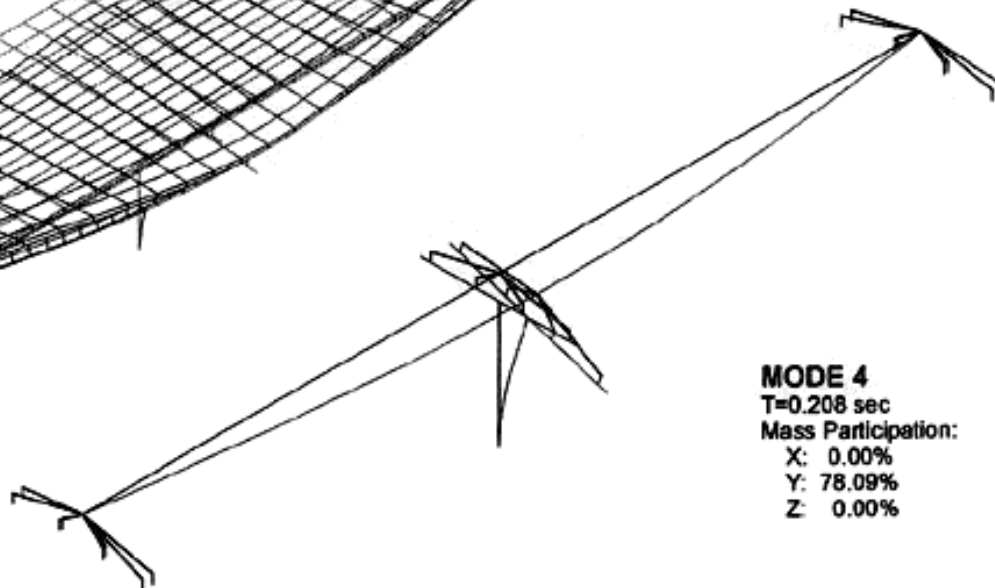
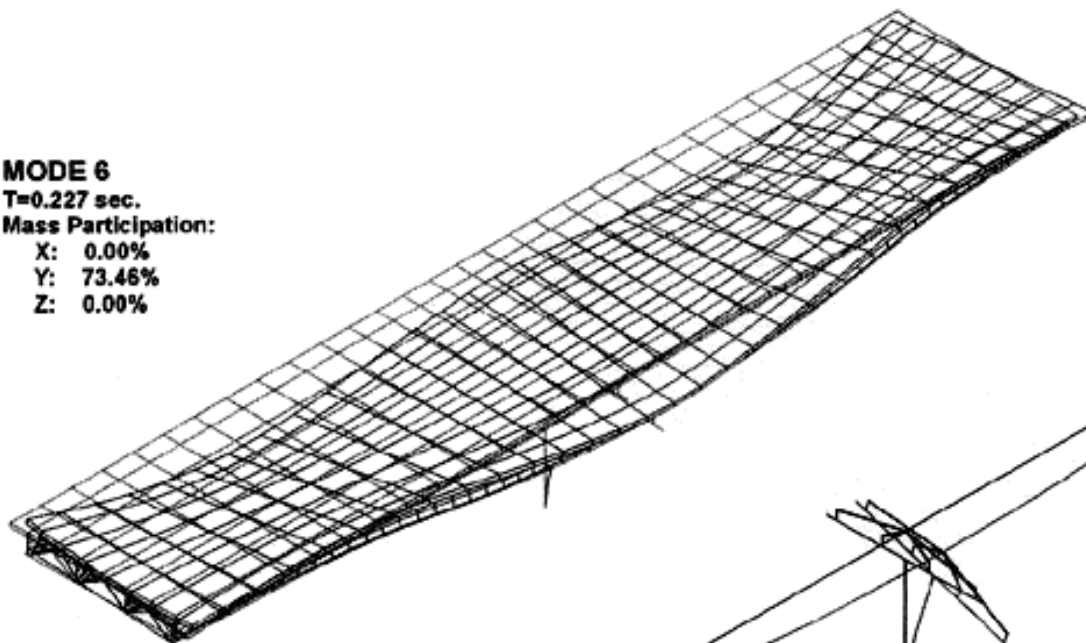


Figure 3.5: Simplified Finite Element Model of the Design Example 4

**MODE 6**  
T=0.227 sec.  
Mass Participation:  
X: 0.00%  
Y: 73.46%  
Z: 0.00%



**MODE 4**  
T=0.208 sec  
Mass Participation:  
X: 0.00%  
Y: 78.09%  
Z: 0.00%

Figure 4.1: Comparison of Mode Shapes of the Model 2

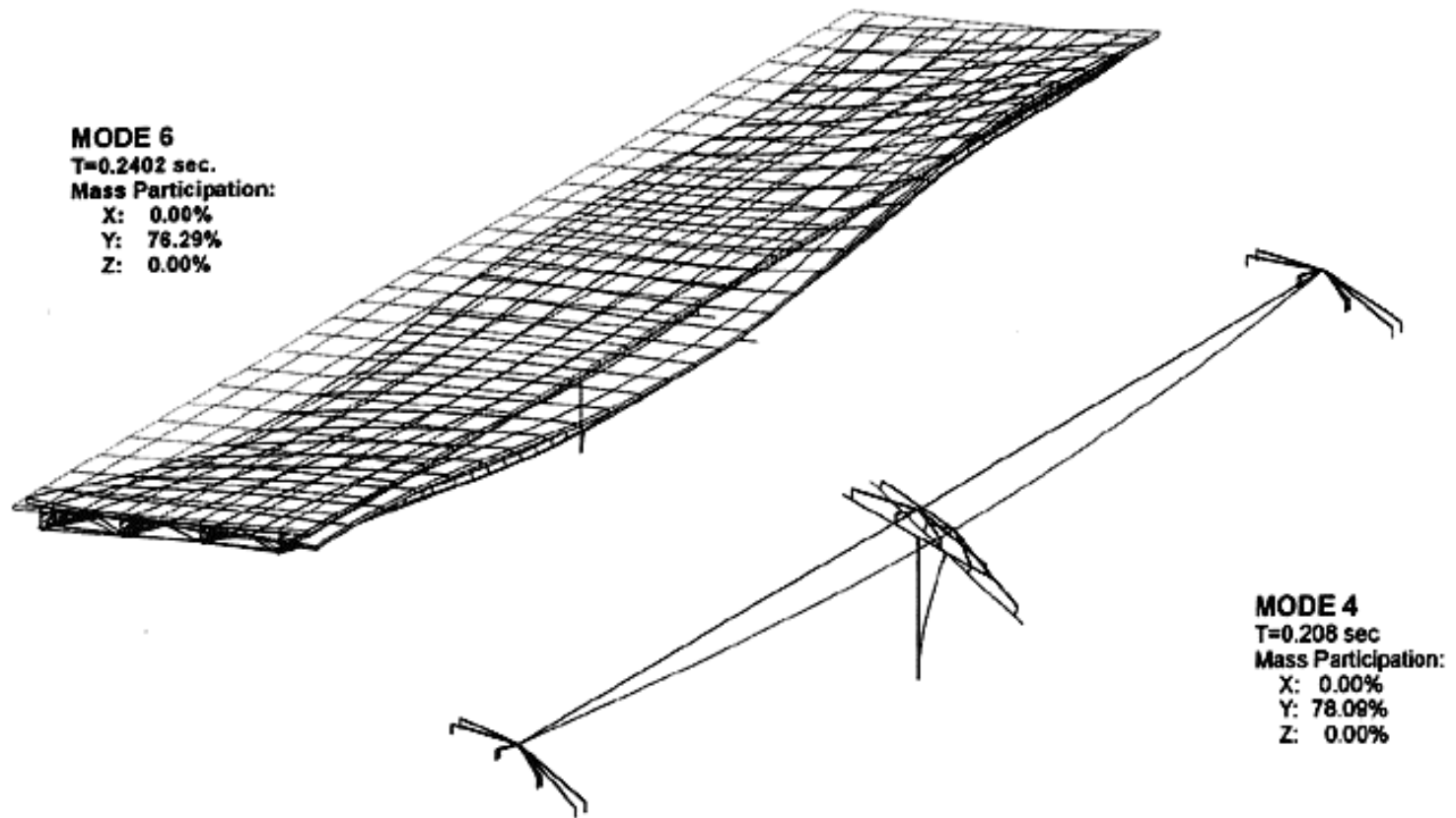


Figure 4.2: Comparison of Mode Shapes of the Model 2M

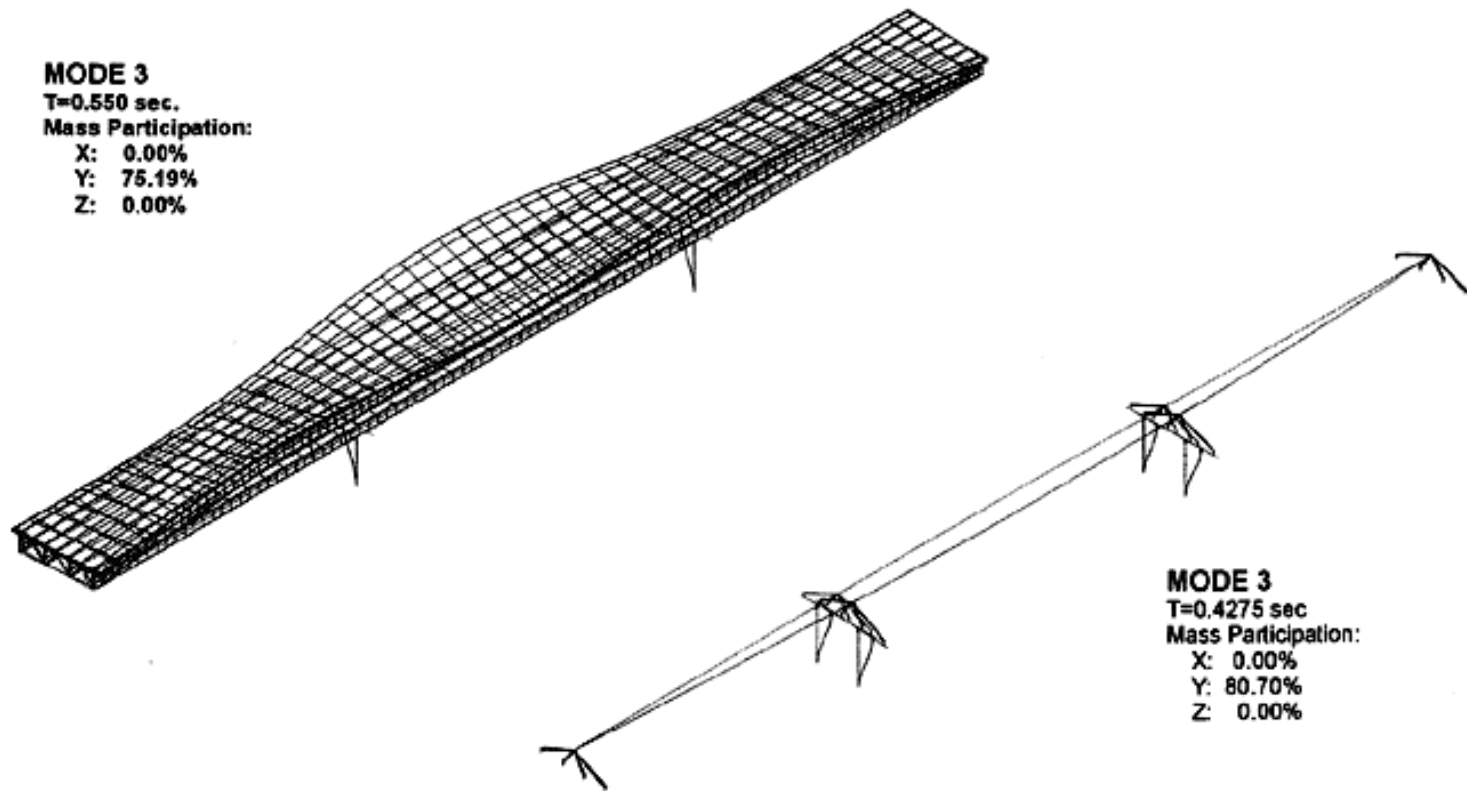


Figure 4.3: Comparison of Mode Shapes of the Model 3 with Fixed Base

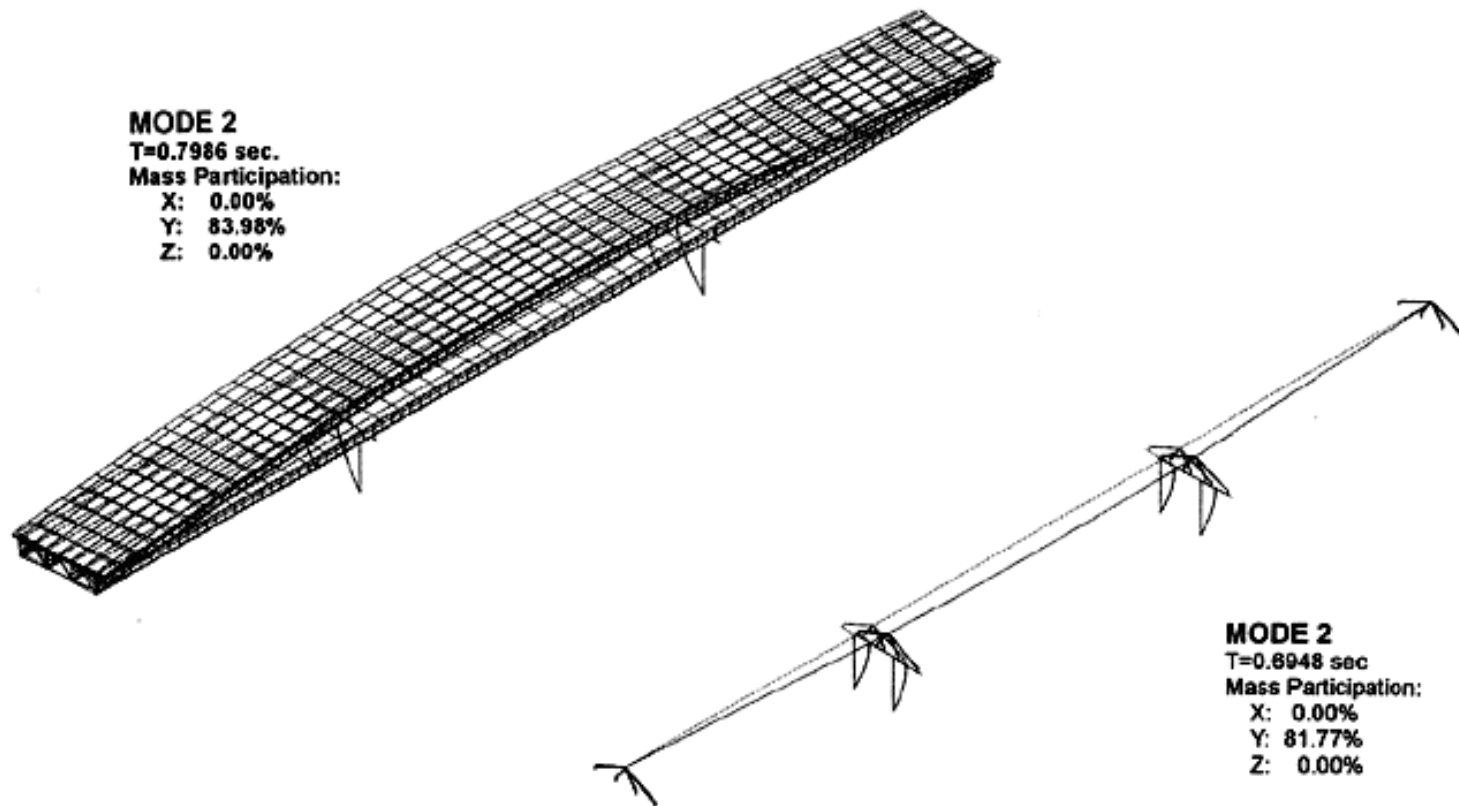


Figure 4.4: Comparison of Mode Shapes of the Model 3M

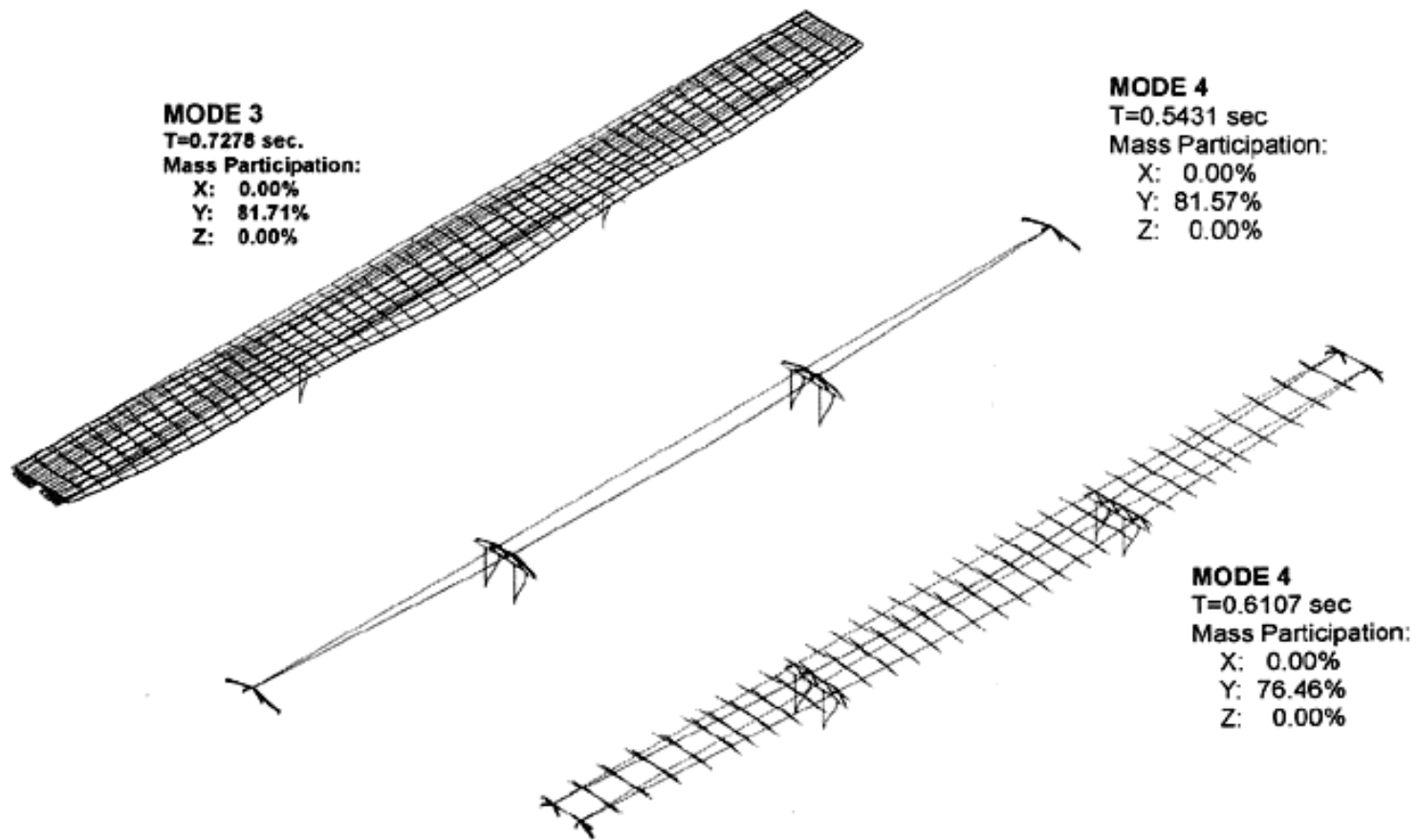


Figure 4.5: Comparison of Mode Shapes of the Model 4



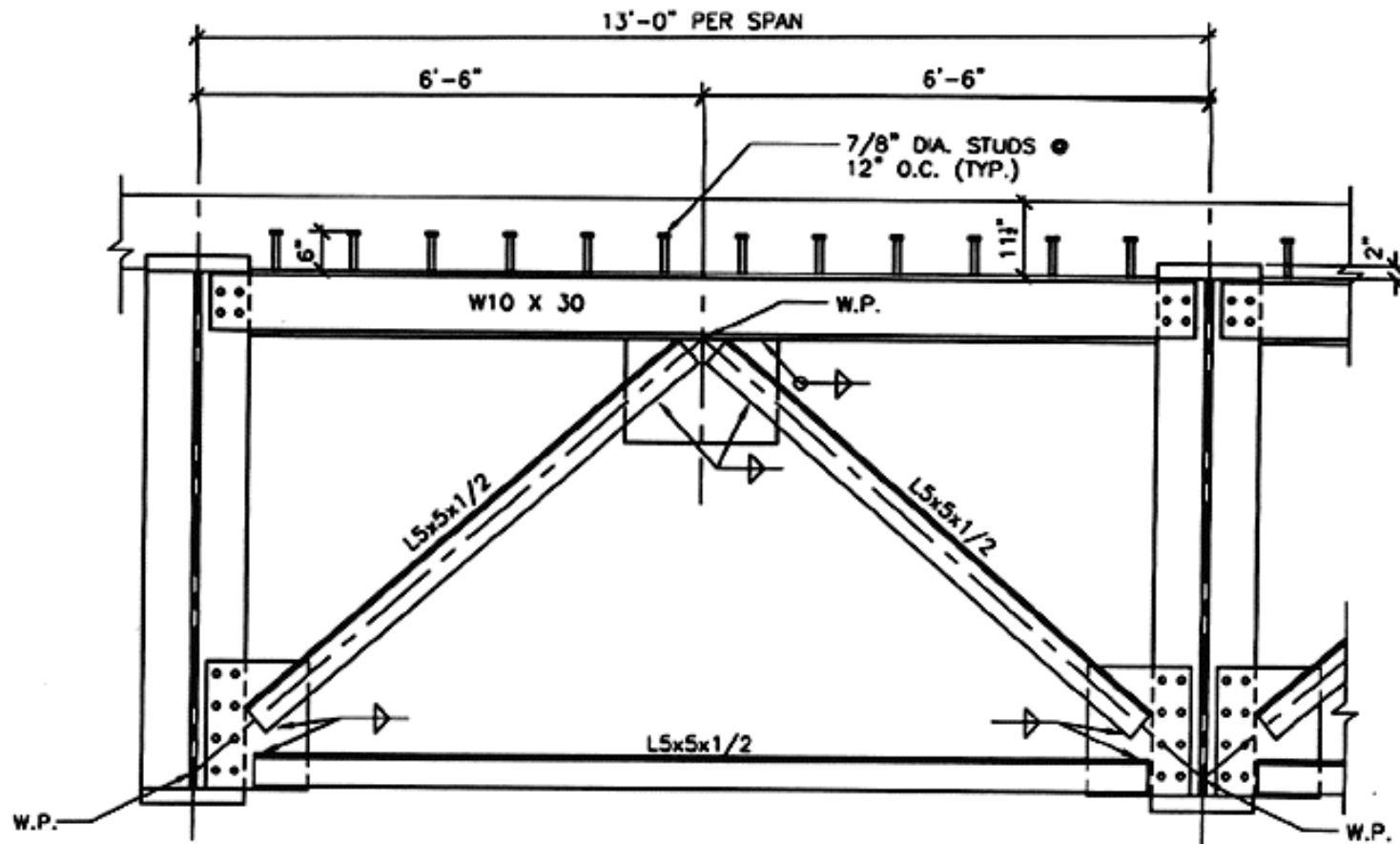


Figure 6.1 Elevation view of end cross frame of Example 1

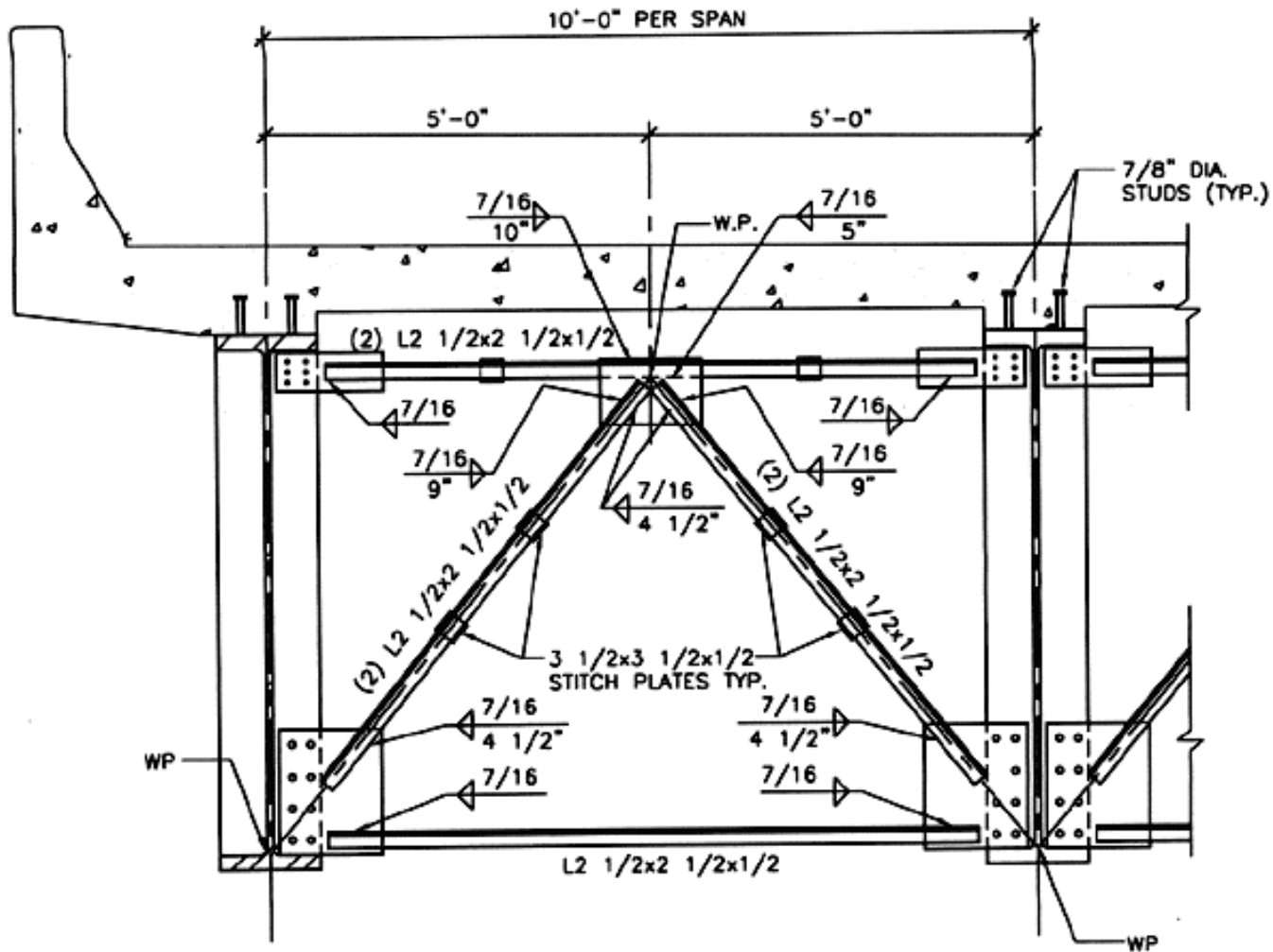


Figure 6.2 Elevation view of intermediate cross frame of Example 2

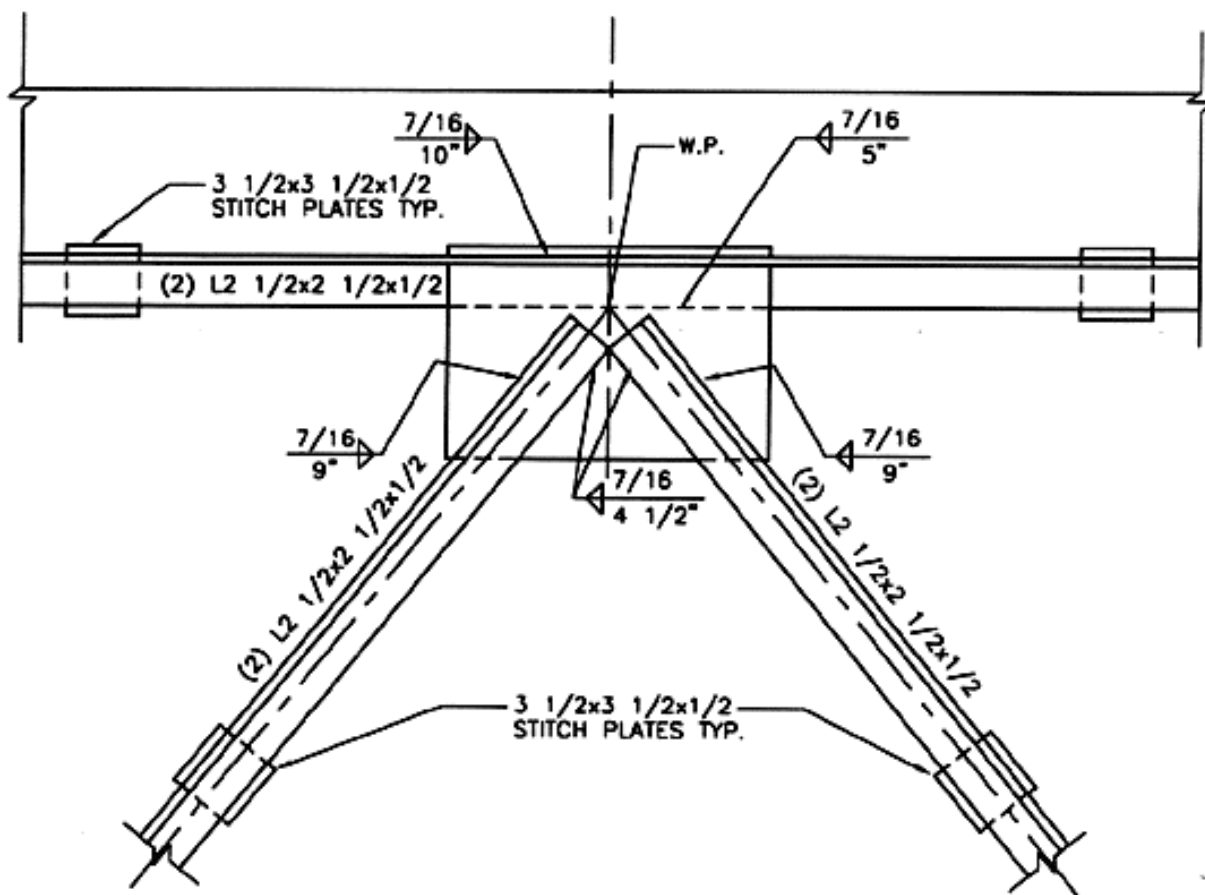


Figure 6.3 Connection details between diagonal members and top strut at bent cross frame

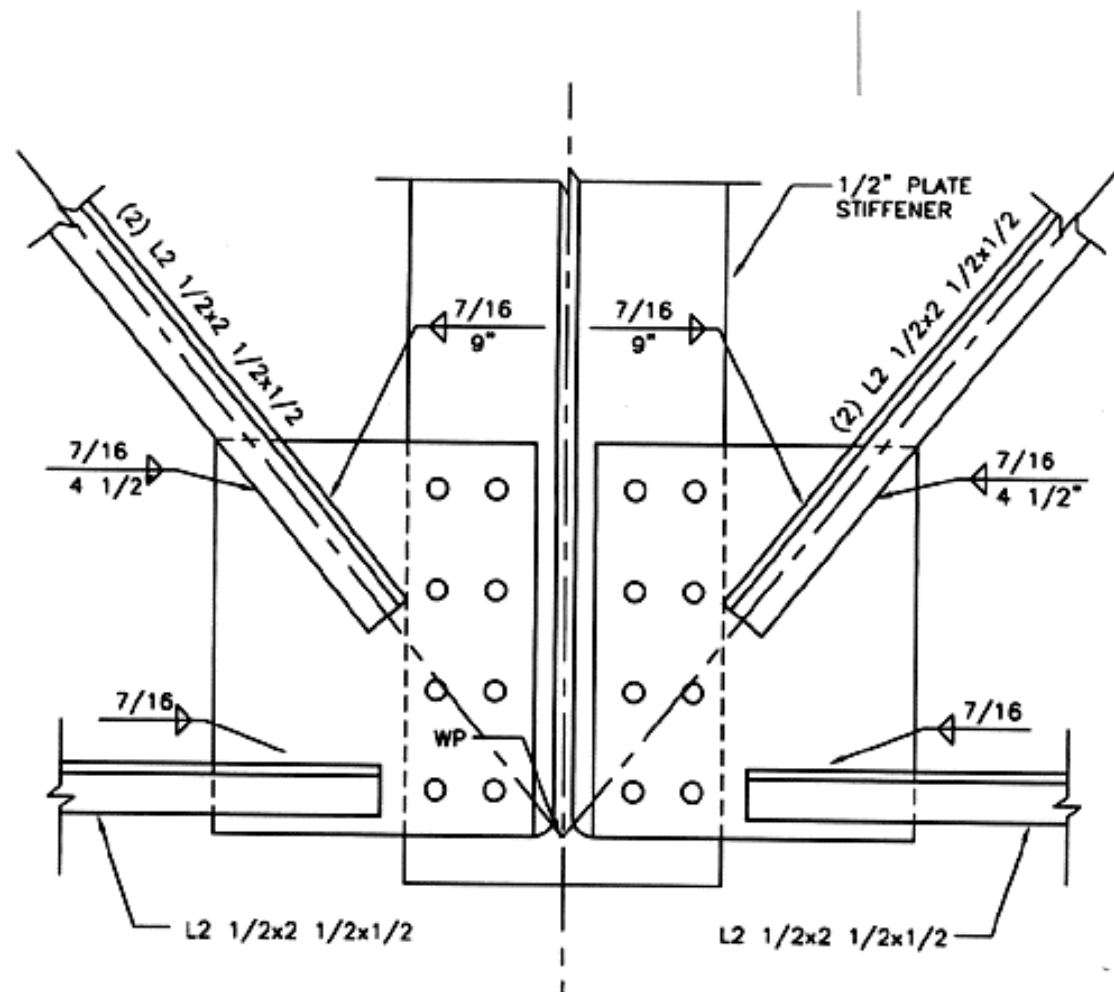


Figure 6.4 Connection details between diagonal members and bottom strut at bent cross frame

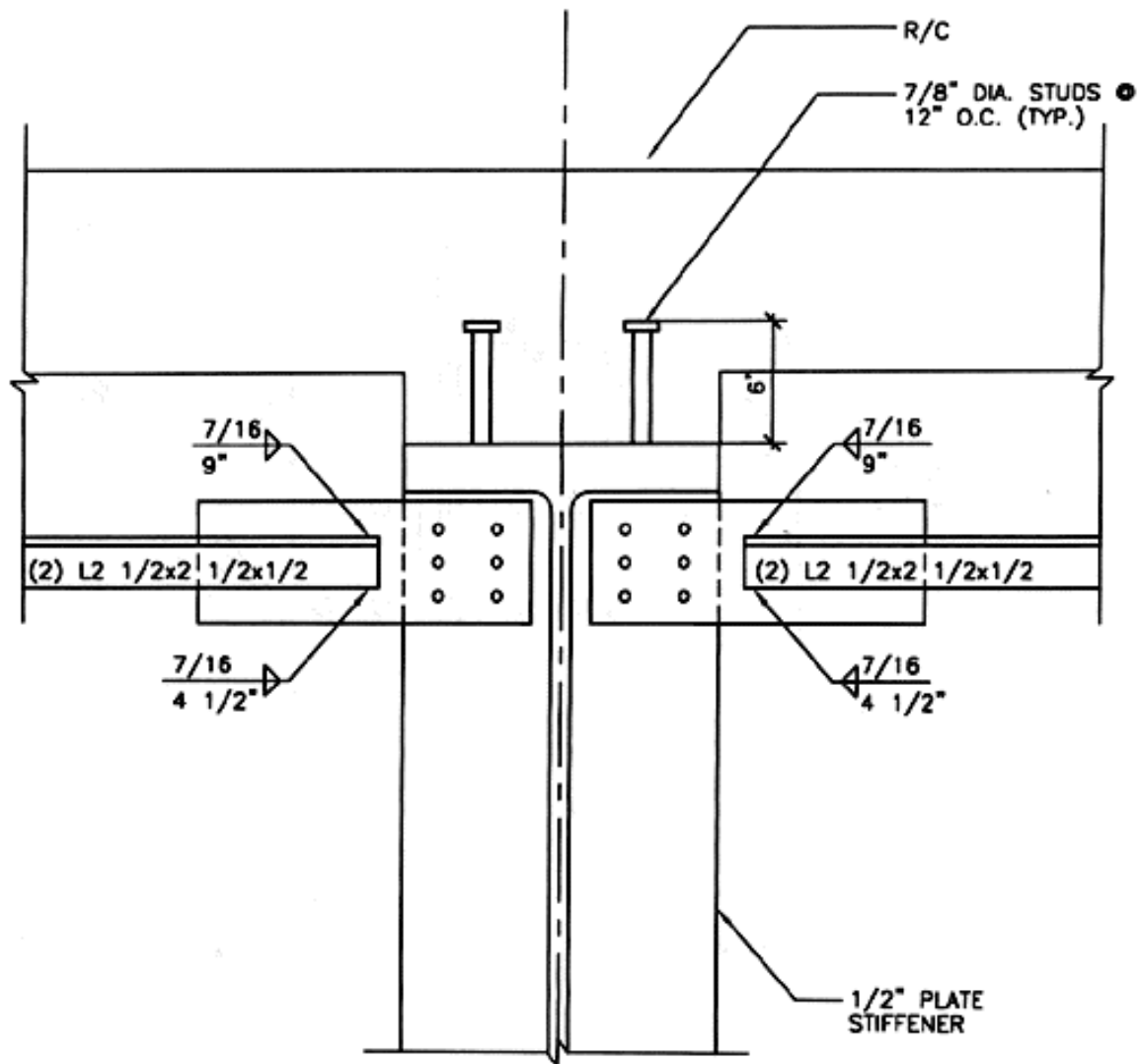


Figure 6.5 Connection details between top strut member at bent cross frame